# Thermodynamic Study of the Supercritical, Transcritical Carbon Dioxide Power Cycles for Utilization of Low Grade Heat Sources Application

**Soheil Moghanlou**

Submitted to the
Institute of Graduate Studies and Research
in partial fulfillment of the requirements for the Degree of

Master of Science
in
Mechanical Engineering

Eastern Mediterranean University
February 2014
Gazimağusa, North Cyprus

Approval of the Institute of Graduate Studies and Research

Prof. Dr. ElvanYılmaz
Director

I certify that this thesis satisfies the requirements as a thesis for the degree of Master of Science in Mechanical Engineering.

Prof. Dr. Uğur Atikol
Chair, Department of Mechanical Engineering

We certify that we have read this thesis and that in our opinion it is fully adequate in scope and quality as a thesis for the degree of Master of Science in Mechanical Engineering.

Prof. Dr. Fuat Egelioğlu
Supervisor

Examining Committee

1. Prof. Dr. Uğur Atikol

2. Prof. Dr. Fuat Egelioğlu

3. Assoc. Prof. Dr. Hasan Hacışevki

# ABSTRACT

Low-grade heat (LGH) sources, here defined as those below 500 $^{o}$C, are a group of abundant energy sources available as industrial waste heat, solar thermal, and geothermal which are not used to their full advantages. For example, they are not adequately for conversion to power because of low efficiency energy conversion. The utilization of LGH can become advantageous for achieving to the highest thermal efficiency. Technologies that allow the efficient conversion of low-grade heat into mechanical and electrical power need to be developed.

Various studies have been carried out to appraise the potential of using supercritical carbon dioxide (S-$CO_2$) in a closed Brayton cycle using LGH source for power generation. In this study, the objective of research is to perform a thermodynamic analysis on five different configurations of S-$CO_2$ Brayton cycle. Different configurations are examined among which recompression and partial cooling have been found very promising.

The main part of this study is focused on carbon dioxide Brayton cycle. $CO_2$ Brayton cycle has wide range of applications such as heat and power generation and in automotive and aircraft industry. Proposed configurations of each carbon dioxide Brayton cycle performance simulation are conducted and subsequently compared with other power cycles utilizing LGH sources.

The $CO_2$ transcritical power cycle (CDTPC) utilizing LGH is also studied. The models are developed by using the Engineering Equation Solver (EES) for several

different Brayton cycle configurations. The choice was made to pursue Brayton cycle with regeneration configuration for further, due to its simplicity and high efficiency.

**Keywords:** Supercritical $CO_2$ Brayton cycle, transcritical $CO_2$ cycle, simulation, low-grade heat.

# ÖZ

Burada, 500 $^{o}$C altında olarak tanımlanan düşük-dereceli ısı kaynakları, tüm avantajları kullanılmayan endüstriyel atık ısı, güneş enerjisi ve jeotermal gibi mevcut bol enerji kaynaklarından bir gruptur. Ancak, düşük enerji dönüşümü verimliliğinden dolayı bu kaynaklardan az yararlanılıyor. Düşük-dereceli ısı kullanımı birçok nedenden dolayı avantajlıdır. Düşük-dereceli ısının mekanik ve elektrik güç haline verimli dönüşümünü sağlayan teknolojileri geliştirmek oldukça önemlidir.

Süper kritik karbon dioksitin, düşük-dereceli ısı kaynaklı kapalı Brayton çevriminin güç üretimide kullanım potansiyelini değerlendirmek için çeşitli çalışmalar gerçekleştirilmiştir. Bu çalışmadaki araştırmanın amacı beş farklı konfigürasyonda süper kritik karbon dioksit Brayton çevriminin termodinamik analizini gerçekleştirmektir. Farklı konfigürasyonlar incelendi ve bunlar arasında tekrar sıkıştırma ve kısmi soğutma çok umut verici bulundu.

Bu çalışmanın ana kısmı, karbon dioksit Brayton çevrimine odaklanmıştır. Karbon dioksit Brayton çevrimi geniş uygulama yelpazesine sahiptir, örneğin ısı ve güç üretimi, otomotiv ve uçak sanayisi. Önerilen karbon dioksit Brayton çevrimi konfigürasyonlarının performans simülasyonu yapıldı ve diğer düşük dereceli ısı kullanan güç çevrimleri ile karşılaştırıldı. Düşük-dereceli ısı kaynağı kullanan $CO_2$ transkritik güç çevrimi ayrıca incelendi. Engineering Equation Solver yazılımı kullanılarak farklı konfigürasyonlardaki Brayton çevriminin modelleri geliştirildi. Rejenaratörlü basit Brayton çevriminin sadeliği ve yüksek verimliliği nedeniyle daha fazla takip edilmesi gerektiği seçimi yapıldı.

**Anahtar kelimeler:** Süper kritik $CO_2$ Brayton çevrimi, transkritik $CO_2$ çevrimi, simülasyon, Düşük-dereceli ısı

***I dedicate my dissertation work to my family and many friends. A special feeling of gratitude to my loving parents, whose words of encouragement and push for tenacity ring in my ears. My sister, Soraya has never left my side and is very special.***

# ACKNOWLEDGMENT

There are so many people that I should like to thank. Without all your assistance, support and encouragement, I would not have achieved this much.

First of all, I would like to express my sincere gratitude to my supervisor, Prof. Dr. Fuat Egelioglu. You opened the door for me to this scientific world and guided me all the way through with your wise ideas, enormous patience, good humor and constant encouragement. I could not have imagined having a better advisor and mentor for my M.S study.

Thanks are also due to:

Prof. Dr. Uğur Atikol, I want to express my hearty thanks to you as Head of the Department of Mechanical Engineering. You are basically an academic man and always inspires me in doing academically and productive works. I am fortunate that I can discuss with you freely and get your advice whenever required. I am thankful also due to providing an office or a safe and calm room to do research.

Dr. Kiyan Parham, my dear friend and brother for your support and help whenever I have had questions. Your guidance helped me in all the time of research and writing of this thesis. You never said ″no″ to me when I needed help and your hard work has always inspired me.

Moreover, I want to thank all my friends those who, in my daily work I have been blessed with a friendly and cheerful environment from them include Keyvan Bahlouli, Mehrdad Khamooshi, Ali Hooshyar, Sina Ghafourpour and especially my parents

Akram Khoshrou and Abdolreza Moghanlou, and my sister, Soraya for your love, support and constant care.

I would also like to thank all the teaching and non-teaching staff of Department of Mechanical Engineering, for their cooperation during this master degree.

# TABLE OF CONTENTS

# LIST OF TABLES

# LIST OF FIGURES

# NOMENCLATURE

| | |
|---|---|
| S-$CO_2$ | Supercritical Carbon Dioxide |
| T-$CO_2$ | Transcritical Carbon Dioxide |
| Max | Maximum |
| Min | Minimum |
| COP | Coefficient of Performance |
| Gen | Generator |
| HEX | Heat Exchanger |
| CIT | Compressor inlet temperature, (°C) |
| TIT | Turbine inlet temperature, (°C) |
| HTR | High-temperature recuperator |
| LTR | Low-temperature recuperator |
| HPT | High-Pressure Turbine, (MPa) |
| LPT | Low-Pressure Turbine, (MPa) |
| LT | Low-temperature |
| HT | High-temperature |
| ORC | Organic Rankin Cycle |
| CDTPC | Carbon dioxide transcritical power cycle |
| CSP | Concentrated solar power |
| LGH | Low-grade heat |

# LIST OF SYMBOLS

| | |
|---|---|
| $\varepsilon$ | Heat exchanger effectiveness |
| T | Temperature ($^{o}$C) |
| P | Pressure (MPa) |
| Q | Heat Capacity (KW) |
| $\dot{m}$ | Mass flow rate (kg/s) |
| h | Enthalpy (kJ/kg) |
| s | Entropy (kJ/kg-K) |
| $P_c$ | Critical pressure (MPa) |
| $P_{max}$ | Maximum operating pressure (MPa) |
| $Q_{in}$ | Input heat to the cycle (kJ/kg) |
| $Q_{out}$ | Output heat from the cycle (kJ/kg) |
| $P_r$ | Cycle pressure ratio |
| $T_c$ | Critical temperature (°C) |
| $T_{max}$ | Maximum temperature of the cycle (°C) |
| $W_{net}$ | Net power generated (kJ/kg) |
| $C_p$ | Isobaric specific heat (kJ/kg K) |

# Chapter 1

# INTRODUCTION

## 1.1 Overview

Global demand for energy has risen inexorably in the last 150 years in step with industrial development and population growth. Hunger for energy is predicted to continue to rise; by at least 50% by 2030. This increase, in turn, has enabled the world economy to expand, raising living standards and helping to meet the aspirations of millions of people around the world.

At present, two-thirds of the world's electricity demand is meet by non- renewable fossil fuels, which has led to serious environmental problems and a widespread energy crisis. The world energy council share of global energy (about 80% at present) is supplied by coal, oil and gas - the 'fossil fuels' that formed long ago from the carbon-rich remains of dead plants and animals [1]. However, these are non-renewable sources that will one day be exhausted. In trying to limit the emissions from the electricity generating sector, new energy resources as well as radically new technologies should be developed and/or current technologies be improved so that the power output per unit of pollution is reduced. Pressure to replace fossil fuels has focused more attention on renewable sources - e.g. solar and wind. Renewable energy sources, such as solar thermal and geothermal, and vast amounts of industrial waste heat are potentially promising energy sources capable, in part, to meet the world electricity demand. However, the above-mentioned energy sources are available

largely at moderate temperatures. Due to all these reasons, utilizing low-grade waste heat for power generation has attracted more and more attention for its potential in reducing the fossil fuel consumption.

## 1.2 Motivation

Huge amount of low or mid-level waste heat are released daily from industrial processes to the atmosphere [2]. The reduction of the waste heat produced by industries is a crucial step toward the successful future utilization of low-grade waste heat. In achieving this goal most work and effort in the past has been done toward the simplification and cost reduction of primary cogeneration systems.

Thus, a power cycle with high efficiency that has small primary resource consumption is sought. There are thermodynamic cycles that can recover these low-grade waste heats such as Organic Rankine cycle (ORC) and $CO_2$ Transcritical power cycle (CDTPC). ORC and CDTPC can efficiently convert low-temperature waste heat into electricity

Compared to steam cycles, closed cycle gas turbines are in general simple, compact, and less expensive and have shorter construction periods, thus reducing the costs during construction. Due to their simplicity, they are well suited to modular construction techniques. Therefore, they are a primary topic of current advanced power cycle research.

For the reasons mentioned above, supercritical $CO_2$ Brayton cycle seems to have a great potential as a conventional thermodynamic power cycles in utilizing the energy in low-grade heat sources and waste heat.

## 1.3 Thesis Objectives

In this study, the objective is particularly to evaluate the performance of various S-$CO_2$ Brayton Cycle configurations in which the efficiency enhancement is sought. A complete thermodynamic analysis and efficiency evaluation of five different configurations will be performed. The main objective is to investigate the effect of some operating parameters such as; high pressure (HP) and low pressure (LP) turbine inlet temperature, gas cooler pressure, first compressor (pre-compressor) and second compressor (re-compressor) temperatures and pressures, heat exchanger (generator or recuperator) efficiencies on the performance of the cycle. Furthermore the cycle is thermodynamically optimized by using the EES software [3].

## 1.4 Structure of Thesis

The organization of thesis is as follow:

Chapter 1 presents a brief introduction on global energy demand and the significant role of low-grade heat sources and the methods to utilize low-grade heat source for power generation.

Chapter 2 provides a comprehensive review about different types of low-grade heat sources. Moreover, history of Brayton cycle has been reviewed. Couple of thermodynamic cycles for the conversion of low-grade heat have been presented in concise. The carbon dioxide as a working fluid is introduced and its properties are discussed.

Chapter 3 addresses the methods employed to model the S-$CO_2$ Brayton cycle. Discussion proceeds from investigation into multiple Brayton cycle configurations

using a simplified methodology. The assessment is based on the analysis performed using cycle models developed as part of this research to simulate the S-$CO_2$ cycle performance over a range of operating conditions.

Chapter 4 focuses on the results that obtained from the simulation for each configuration of S-$CO_2$ Brayton cycle. Some key parameters which are mentioned in former parts, has been investigated to find comparisons between the configurations. The chapter also provides an examination of how various design parameters affect performance of the S-$CO_2$ Brayton cycle. The cycles are also compared against carbon dioxide transcritical power cycle results from Y.M. Kim et al.[4] work simulating the transcritical and supercritical $CO_2$ cycle using both low and high-temperature heat sources.

Chapter 5 presents the conclusions and recommendations drawn from the study. The chapter also puts forth potential areas of future work.

# Chapter 2

# LITERATURE REVIEW

Renewable energy sources, such as solar thermal and geothermal, and vast amounts of industrial waste heat are potentially promising energy sources capable, in part, to meet the world electricity demand. However, low and the moderate temperature heat from these sources cannot be converted efficiently to electrical power by employing conventional power cycles, i.e., steam Rankine cycle or gas turbine using air as working fluid, and a large amount of low and moderate temperature heat is simply wasted.

In this context, developing other thermodynamic cycles to convert the low-grade heat into electrical power is of great significance. Organic Rankine cycle, supercritical Rankine cycle, Kalina cycle, Goswami cycle, trilateral flash cycle, S-$CO_2$ Brayton cycle and Transcritical $CO_2$ power cycle are the major cycles that have been developed for the conversion of low-grade heat into electricity.

## 2.1 Low-Grade Heat Source

In following subsections, various low-grade heat sources are presented in brief.

### 2.1.1 Solar Thermal

Every year, the sun irradiates the landmasses on earth with the equivalent of 19,000 billion tons of oil equivalent (toe). Only a fraction (9 billion toe) would satisfy the world's current energy requirements. Put differently, in 20 minutes, the amount of solar energy falling on the earth could power the planet for one year[5]. In order to be

more usable, however, the energy must be collected and converted to a suitable form. Solar thermal energy can be produced by using solar thermal collectors, solar ponds and etc.

Solar ponds are large-scale solar thermal energy collectors, which are pools filled with saltwater with a density gradient from the bottom to the top. A solar pond combines heat collection and storage. With a 20°C ambient temperature, the thermal energy obtained from the solar ponds is in the form of low-grade heat at 70 to 80°C. There are low-, medium- and high- temperature solar thermal collectors, depending on their collecting temperature [6].

### 2.1.2 Geothermal Energy

The Earth's temperature increases with the depth from the ground. It was reported that the geothermal gradient is 25-30 ºC per km of depth in most of the world, not including the tectonic plate boundaries adjacent area. Geothermal reservoirs can reach temperature up to 370 ºC, and they are powerful sources of energy.

A typical geothermal extraction process would be injecting a cold fluid deep into the ground, and pumping it back when it is heated by the underground heat. Geothermal is cost effective, sustainable, and reliable. Although geothermal wells release greenhouse gases trapped deep within the earth, these emissions are much lower per energy unit than burning fossil fuels. Therefore, geothermal is environmental more friendly.

### 2.1.3 Industrial Waste Heat

Statistical investigations indicate that the energy lost in industrial waste heat is huge. Nearly a third of the world's energy consumption and 36% of carbon dioxide ($CO_2$) emissions are attributable to manufacturing industries[7]. About 50% of all fuel

burned by industrial sources becomes waste heat, mostly low-grade. Approximately two-thirds of these amounts are contributed by the basic materials industries, i.e. chemical, petrochemicals, iron and steel, cement, paper and pulp, and other minerals and metals. Altogether, industry's use of energy has grown by 61% between 1971 and 2004, albeit with rapidly growing energy demand in developing countries and stagnating energy demand in developed countries.[8]

The thermal conditions of the industrial waste heat are industry dependent. In glass and metals industry, the waste heat can be at the temperature level of 300 400 ºC; in Petro Chemicals & and refining industry, it can be at the level of 150 ºC; in food & beverage industry, the level can be 80 ºC. The Fig. 2.1 shows the world's industrial energy consumption by fuel for 2011, 2025, and 2040.

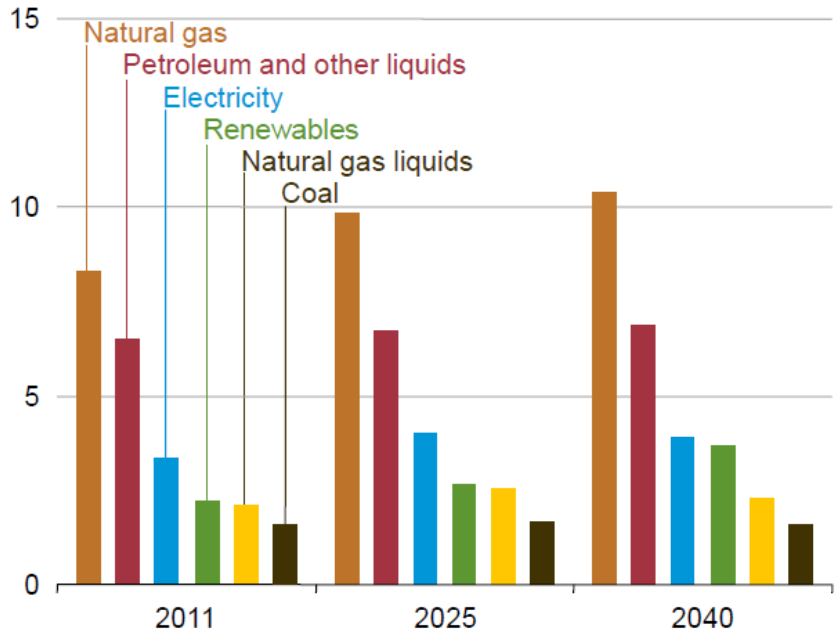


Figure 2.1 Industrial energy consumption by fuel, 2011, 2025, and 2040 (quadrillion Btu) [9]

Much of the growth in industrial energy consumption in the annual energy outlook 2013 Reference case is accounted for by natural gas use, which increases by 18 percent from 2011 and 2025 and by 6 percent from 2025 to 2040[9].

Although abundantly exists, a large amount of the low-grade heat has not been efficiently utilized, and discarding it has become an environmental concern which lead to thermal pollutions.

## 2.2 History of Brayton Cycle

The basic gas turbine cycle is named for the Boston engineer, George Brayton, who first proposed the Brayton cycle around 1870 [10]. The Brayton cycle is used for gas turbines only where both the compression and expansion processes take place in rotating machinery [11]. John Barber patented the basic gas turbine in 1791 [12]. The two major application areas of gas-turbine engines are aircraft propulsion and electric power generation. Gas turbines are used as stationary power plants to generate electricity as stand-alone units or in conjunction with steam power plants as a combined power plant.

The Brayton cycle depicts the air-standard model of a gas turbine power cycle. A simple gas turbine is comprised of three main components: a compressor, a combustor, and a turbine. According to the principle of the Brayton cycle, air is compressed in the compressor. The air is then mixed with fuel, and burned under constant pressure conditions in the combustor or heated by a waste heat flow. The resulting high pressure and temperature gas is allowed to expand through a turbine to perform work. Most of the work produced in the turbine is used to run the compressor and the rest is available to run auxiliary equipment and produce power. The gas turbine is used in a wide range

of applications. Common uses include stationary power generation plants (electric utilities) and mobile power generation engines (ships and aircraft). In power plant applications, the power output of the turbine is used to provide shaft power to drive a generator. A jet engine powered aircraft is propelled by the reaction thrust of the exiting gas stream. The turbine provides just enough power to drive the compressor and produce the auxiliary power. The gas stream acquires more energy in the cycle than is needed to drive the compressor. The remaining available energy is used to propel the aircraft forward.

## 2.3 Thermodynamic Cycles for the Conversion of Low-Grade Heat

Various thermodynamic cycles have been developed for the conversion of low-grade heat into electricity, among which the major ones are: Kaline Cycle, Goswami cycle, Trilateral Flash cycle, organic Rankine cycle, and supercritical Rankine cycle. The cycles are briefly discussed in the following subsections.

### 2.3.1 Kalina Cycle

The Kalina cycle was first developed by Aleksandr Kalina in the late 1970s and early 1980s [13]. Since then, several Kalina cycles have been proposed based on different applications. The Kalina cycle uses a mixture as the working fluid, instead of a pure fluid like water, the mixture being composed of at least two different components, typically water and ammonia. The ratio between those components varies in different parts of the system to decrease thermodynamic irreversibility and therefore increase the overall thermodynamic efficiency. A basic configuration of the Kalina cycle is shown in Fig 2.2.

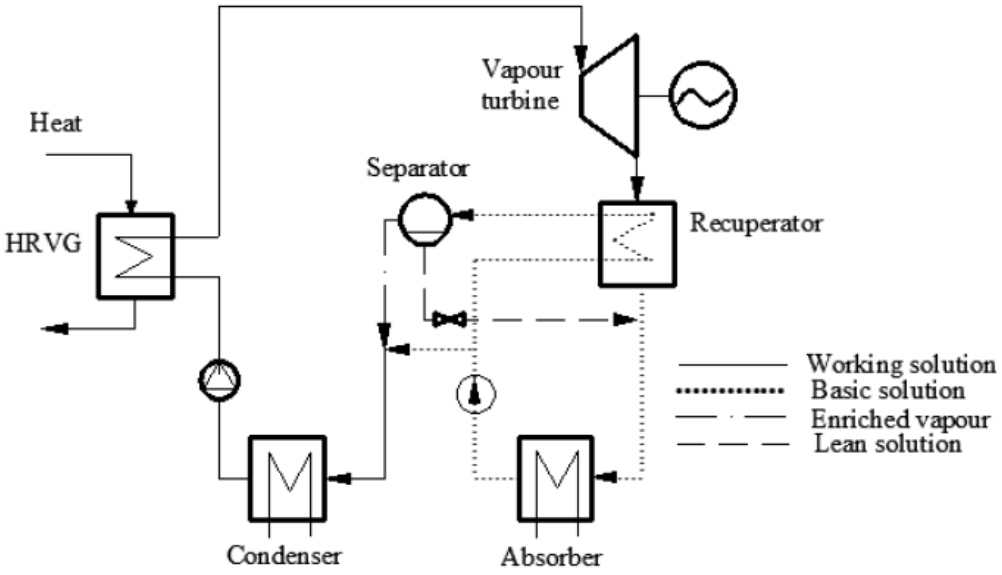


Figure 2.2 Flow Scheme of The Basic Kalina Cycle [14]

In the Kalina cycle, the use of a mixture results in a good thermal match in the boiler due to the non-isothermal boiling created by the shifting mixture composition. Several studies have shown that the Kalina cycle performs substantially better than a steam Rankine cycle system [15-17]. A second law analysis showed that by using a binary fluid, irreversibility is reduced in the boiler, resulting in improved efficiency of the cycle [18].

One drawback of the Kalina cycle is the fact that high vapor fraction is needed in the boiler; however, the heat exchanger surface is easy to dry out at high vapor fractions, resulting in lower overall heat transfer coefficients and a larger heat exchange area. Another drawback relates to the corrosivity of ammonia. Impurities in liquid ammonia such as air or carbon dioxide can cause stress corrosion cracking of mild steel and also ammonia is highly corrosive towards copper and zinc.

### 2.3.2 Goswami Power and Cooling Cogeneration Cycle

Goswami cycle, proposed by Dr. Yogi Goswami (1998) is a novel thermodynamic cycle that uses binary mixture to produce power and refrigeration simultaneously in

one loop [19].This cycle is a combination of Rankine power cycle and an absorption cooling cycle. Its advantages include the production of power and cooling in the same cycle, the design flexibility to produce any combination of power and refrigeration, the efficient conversion of moderate temperature heat sources, and the possibility of improved resource utilization compared to separate power and cooling systems [20]. The binary mixture first used was ammonia-water, and later on new binary fluids were proposed and studied. A configuration of the cycle is shown in Fig. 2.3.

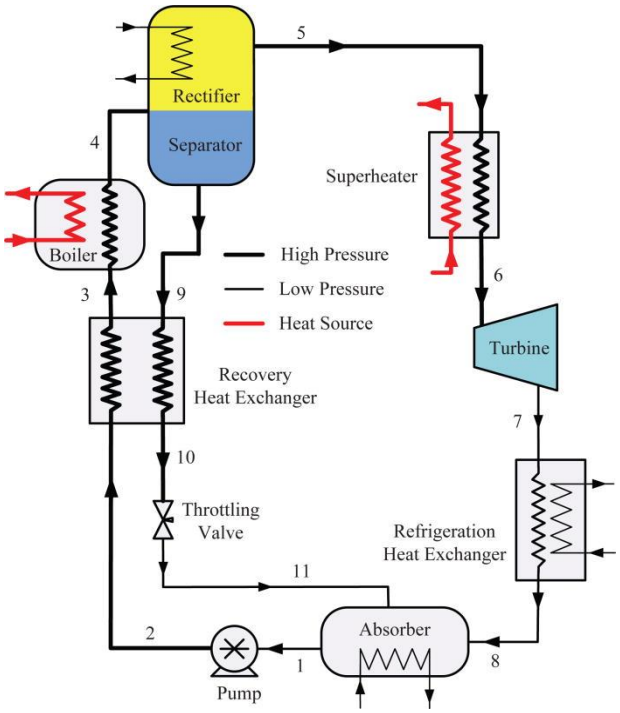


Figure 2.3 The Basic Configuration of the Combined Power and Cooling Cycle[22]

A stream of the mixture is pumped to a high pressure, and then preheated and pumped to the boiler, where is it partially boiled. A rectifier is used to purify the vapor by condensing the water, if needed. Then the rectified vapor is superheated before expanding to a low temperature in an expander such as a turbine. Since the working fluid is condensed by absorption, it can be expanded to a temperature lower than the ambient, which provides a refrigeration output in addition to the power output. The

remaining hot weak solution from the boiler is used to preheat the working fluid, and then throttled back to the absorber.

### 2.3.3 Trilateral Flash Cycle

The Trilateral Flash Cycle (TFC) is a thermodynamic power cycle whose expansion starts from the saturated liquid rather than a vapor phase. By avoiding the boiling part, the heat transfer from a heat source to a liquid working fluid is achieved with almost perfect temperature matching. Irreversibilities are thereby minimized. According to Ng, K. C. et. al. [21], its potential power recovery could be 14 - 85% more than from ORC or flash steam systems provided that the two-phase expansion process is efficient. Figure 2.4 is the configuration of a trilateral flash cycle.

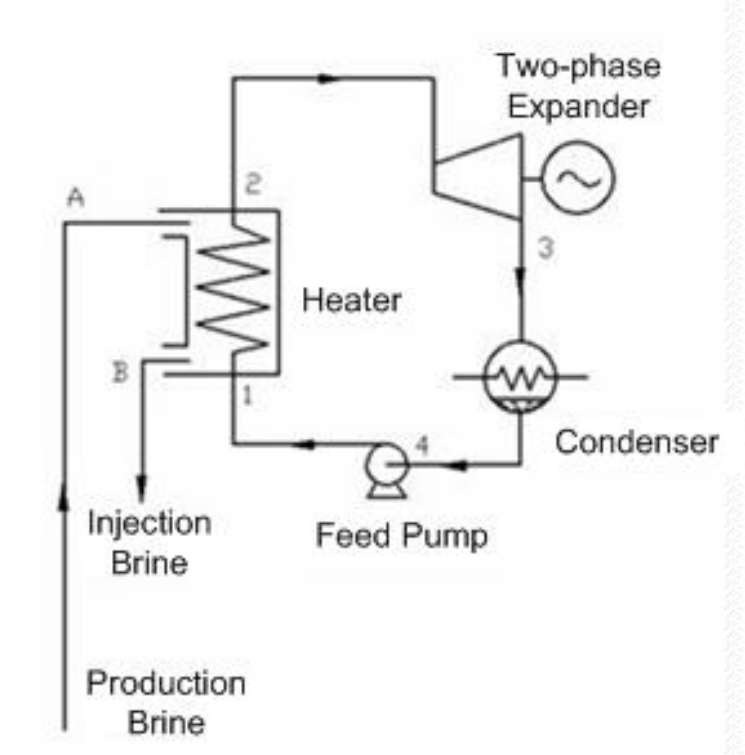


Figure 2.4 The Configuration of a Trilateral Flash Cycle [22]

### 2.3.4 Organic Rankine Cycles (ORCs)

The ORC applies the principle of the steam Rankine cycle, but uses organic working fluids with low boiling points, instead of steam, to recover heat from a lower temperature heat source. Figure 2.5 shows a schematic of an ORC and its process plotted in a T-s diagram in Fig. 2.6. The cycle consists of an expansion turbine, a condenser, a pump, a boiler, and a superheater (provided if superheat is needed).

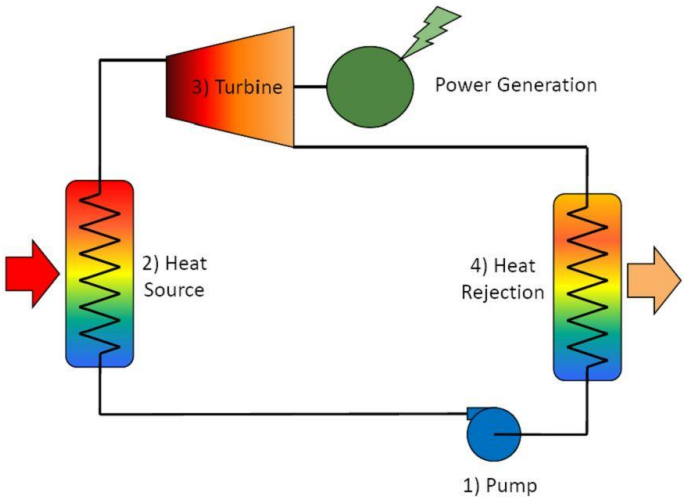


Figure 2.5 A Schematic of an Organic Rankine Cycle [22]

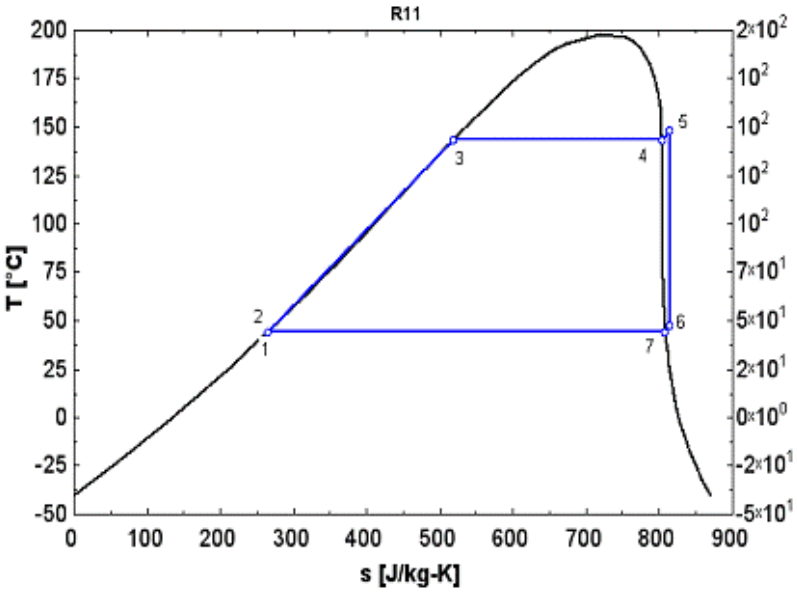


Figure 2. 6 The T-S Diagram Process of an Organic Rankine Using R11 as the Working Fluid [23]

The working fluid of an ORC is very important. Pure working fluids such as HCFC123 ($CHCl_2CF_3$), PF5050 ($CF_3(CF_2)_3CF_3$), HFC-245fa ($CH_3CH_2CHF_2$), HFC-245ca ($CF_3CHFCH_2F$), isobutene ($(CH_3)_2C=CH_2$), n-pentane and aromatic hydrocarbons, have been studied for organic Rankine cycles. Fluid mixtures were also proposed for organic Rankine cycles [24-28]. The organic working fluids have many different characteristics than water [29]. The slope of the saturation curve of a working fluid in a T-S diagram can be positive (e.g. isopentane), negative (e.g. R22) or vertical (e.g. R11), and the fluids are accordingly called wet, dry or isentropic, respectively. Wet fluids, like water, usually need to be superheated, while many organic fluids, which may be dry or isentropic, do not need superheating. Another advantage of organic working fluids is that the turbine built for ORCs typically requires only a single-stage expander, resulting in a simpler, more economical system in terms of capital costs and maintenance [30].

### 2.3.5 Supercritical Rankine Cycle

Working fluids with relatively low critical temperature and pressure can be compressed directly to their supercritical pressures and heated to their supercritical state before expansion to obtain a better thermal match with the heat source. Figures 2.7 and 2.8 show the configuration and process of a $CO_2$ supercritical Rankine cycle in a T-s diagram, respectively.

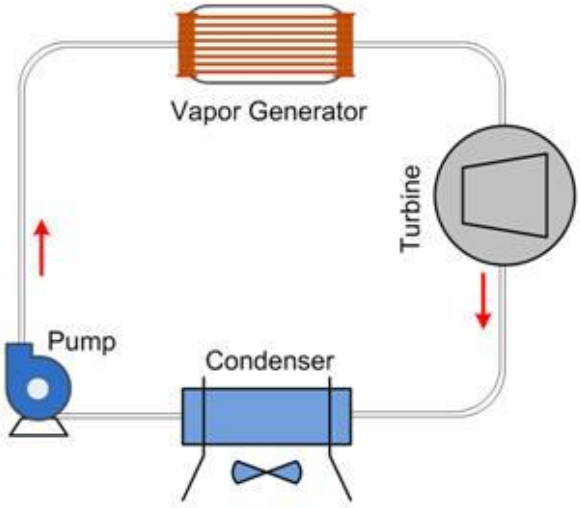


Figure 2.7 The Configuration of a Supercritical Rankine Cycle [31]

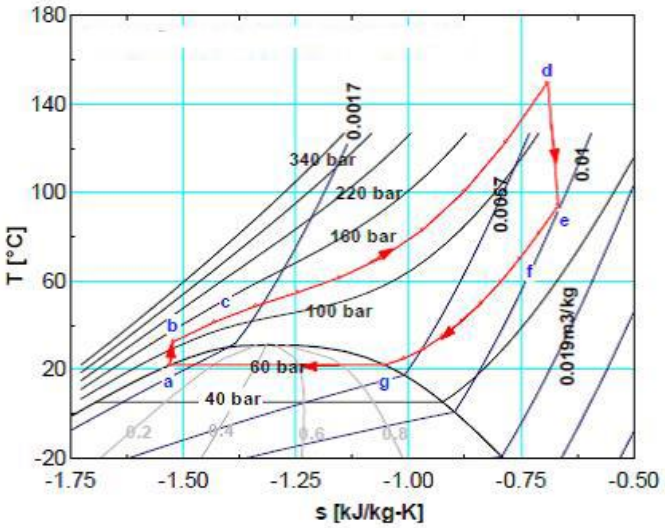


Figure 2.8 The Process of a Supercritical Rankine Cycle Using $CO_2$ as the Working Fluid [32]

The heating process of a supercritical Rankine cycle does not pass through a distinct two-phase region like a conventional Rankine or organic Rankine cycle thus getting a better thermal match in the boiler with less irreversibility.

Chen et al. [33-35] did a comparative study of the carbon dioxide supercritical power cycle and compared it with an organic Rankine cycle using R123 as the working fluid in a waste heat recovery application. It is shown that a $CO_2$ supercritical power

cycle has higher system efficiency than an ORC when taking into account the behavior of the heat transfer between the heat source and the working fluid. The $CO_2$ cycle shows no pinch limitation in the heat exchanger. Zhang et al. [36-38] have also conducted research on the supercritical $CO_2$ power cycle. Experiments revealed that the $CO_2$ can be heated up to 187℃ and the power generation efficiency was 8.78% to 9.45% [39], and the COP for the overall outputs from the cycle was 0.548 and 0.406, respectively, on a typical summer and winter day in Japan [38].

There is no supercritical Rankine cycle in operation up to now. However, it is becoming a new direction due to its advantages in thermal efficiency and simplicity in configuration.

## 2.4 Working Fluid

A key advantage of the $CO_2$ Brayton Cycle is the employment of supercritical $CO_2$ as a working fluid for heat recovery and power generation. A supercritical fluid is a substance at a temperature and pressure above its critical temperature and pressure. The critical point represents the highest temperature and pressure at which the substance can exist as a vapor and liquid in equilibrium. As shown in Fig 2.9, above its critical point of 30.98°C at 7.38 MPa (304.25 K at 73.78 bar), carbon dioxide is a supercritical fluid and adopts properties midway between a gas and a liquid [40].

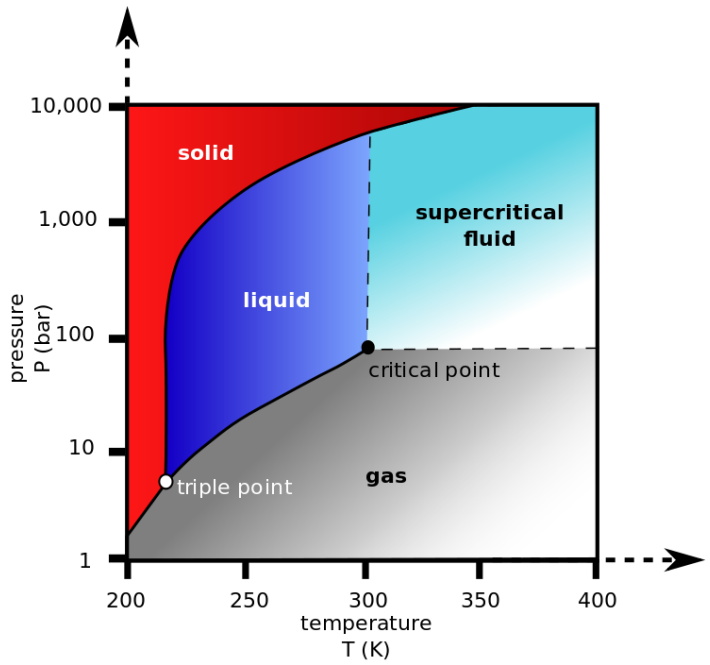

Figure 2. 9 Carbon Dioxide Pressure-Temperature Phase Diagram [41]

Supercritical $CO_2$ viscosity is similar to that of gas but far less than liquid viscosity. Its diffusion coefficient is close to that of gas and far greater than the coefficient of liquid, so it has good flowability and transmission characteristics.

Other benefits of Carbon dioxide are:

- S-$CO_2$ cycles achieve high efficiency at low temperatures
- High operating pressure allows small size components
- More than twenty years experiences of $CO_2$ application in nuclear reactors
- Well known thermodynamic properties
- Stability
- Non-toxicity
- Abundance
- Low molecular leak due to higher molecular mass
- Low cost

## 2.5 Supercritical $CO_2$ Cycle- Characteristics and Variations

In the temperature, range of interest $CO_2$ is not an ideal gas. This is caused by the fact that the critical point of $CO_2$. The behavior of a gas near its critical point is very sensitive to pressure and temperature. Fluid properties are significantly affected. Therefore, unlike for an ideal gas, cycle operating conditions have a strong effect on cycle performance. This results in a net cycle efficiency increase. The cycle efficiency is defined as:

$$\eta_{Cycle} = \frac{W_T - W_C}{q_{in}} \quad \textbf{(3-1)}$$

Where $\eta_{Cycle}$ is the cycle efficiency, $w_T$ is the turbine work, $w_C$ is the compressor work and $q_{in}$ is the heat input.

The cycle, in its simplest practical form, is represented in the schematic equipment and temperature-entropy diagram shown in Figures 2.10 and 2.11, respectively.

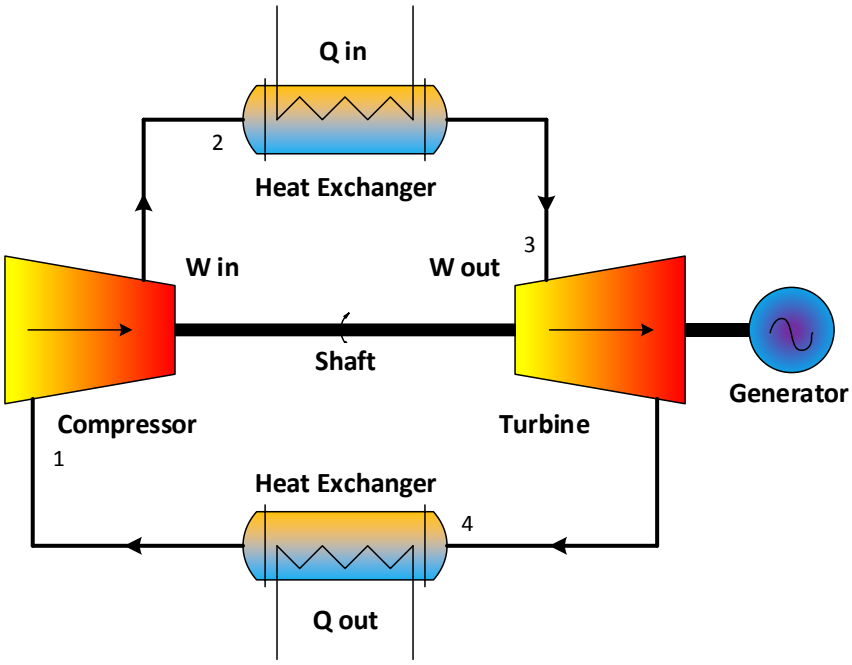


Figure 2.10 Simple Brayton cycle layout

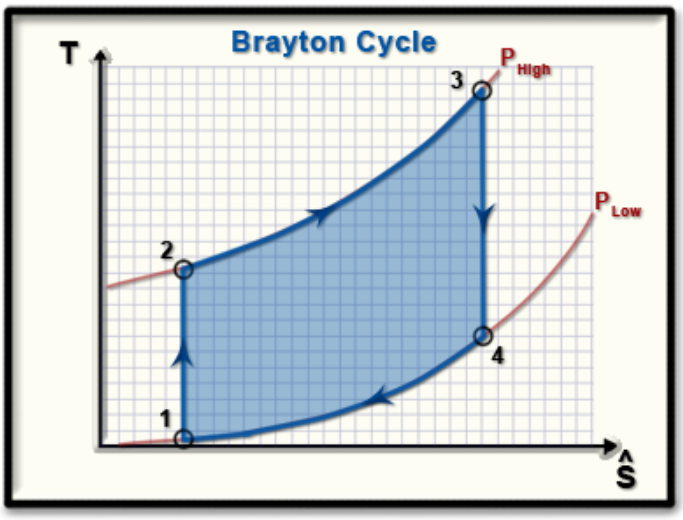

Figure 2.11 Temperature-Entropy Diagram of Simple Brayton [23]

The Low-pressure carbon dioxide enters into a compressor (1) where it is compressed to a higher pressure (2). After compression state, the $CO_2$ receives certain amount of heat to reach the maximum temperature of the cycle. The outcome hot gases go through the turbine (3) and expand to state (4) which is cooling the exhausted gas to be prepared for compression stage again.

The ideal simple Brayton cycle is comprised of four main processes:

- 1-2 Isentropic compression (in a compressor)
- 2-3 Constant pressure heat addition
- 3-4 Isentropic expansion (in a turbine)
- 4-1 Constant pressure heat rejection

With supercritical $CO_2$ as a working fluid, the efficiency enhancement, which is main mechanism, can be obtained by carrying out the compression process near to the critical point in order to reduce the compressor work. To understand the effect, first consider turbine work. Figure 2.12 shows the turbine work for different turbine inlet

pressures and turbine pressure ratios for turbine efficiency of 90 % and turbine inlet temperature of 550 °C.

Apparently, from Fig. 2.12 the turbine work is almost independent of operating pressure. For an ideal gas, as pressure ratio increases as a result a bare rise in turbine work is expected but the increment becomes small and smaller. Since the turbine work of $CO_2$ follows this behavior, one can see that in the turbine the fluid behaves almost as an ideal gas. Only at very high-pressure ratios is the deviation from this behavior is noticeable. However, these ultra-high-pressure ratios are not relevant since the cycle would not be operated in this region because of efficiency and material considerations.

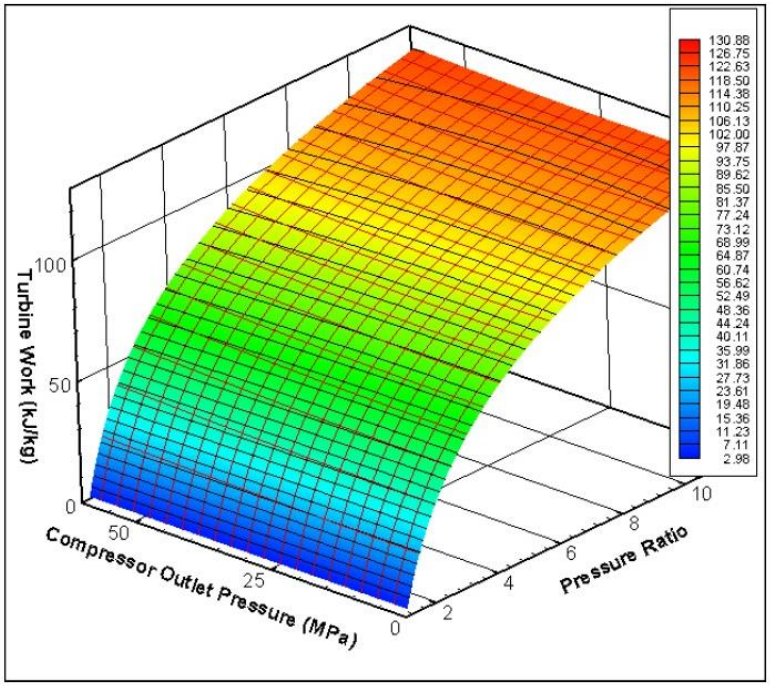


Figure 2.12 $CO_2$ Turbine Work [42]

Since the compressor operates close to the critical point one would expect to see significant deviations from ideal gas behavior in compressor work. A figure similar to Fig. 2.13 showing the compressor work for different pressure ratios and different

compressor outlet pressures was developed using compressor efficiency of 89% and compressor inlet temperature of 32°C.

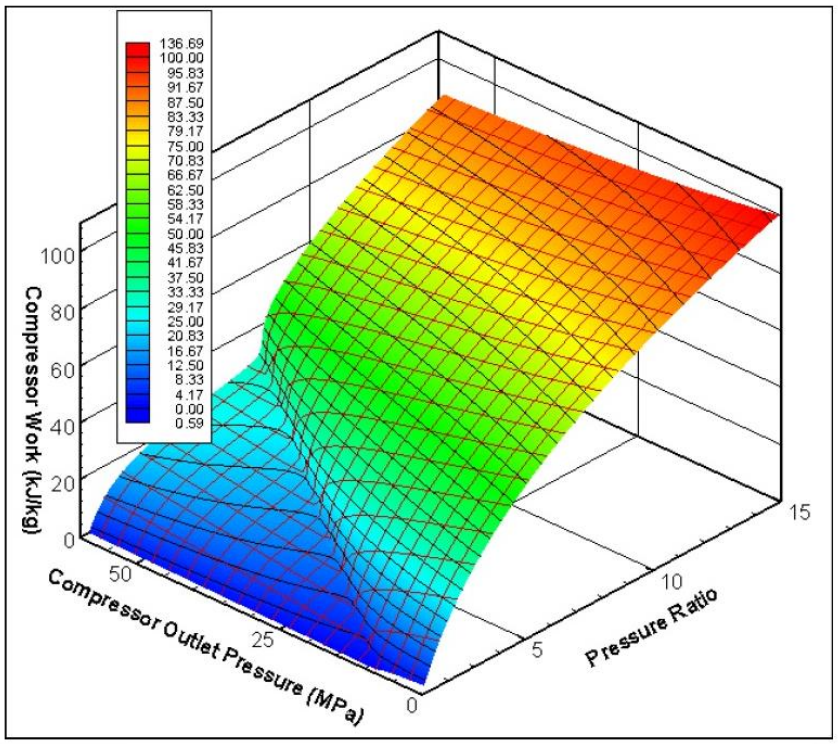


Figure 2. 13 $CO_2$ Compressor Work [42]

Figure 2.13 shows that the compressor work changes significantly as a function of operating pressure and pressure ratio; both parameters are linked to the deviation from ideal gas behavior. For a compressor operating with ideal gas one would see the same profile as was observed for the turbine. However, the proximity of the critical point significantly affects the compressor work. Once the inlet pressure exceeds the critical pressure (7.38 MPa), the compressor work is significantly reduced. One can also observe the less steep rise of compressor work with the pressure ratio than in the case of the turbine. Therefore, the cycle optimum pressure ratio will have lower values, since at those values, the compressor work is low and the turbine output is high. The reduction of the compressor work comes from the low compressibility of $CO_2$ near the

critical point. The density change for different pressures is not very high and thus the compression work is reduced. This is the main reason why supercritical $CO_2$ cycles achieve an advantage over the ideal gas Brayton cycle, where the gas exhibits the same trends in both turbine and compressor.

Unfortunately, the reduction of the compressor work is only one of the effects caused by the non-ideal properties. The specific heat, which affects recuperator design in particular, also varies widely. It is known that for certain cycle operating conditions a pinch-point exists in the recuperator [43]. Due to the radical temperature and pressure dependence of specific heat, the temperature difference between the hot and the cold fluid varies widely within the recuperator. Thus, even for the single-phase state of the $CO_2$ working fluid the minimum value of the temperature difference is not always achieved at the recuperator inlet or outlet, but sometimes somewhere along the recuperator. An overly simple analysis of the cycle based only on identifying component end state points would not reveal this behavior. Therefore, it is necessary to evaluate the local temperature difference throughout the recuperator, and the minimum temperature difference encountered is an important parameter in cycle evaluation. In the case of $CO_2$ the operating pressure is important as it affects the temperature difference in the recuperator and the resulting regenerated heat, which affects the cycle efficiency and the size of the recuperator. For these reasons, it is necessary to investigate the behavior of the cycle over a wide range of possible operating pressures in order to find the optimum for cycle design [42].

The supercritical $CO_2$ Brayton cycle is of interest both to the solar energy and nuclear energy communities. One characteristic that is driving interest in the $S-CO_2$ cycle is that the working fluid operates at or near its critical point (at 30.98 °C and

7.38 MPa) where it has extremely high density. The density of carbon dioxide as a function of temperature for a range of pressures at and above the critical point is shown below in Fig. 2.14.

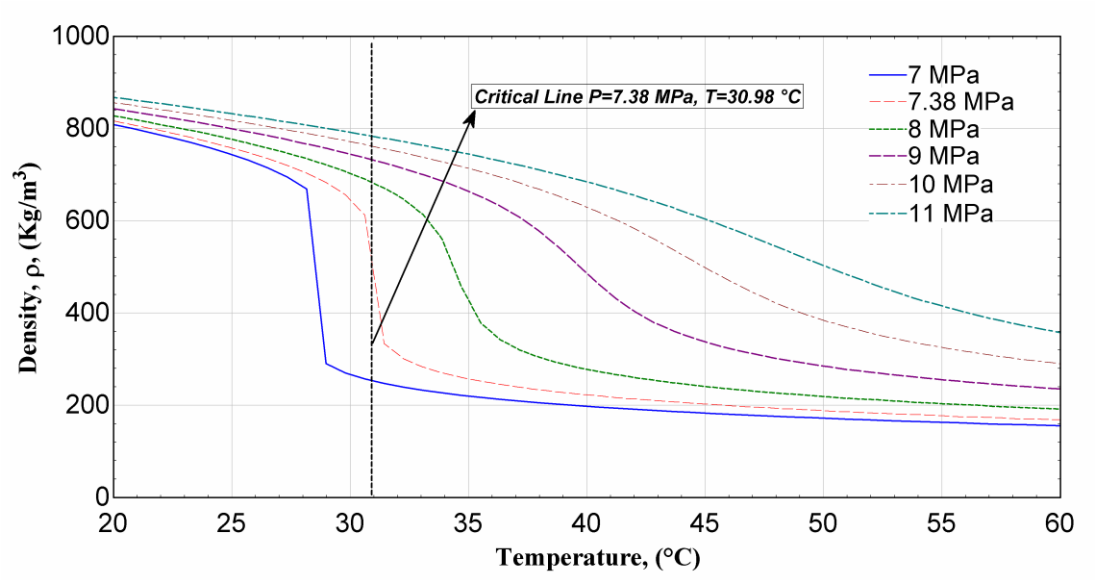


Figure 2.14 $CO_2$ Density near Critical Point

As can be seen in Fig. 2.14, $CO_2$ density changes quickly near the critical point. High fluid density offers the potential to reduce both compressor power and size; thereby, leading to greater efficiency than an ideal-gas Brayton cycle and greater power density when compared to a superheated Rankine cycle [44]. These characteristics allow for smaller and less expensive equipment. In the case of isobaric specific heat capacity, property changes are more severe near the critical point, as seen in Fig. 2.15.

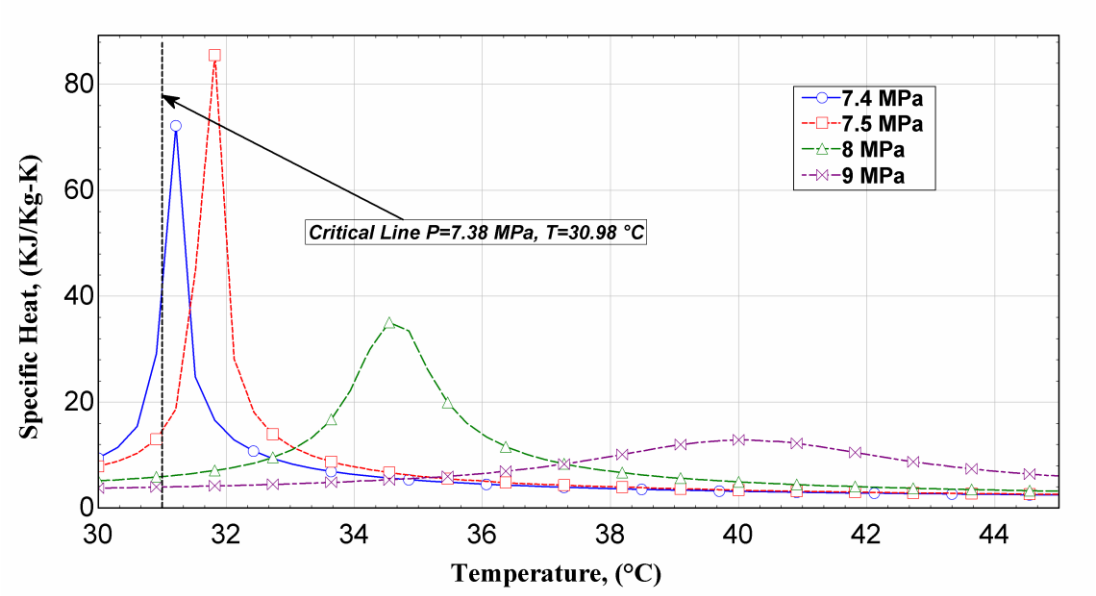


Figure 2. 15 $CO_2$ Isobaric Specific Heat Capacity

The S-$CO_2$ Brayton cycle is also seen as attractive due to its heat rejection characteristics. Since the Brayton cycle rejects heat across a range of relatively high temperatures, unlike the Rankine cycle, there is potential for novel heat rejection strategies, including dry and hybrid cooling.

## 2.6 History of the Supercritical $CO_2$ Cycle

In some thermodynamic texts this kind of cycle would be called transcritical or hypercritical. The reason for this is to distinguish this type of cycle from the supercritical Rankine steam cycle, where the working fluid is compressed to pressures above the critical pressure and expands to subcritical pressure, e.g. only the high-pressure part of the cycle operates above the critical pressure. The first $CO_2$ cycle design in the USA was proposed by E. G. Feher [43]. In the case of the Feher cycle all pressures are supercritical, however he does not call the cycle trans - or hyper-critical, but supercritical. For these historical reasons, it was decided for the purpose of this work to adopt the Feher nomenclature and call the cycle supercritical without regard

to whether it operates entirely or partly above the critical pressure since in our case both situations may occur.

The S-$CO_2$ Brayton cycle has a very long history. The oldest reference found is from 1948, when Sulzer Bros patented a partial condensation $CO_2$ Brayton cycle [42]. The advantage of $CO_2$ fluid was quickly realized and investigation of supercritical $CO_2$ cycles was carried on in many countries: by Gokhstein and Verhivker in the Soviet Union [45], [46] and Angelino in Italy [47] are the most famous and important among many others.

## 2.7 Improving Supercritical $CO_2$ Cycle

In 1997 an investigation of the supercritical $CO_2$ cycle for possible use in new power plants was conducted at the Czech Technical University in Prague, Czech Republic [48]. The study focused on the Brayton and recompression supercritical $CO_2$ cycles. The effect of re-heating on the recompression cycle was investigated as well. The re-compression cycle with re-heating achieved the best cycle efficiency.

Another institute that is currently investigating the supercritical $CO_2$ cycle is the Tokyo Institute of Technology in Japan [49]. The work here at first focused on partial condensation cycles, but given the difficulties with the supply of the cold cooling water the current reference design is a partial cooling cycle. A thermal efficiency of 50% at 12 MPa was achieved with the partial cooling cycle operating at a reactor outlet temperature of 800°C.

In the USA, the investigation of the recompression supercritical $CO_2$ cycle was resumed in the year 2000 at MIT under collaboration with Idaho National Engineering

and Environmental Laboratory (INEEL). An indirect supercritical $CO_2$ recompression cycle was designed for a lead-bismuth eutectic (LBE) cooled reactor [50]. A net efficiency of 41% was calculated for a compressor outlet pressure of 20 MPa and LBE reactor outlet temperature of 555°C. Currently, both direct and indirect versions for fast gas cooled reactors are being pursued.

In a recent paper in 2013 which is conducted by Turchi [51], the possibility of high-performance, air-cooled S-$CO_2$ cycle configurations that can be applied for an advanced concentrated solar power (CSP) plant has been explored. They found distinct S-$CO_2$ Brayton cycle configurations that have capability to achieve greater than 50% efficiency by ability to accommodate dry cooling from the viewpoint of CSP purpose. Observations revealed that with cycle configuration include the partial cooling cycles and recompression with reheat, reaching 50% efficiency goal is feasible even when it is combined with dry cooling. In addition, the intercooled cycles distend the temperature disparity across the primary heat exchanger, which is suitable for CSP systems.

In 2013, Besarati and Yogi Goswami [52] considered three different configurations of S-$CO_2$ Brayton cycle, i.e., simple, recompression, and partial cooling are as the top cycles which provided heat for an organic Rankine bottoming cycle. They simulated the three configurations then compared their results with the available data from the literature. As a result, they realized that adding an efficient bottoming cycle can raise the overall cycle efficiency by 3-7 percent under the determinate conditions. It was also clear that the maximum efficiency is achievable by using a simple S-$CO_2$ as the top cycle. This study indicates that the maximum combined cycle efficiency is obtained by the recompression combined S-$CO_2$-ORC cycle. In addition, different

working fluids are examined for the ORC for each configuration and the operating conditions are optimized. The results revealed that that among the working fluids considered for the ORC, butene and cis-butene are found to be the most appropriate for that application.

## 2.8 History of the Transcritical $CO_2$ Power Cycle

The research on $CO_2$ power cycles is however limited. Besides the research on $CO_2$ Brayton cycles for power production with nuclear reactors as heat sources (which work with high temperature (600 °C) and pressure [42, 43]), there is very little information available for power cycle research with $CO_2$ as working fluid in the low-grade energy source utilization area.

Angelino [43] conducted one of the most detailed investigations on transcritical $CO_2$ (T-$CO_2$) cycles and primarily focused on condensation cycles. It is found that at turbine inlet temperatures higher than 650 °C single heating $CO_2$ cycles exhibit a better efficiency than reheat steam cycles.

Emmanuel Cayer et al. [53] argued that for limited capacity heat sources as is the case with thermal wastes, a more detailed study is necessary. The study began with a methodology involving the first and second law of thermodynamics, a modified Logarithmic Mean Temperature Difference (LMTD) method and heat transfer correlations has been applied to analyze the performance of a $CO_2$ transcritical cycle using low enthalpy waste heat as its energy source. The transcritical cycle was chosen because it shows a good potential of converting heat from a sensible heat source into electricity owing to its variable temperature phase change in the vapor generator.

The most interesting approach to this issue has been proposed by Yang Chen et al. [54]. The study showed that the matching of the temperature profiles in the system heat exchangers has crucial influences on their exergy destructions and entropy generations. It is also an essential factor that influences the system thermodynamic efficiencies. They have also found that the exergy destruction and the entropy generation are increasing in all the system components, although the increasing trend is more obvious in the gas cooler & condenser than in other components.

Recently, several authors [4] have proposed Transcritical $CO_2$ Rankine cycles or fully-cooled S-$CO_2$ cycles using both the low and high temperature heat sources can maximize the power output of the $CO_2$ power cycle with the given high-temperature heat sources. Moreover, the proposed $CO_2$ cycles combined with the low-temperature thermal energy storage offer the advantage of load leveling over other $CO_2$ cycles, with the given high temperature heat sources. The results showed that of the T-$CO_2$ Brayton cycle with an high temperature (HT) heat source, the proposed low temperature (LH) T-CO2 cycle can produce approximately 25% more power by reducing the compression work and enhancing the cycle efficiency by approximately 10% at 600 °C with the same heat input from the HT heat source by utilizing an LT heat source. The exergy efficiency of the LH T-CO2 cycle using both the LT and the HT heat sources is approximately 10% higher than that of the T-CO2 Brayton cycle with an HT heat source.

# Chapter 3

# SUPERCRITICAL $CO_2$ BRAYTON CYCLE APPLICATIONS AND PERFORMANCE SIMULATIONS

## 3.1 Basic Cycles and the Parameters That Influence the Cycle Performances

As mentioned in the previous chapter, there are two cycles, namely carbon dioxide Transcritical power cycle and carbon dioxide Brayton cycle, which have been proposed in the current study for utilizing the energy in low-grade heat sources and waste heat.

Thermodynamically, the larger the temperature difference between the cycle's heat absorbing temperature and its heat rejecting temperature, the higher the cycle efficiency. From this viewpoint, for the same heat absorbing temperature, the $CO_2$ transcritical power cycle will achieve a higher efficiency than the $CO_2$ Brayton cycle if a low temperature heat sink is available. To achieve a satisfactory efficiency from a carbon dioxide Brayton cycle, a significantly higher heat source temperature is needed. The current study mainly focuses on the systems that work with carbon dioxide supercritical Brayton cycles in low-grade heat source utilization. However, the carbon dioxide transcritical Brayton cycle has also been analyzed for its potential in waste heat utilization.

Several definitions are needed to analyze the performance of the proposed carbon dioxide systems in low-grade heat source:

The cycle thermal efficiency ($\eta_{th}$) is:

$$\eta_{th} = \frac{W_{net}}{Q_{in}} = \frac{W_{exp.} - W_{comp.}}{Q_{in}} \quad \textbf{(3-1)}$$

Where Q in is the heat input to the system and $w_{net}$ is the power production by the system.

The Coefficient of Performance (COP) of the carbon dioxide refrigeration cycle and the COP of the cooling part of the carbon dioxide cooling and power combined cycle can be defined as Equation 3-2:

$$COP = \frac{Q_{cooling}}{W_{basic}} \quad \textbf{(3-2)}$$

Where $Q_{cooling}$ is the cooling capacity of the cooling system and $w_{basic}$ is the required compression work of the compressor.

One of the original motivations of the current study was to reduce the energy usage of refrigeration / air conditioning systems by utilizing the energy in low-grade heat source or waste heat by carbon dioxide power systems. The produced power will be then used to partly, or totally, to cover the compressor power demand in a refrigeration system or in the cooling part of the carbon dioxide combined system. In such applications, the COP of the cooling system can be redefined as equation 3-3, since the power produced by the $CO_2$ power system or the power part of the combined system is gained "free of charge" from the low-grade heat source or waste heat.

$$COP_{new} = \frac{Q_{cooling}}{W_{basic} - W_{output}} = \frac{Q_{cooling}}{W_{new}} \quad \textbf{(3-3)}$$

Where $Q_{cooling}$,is the required cooling capacity, $w_{basic}$ is the original compression work of the cooling cycle, and $w_{output}$ is the work output from the $CO_2$power system or the power part of the combined system, i.e. the "free" energy gained from the low-grade heat source or waste heat. At the end $w_{new}$ is the work needed by the compressor after taking away the energy gained from low-grade heat source or waste heat.

Although the applications will determine the possible temperature levels and the capacity as well as the obtainable efficiencies for the various components, several assumptions are made in this chapter based on the published literatures to be able to specify the cycle working conditions and gain a general picture of basic cycle performance.

## 3.2 Supercritical $CO_2$ Brayton Cycle Configurations

Five different S-$CO_2$ Brayton cycle are studied in the present work. These configurations are briefly discussed in the following sub-sections.

### 3.2.1 Simple Carbon dioxide power cycle

The simple cycle is the one from which the other two configurations are derived, which is shown in Fig. 3.1. High temperature S-$CO_2$ enters the turbine where it is expanded to the low pressure of the cycle. Then, it is cooled by rejecting heat to the cold sink and pressurized by the compressor, respectively. The pressurized S-$CO_2$ gains energy in the heater or combustor and enter to turbine again. The cycle efficiency can be increased by dividing the compression into two stages and using an intercooler in between. Similarly, using a two-stage expansion and a reheater can be beneficial.

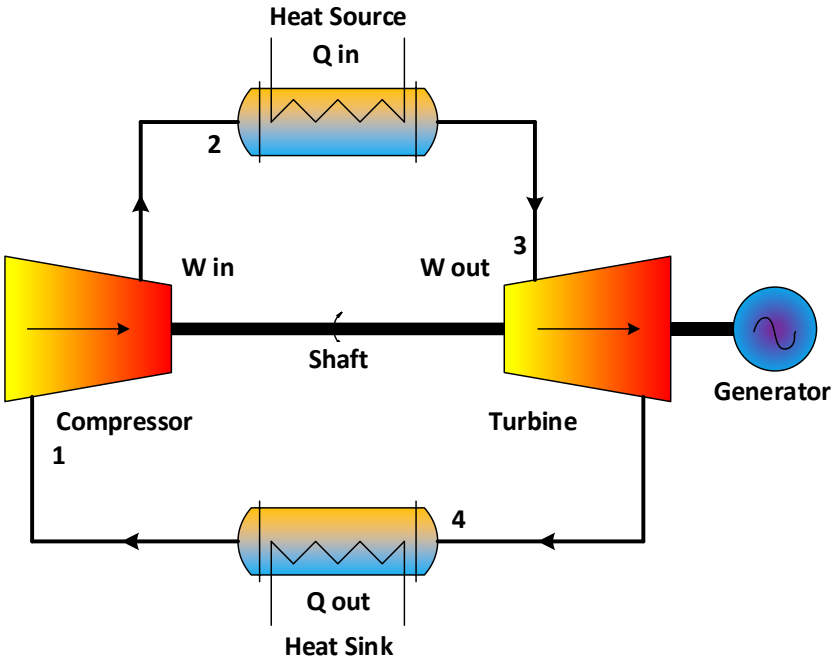

Figure 3.1 Simple Bryton Cycle Layout

The thermal efficiencies of all the proposed five cycles are obtained by simulation for different temperatures and pressures based on the First Law of Thermodynamics. The following general assumptions are made for the thermodynamic analysis of the carbon dioxide power cycles:

- The maximum temperature and pressure of a cycle were fixed at 550 ºC and 25 MPa, respectively based on Vaclav Dostal work [42].
- Isentropic efficiencies of the turbomachinery were specified as 90% and 89% for the turbine and compressor, respectively based on Marc T. Dunham study [55].
- The cycle is considered to work at steady state
- Pressure drops in the heat exchangers are neglected
- The lowest cycle temperature (T1) is set notionally at 32 °C.
- The regenerator effectiveness was specified as 80%. Typical regenerator effectiveness range is from 60 to 80%. Further increases in effectiveness is typically

not economical due to the large capital expenditures required to achieve these increases.

The energy equations are follows:

For the compressor:

$$w_c = h_2 - h_1 \quad \textbf{(3-4)}$$

Where $w_c$ is the work done by compressor (input work), $h_1$ is the specific enthalpy of inlet fluid to the compressor and $h_2$ present the enthalpy of outlet from compressor.

For the turbine:

$$w_t = h_3 - h_4 \quad \textbf{(3-5)}$$

Where $w_t$ is the turbine work per unit mass (output work), $h_3$ is the specific enthalpy of fluid entering the turbine and $h_4$ is the specific enthalpy of fluid exiting the turbine.

For the heat source (gas heater):

$$q_{in} = h_3 - h_2 \quad \textbf{(3-6)}$$

Where as $q_{in}$ is the heat transferred to fluid from heat source, $h_3$ is the enthalpy of leaving the gas heater and $h_2$ is the enthalpy of entering to gas heater.

For the heat exchanger (gas cooler):

$$q_{out} = h_4 - h_1 \quad \textbf{(3-7)}$$

Where as $q_{out}$ is the heat rejected from the working fluid, $h_4$ is the specific enthalpy of turbine exit and $h_1$ is the enthalpy of gas cooler exit.

Then the work net output:

$$W_{net} = W_t - W_c \quad \textbf{(3-8)}$$

Where as $w_{net}$ is the net work of the cycle, $w_t$ is the work done by turbine ($w_{out}$) and $W_c$ is the work done by compressor ($w_{in}$).

### 3.2.2 Carbon dioxide power cycle with Intercooling

In this cycle multi stage compression with intercooling is employed. Recompression with intercooling is a common addition to gas cycles that decreases compression work. This arrangement also benefits the S-$CO_2$ cycle by decoupling the main compressor inlet pressure from the low-pressure turbine outlet pressure. Intercooling divides compression into two stages. First, the low-pressure stream enters a heat exchanger (precooler) and is cooled. The cooled flow then enters the precompressor, where it is compressed to an intermediate pressure. Next, the fluid enters the intercooler and is cooled again before entering the main compressor. Figure 3.2 shows the Brayton cycle with intercooling layout.

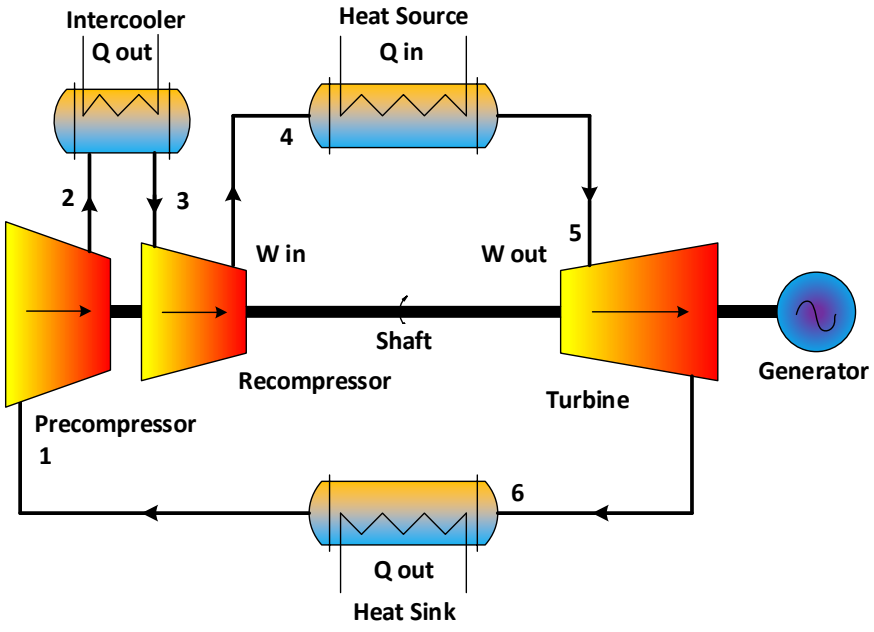


Figure 3.2 Bryton Cycle with Intercooling Layout

The inlet temperatures of the compressors are not required to be equal, but since only one cold sink is likely to be used, the temperatures will typically be equal. Therefore, the compressor inlet temperatures are identical in this study.

### 3.2.3 Carbon dioxide power cycle with Reheating

The third investigated cycle layout is the reheated Brayton cycle. The cycle layouts are depicted in Fig. 3.3. The cycle is similar to the simple Brayton cycle. For example, the working fluid is compressed in the compressor and then heated in the recuperator (gas heater) by the external heat source. The only difference from the simple Brayton cycle is the split of the turbine into the high pressure and low-pressure turbine and considering a reheat stage to increase the temperature of $CO_2$.

The reheating improves the cycle efficiency by increasing the equivalent Carnot temperature for the cycle. High-pressure supercritical $CO_2$ exits the compressor and enters the heat exchanger or gas heater as the cold stream (2). The high temperature and pressure $CO_2$stream enters to the HP turbine (3) and loses its energy in the HP turbine exit (4). Low-pressure S-$CO_2$ stream gains energy in the reheater and exits to the LP turbine (5). It is possible to introduce more than just one reheat stage where two reheat stages are used. In the case of three stages of reheat, there will be an addition of another turbine body into the system. Finally, the heat is rejected in the precooler (6), where the working fluid is cooled to the compressor inlet temperature.

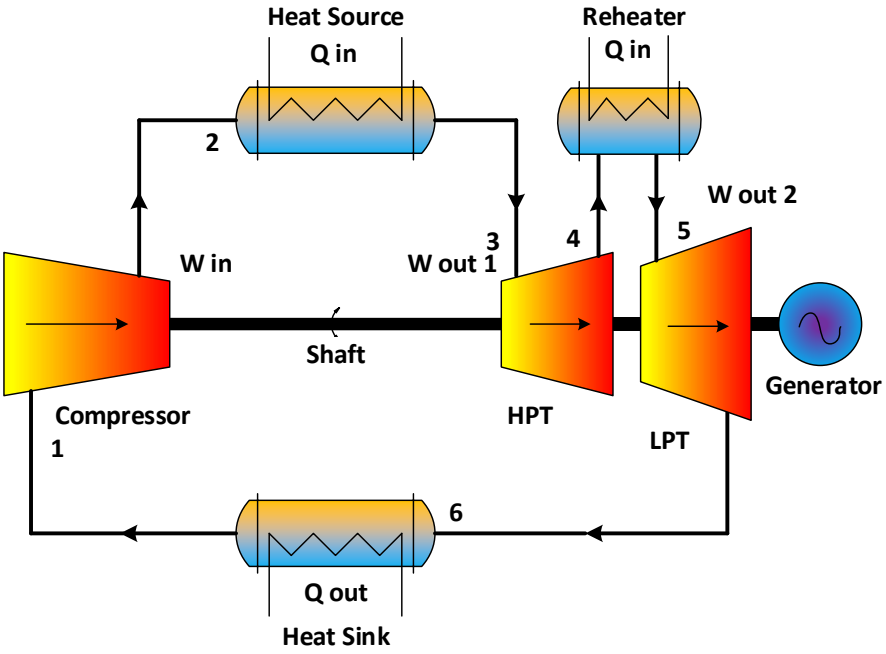

Figure 3.3 Bryton Cycle with Reheat Layout

To increase the efficiency of a real cycle one has to either increase the average temperature of heat addition or reduce the average temperature of heat rejection. With this view, it is easy to see that reheating is the first strategy. Therefore, to get the best efficiency improvement from reheating one would like to keep the inlet temperature the same and the outlet temperatures the same for all turbines. For an ideal gas cycle, due to the constant pressure ratio this leads to the equal split of the total pressure ratio among the turbines.

For a real gas cycle such as $CO_2$ the pressure ratio split should be optimized to give the same equivalent temperatures of heat addition. However, the optimized value is not expected to significantly differ from the equal pressure ratio split, because $CO_2$ is very close to ideal gas behavior in the turbine. The situation may be different for the intercooling, where the specific heat varies more widely.

### 3.2.4 Carbon dioxide power cycle with Intercooling and Reheating

In this cycle, there is multistage compression and expansion. The S-$CO_2$, which exits from precooler, enters into the precompressor (1) see Fig. 3.4. After compression stage, the fluid enters to an intercooler to reject heat (2). After the intercooler, S-$CO_2$ enters to the main compressor (recompressor) where its pressure and temperature increased (3). Then, S-$CO_2$ flows to a HP turbine after absorbing heat from the heat exchanger (gas heater) (4 to 5). The outlet fluid from HP turbine is heated in the reheater at constant pressure (6). The low-pressure heated fluid (7) enters the LP turbine and expands (8). After generating electricity, the fluid goes through heat sink where the remaining heat is rejected and then enters to a precompressor and the total process begins all over again.

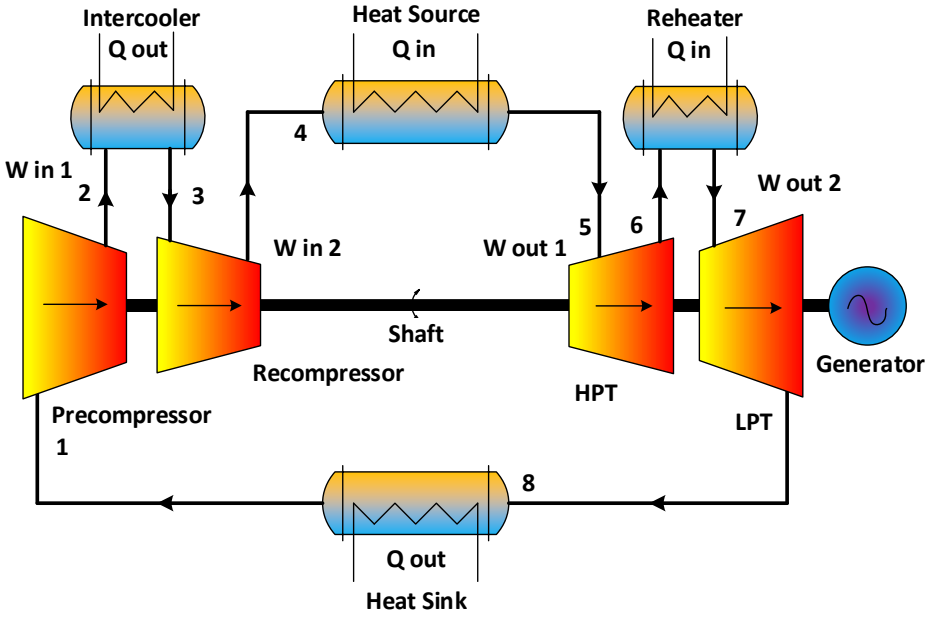


Figure 3.4 Bryton Cycle with Intercooling and Reheat Layout

### 3.2.5 Carbon dioxide power cycle with Intercooling, Reheating, and Regeneration

A schematic for a Brayton cycle with intercooling, reheating and regeneration is shown in Fig. 3.5. The cycle is composed of five components, a heat exchanger (HEX)

or gas heater, turbine, regenerator (recuperator), precooler (heat sink), and compressor. In this cycle configuration, a low temperature $CO_2$ enters to precompressor where it is compressed. Intercooling decrease the temperature, of the working fluid entering the recompressor. Thus, work input decreased and regeneration become more and more effective. The working fluid is heated from the higher temperature fluid, which comes from the LP turbine within the regenerator as a pre-warming flow. Afterward heater rise the temperature to the maximum (550 °C) to be ready for HP turbine. To increase the efficiency of a real cycle one has to either increase the average temperature of heat addition or reduce the average temperature of heat rejection. With this view, it is easy to see that re-heating is the first strategy. By the introduction of a re-heat stage the turbine outlet temperature increases, which leads to the increase of the heat source inlet temperature and thus to the increase of the medium temperature at which the heat is added to the cycle. Therefore, to get the best efficiency improvement from re-heating one would like to keep the inlet temperature the same and the outlet temperatures the same for all turbines. After reheating fluid goes to LP turbine to expand for the second time by losing pressure and generating power in generator. The hot exhaust carbon dioxide which exits from LP turbine has high potential to transfer part of its energy to the main compressor outlet flow by going trough of a recuperator and then reject energies in the precooler or gas cooler.

For a real gas cycle such as $CO_2$ the pressure ratio split should be optimized to give the same equivalent temperatures of heat addition. However, the optimized value is not expected to significantly differ from the equal pressure ratio split, because $CO_2$ is very close to ideal gas behavior in the turbine.

The overall effectiveness of a heat exchanger is defined as the ratio of actual heat transfer to the maximum possible heat transfer through the heat exchanger, were the heat exchanger infinitely large. This is shown in equation 3-10.

$$\varepsilon = \frac{\dot{q}}{q_{max}} \tag{3-9}$$

Where ε, is the effectiveness of the overall heat exchanger, $\dot{q}$ is the actual heat transfer through the heat exchanger, and $q_{max}$ is the maximum possible heat transfer through the heat exchanger.

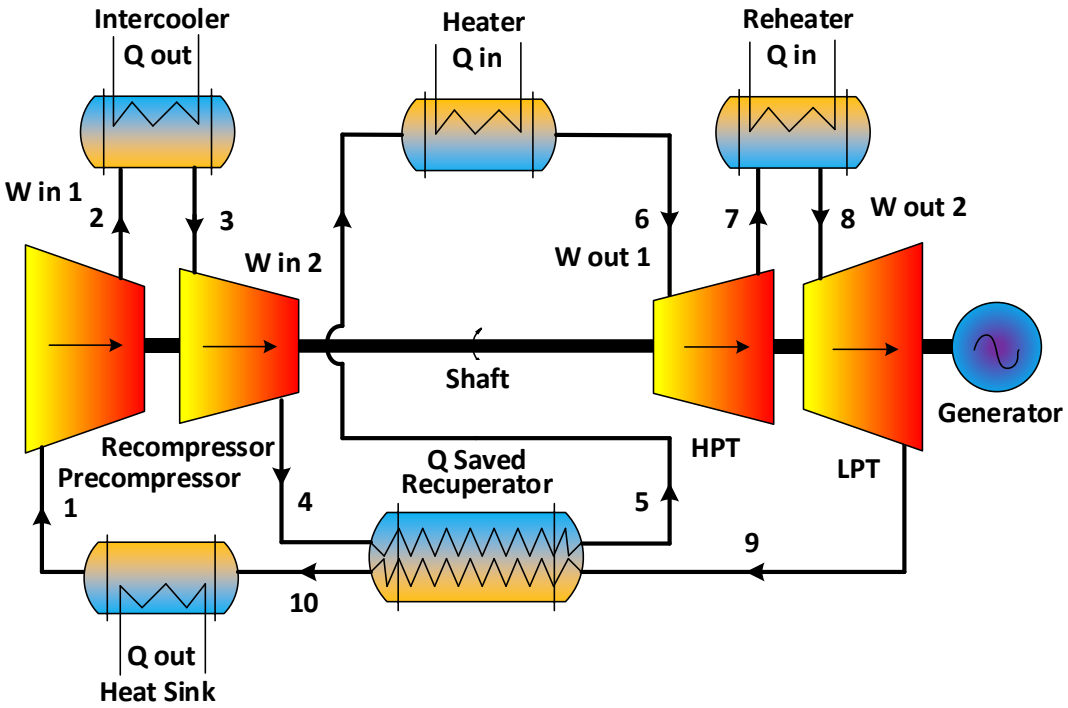


Figure 3.5 Bryton Cycle with Intercooling, Reheat and Regenerator Layout

The assumption of 80% effectiveness for the recuperator is reasonably practical, and significantly reducing the exergy destructions by improving their efficiencies is technologically challenging.

### 3.2.6 Carbon Dioxide Transcritical Power Cycle

The present study also focuses on the transcritical cycle because of its high potential usage in the industry and due to the limited studies found in the literature. The transcritical cycle, whose heat rejection takes place at a subcritical pressure, must not be confused with the entirely supercritical cycle proposed by Feher [43]. Actually, coal fired transcritical power plants at high temperatures (above 500 °C) constitute a mature technology and are among the best performing heat engines with a thermal efficiency as high as 49% [56]. As far as it is known the carbon dioxide will be considered as transcritical cycle where the temperature is above critical temperature i.e, 31 °C.

For transcritical $CO_2$ as it is depicted in Fig 3.6 and the T-S diagram in Fig. 3.7 same as Brayton cycle the transcritical carbon dioxide cycle will experience processes: compression (1-2), isobaric heat supply (2-3), expansion (3-4), and isobaric heat rejection (4-5). The only difference between these two cycles is whether part of the cycle is located in the subcritical region or not. Therefore, both cycles are sometimes related to supercritical cycles in the literature.

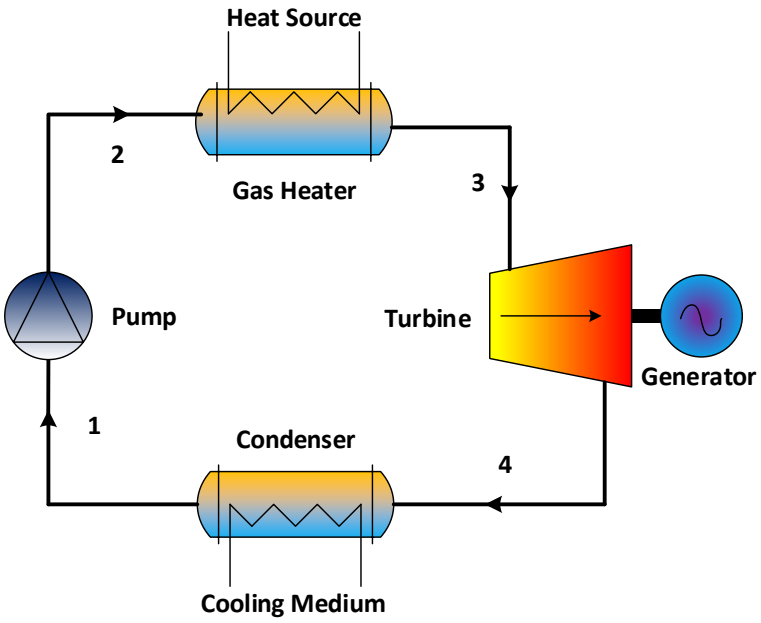


Figure 3.6 Carbon Dioxide Transcritical Power Cycle Layout

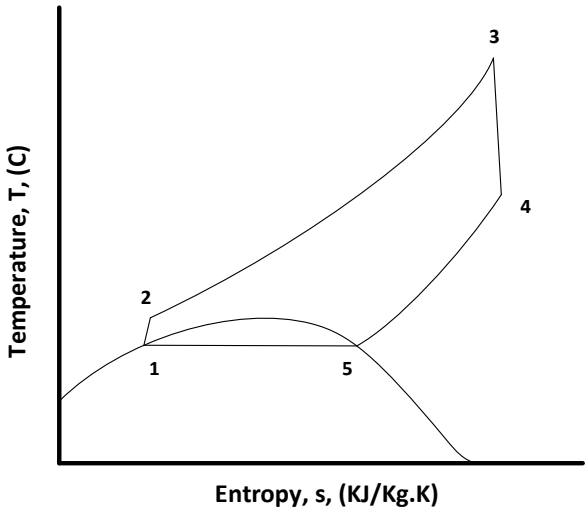


Figure 3.7 Carbon Dioxide Transcritical Power Cycle T-S Diagram

The energy analysis is based on the first law of thermodynamics. The thermal efficiency and the specific net output are its results. With the assumptions previously stated, their values depend only on one independent parameter: the high pressure, which are P2=P3. In particular, these results do not depend on the working fluid mass flow rate. The equations for the different components are the following.

For the pump:

$$\eta_p = \frac{h_{2,s} - h_1}{h_2 - h_1} \quad \textbf{(3-10)}$$

Where the $\eta_p$ is the efficiency of the pump, $h_1$ is the specific enthalpy of the pump inlet fluid, $h_2$ is the enthalpy of pump outlet fluid and $h_{2,s}$ is the isentropic enthalpy of outlet fluid.

$$w_p = h_2 - h_1 \quad \textbf{(3-11)}$$

Where the $w_p$ is the work of the pump, $h_1$ is the specific enthalpy of the inlet fluid and $h_2$ is the enthalpy of outlet fluid.

For the turbine:

$$\eta_t = \frac{h_3 - h_4}{h_3 - h_{4,s}} \quad \textbf{(3-12)}$$

Where the $\eta_t$ is the efficiency of the turbine, $h_3$ is the specific enthalpy of $CO_2$ at the turbine inlet, $h_4$ is the enthalpy of outlet fluid and $h_{4,is}$ is the isentropic enthalpy of outlet fluid.

$$w_t = h_3 - h_4 \quad \textbf{(3-13)}$$

Where the $w_t$ is the work of the pump, $h_3$ is the specific enthalpy of the turbine inlet fluid and $h_4$ is the specific enthalpy of outlet fluid.

For the vapor generator:

$$q_{in} = h_3 - h_2 \quad \textbf{(3-14)}$$

Where the $q_{in}$ is the heat transferred to the fluid in vapor generator, $h_2$ is the specific enthalpy of the gas heater inlet fluid and $h_3$ is the enthalpy of outlet fluid.

For the condenser:

$$q_{out} = h_4 - h_1 \quad \textbf{(3-15)}$$

Where the $\mathbf{q_{out}}$ is the heat rejected from the working fluid in condenser, $h_4$is the enthalpy of the fluid entering the condenser and $h_1$ is the enthalpy exiting of fluid leaving the condenser.

The thermal efficiency of the cycle:

$$\eta_{th} = \frac{W_t - W_p}{q_{in}} = \frac{(h_3 - h_4) - (h_2 - h_1)}{h_3 - h_2} \quad \textbf{(3-16)}$$

Where the $\boldsymbol{\eta_{th}}$ is the thermal efficiency of the cycle, $w_t$ is the turbine work, $W_p$ is the pump work and $q_{in}$ is heat transferred to the working fluid in gas heater.

In compare with an organic Rankin cycle (ORC), the $CO_2$ transcritical power cycle has a higher capability in taking advantages of the energy in a low-grade waste heat with gradient temperature, such as exhaust gases. The temperature glide (Temperature change during take-up of heat energy) for $CO_2$ above the critical point allows for a better matching to the heat source temperature glide than an organic working fluid working below the critical point. Therefore, the so-called pinching problem, which may occur in ORC's counter current heat exchanger, can be avoided by carbon dioxide transcritical power cycle.

# Chapter 4

# RESULTS AND DISCUTION

Typically, in the thermodynamics analysis of cycles, the most important aim is to increase the efficiency of the cycle. Then, the whole cycle is modeled by using the energy balance, after which weaknesses are identified. In the present study, in addition to this conventional approach, there is one major objective; namely, optimum gas heater and cooler pressure.

Each component of the considered system has been treated as a control volume and the principal of the mass and energy conservation are applied to them. The EES software package is used for solving the equations.

The mass balance can be expressed as:

$$\Sigma \dot{m}_{in} - \Sigma \dot{m}_{out} = 0 \qquad \textbf{(4-1)}$$

The first law of thermodynamic yields the energy balance for each component as follows:

$$\Sigma (\dot{m}h)_{in} - \Sigma (\dot{m}h)_{out} + \dot{Q}_{cv} - \dot{W}_{cv} = 0 \qquad \textbf{(4-2)}$$

In following subsections, the simulation results are discussed in detail.

## 4.1 Simple Actual Supercritical Carbon Dioxide Brayton Cycle

In the following section, a simple actual supercritical $CO_2$ Brayton cycle has been investigated and couple of key parameters of the cycle (i.e., Compressor inlet temperature, compressor inlet pressure, turbine inlet temperature, gas cooler pressure,

gas heater pressure, cycle pressure ratio, cycle efficiency, total cycle work, compressor and turbine work) has been analyzed.

### 4.1.1 The Effect of Compressor Inlet Pressure

Figure 4.1 shows the effect of compressor inlet pressure on the cycle efficiency and the amount of the work done by the cycle at four different values of turbine inlet temperature. As indicated in figure 4.1, for a given value of $P_1$, increasing the turbine inlet temperature ($T_3$) results in an increase of cycle efficiency. This is due to the fact that as the $T_3$ increases, the fraction denominator decreases and as a result the cycle efficiency will raise ($\eta_{th} = 1 - T_4/T_3$). On the other hand, the same trend can be seen for the total cycle work but obviously the variation of efficiency is more than work that is done by the cycle along the increment of the compressor inlet pressure. It is noted that for the given condition, the compressor inlet pressure does not have a significant impact on the total cycle work produced, since the compressor inlet conditions are fixed above working fluid's critical condition.

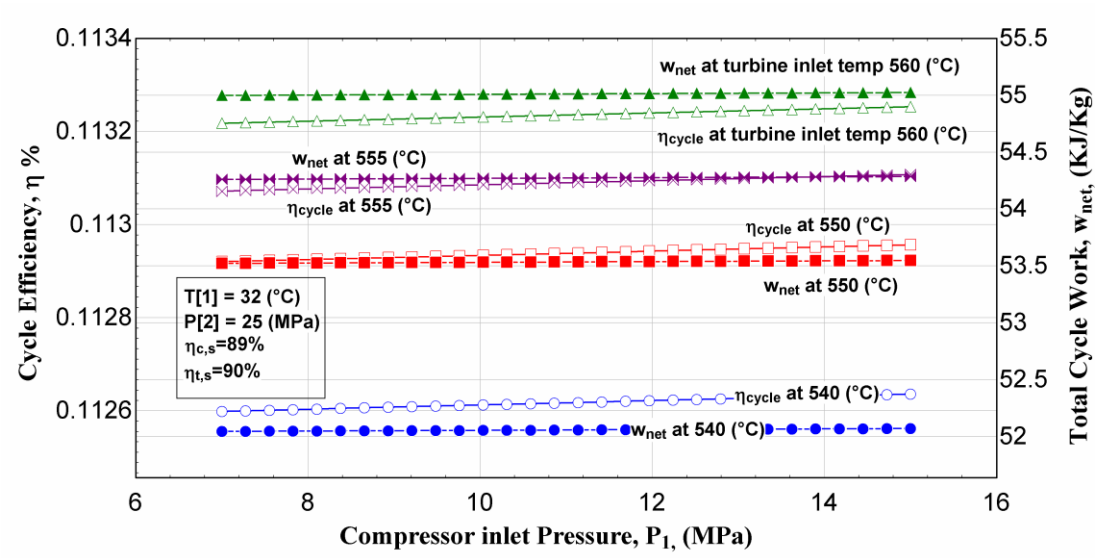


Figure 4.1 Cycle Efficiency and Total Cycle Work vs. Compressor Inlet Pressure at Different Turbine Inlet Temperatures for the Simple Actual S-CO2 Brayton Cycle

### 4.1.2 The Effect of Pressure Ratio

The variation of cycle efficiency and total cycle work with pressure ratio of cycle at different values of turbine inlet temperature ($T_3$) is shown in figure 4.2. The figure shows the trend of the cycle efficiency vs. the pressure ratio for actual cycle assumption, while compressor efficiency, turbine efficiency, compressor inlet pressure and temperature are fixed at constant with reference values mentioned above.

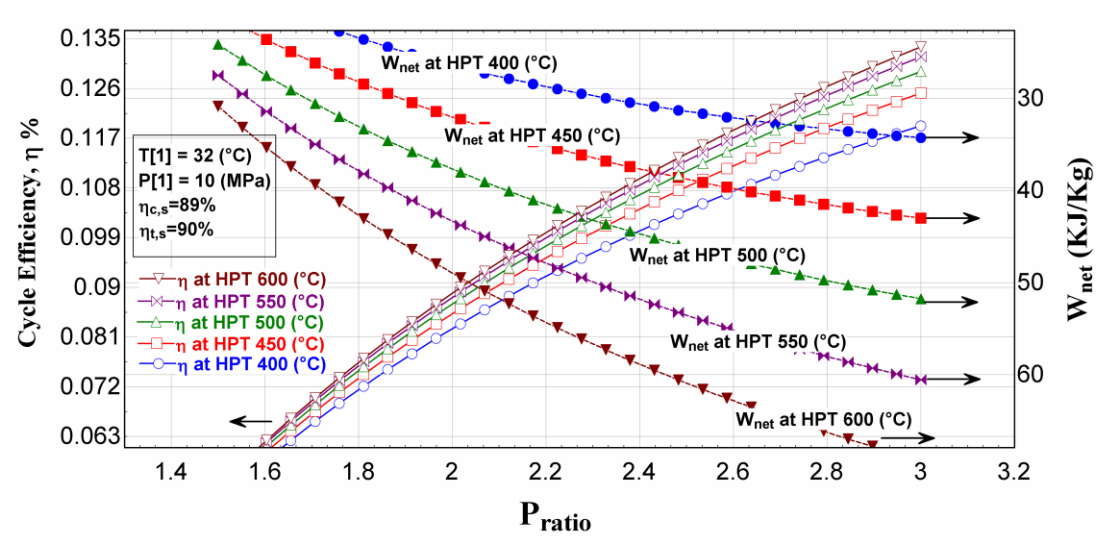


Figure 4.2 Cycle Efficiency and Total Cycle Work vs. Pressure Ratio at Different Turbine Inlet Temperatures for the Simple Actual S-$CO_2$ Brayton Cycle

The total cycle efficiency increases sharply with increasing pressure ratio since the work net produced by turbomachinery gradually increases. The upper range of total cycle efficiency is varying from 6.3% to 13% when the outlet pressure of compressor is changed from 16 MPa to 30 MPa.

### 4.1.3 The Effect of Minimum Operation Temperature

The effect of the compressor inlet temperature on the cycle efficiency is especially important for the supercritical $CO_2$ cycles because it significantly affects the compression process. Since the cycle takes, advantage of the property changes near the critical point the change of the compressor inlet temperature results in a significant

change of $CO_2$ properties and the compression process may not be performed at the optimum conditions.

The efficiency and cycle work against compressor inlet temperature for the $SCO_2$ cycle (in the range of $T_1$ = 30–50 ºC and $P_r$ (pressure ratio) = 2, 2.2, 2.5 and 2.8) has been presented in figure 4.3.

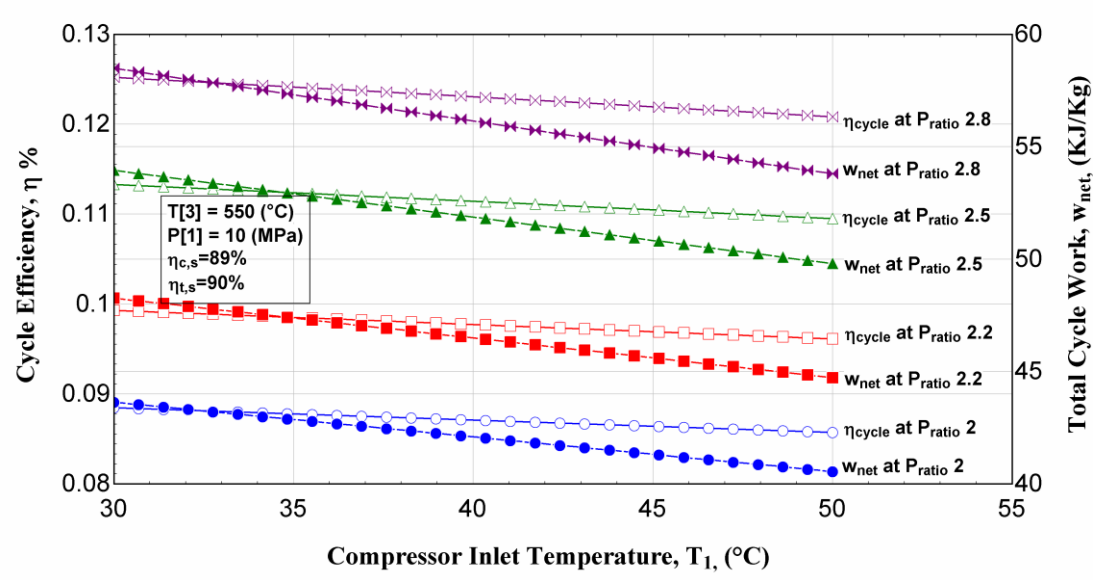


Figure 4.3 Cycle Efficiency and Total Cycle Work vs. Compressor Inlet Temperature at Different Pressure Ratios for the Simple Actual S-$CO_2$ Brayton Cycle

For the various range of pressure ratio figure 4.3 shows the effect of compressor inlet temperature on the total work production of the cycle. It is noted that for the given condition, the pressure ratio has a significant impact on the efficiency and the total work produced.

### 4.1.4 The Effect of Pressure Ratio on the Compressor and Turbine Work

The effect of pressure ratio on the compressor and turbine work is presented in Figure 4.4. All the parameters are fixed except turbine inlet temperature, which is varied from 510 to 570 ºC.

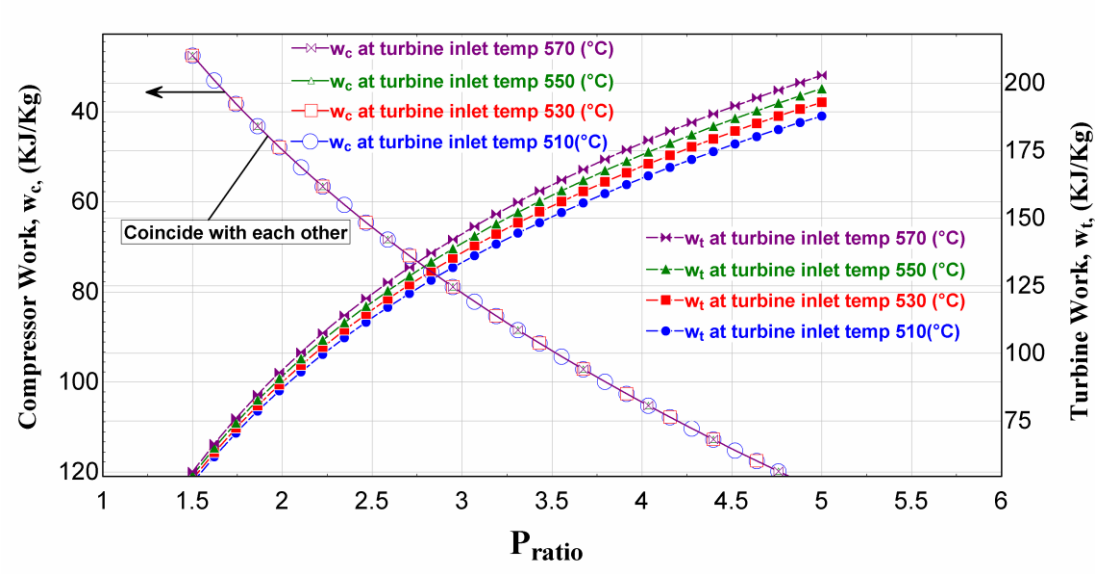


Figure 4.4 Compressor Work and Turbine Work vs. Pressure Ratio at Different Turbine Inlet Temperatures for the Simple Actual S-$CO_2$ Brayton Cycle

Inspection of figure 4.4 reveals that compressor work and turbine work increases with pressure ratio whereas net thermal efficiency is relatively sensitive to pressure ratio. The variation of turbine inlet temperature does not affect the work input of the compressor.

## 4.2 Actual Supercritical Carbon Dioxide Brayton Cycle with Intercooling

### 4.2.1 The Effect of Gas Cooler Pressure

The effect of first compressor outlet pressure ($P_2$) on thermal efficiency of the cycle is shown in Figure 4.5. The dash line in the figure shows the maximum thermal efficiency points for different turbine inlet temperature lines whereas the optimum pressure can be obtained by the first compressor is equal to 11.9 MPa for each case. As $P_2$ increases beyond the optimum value (i.e., 11.9 MPa) the efficiency will decreases remarkably.

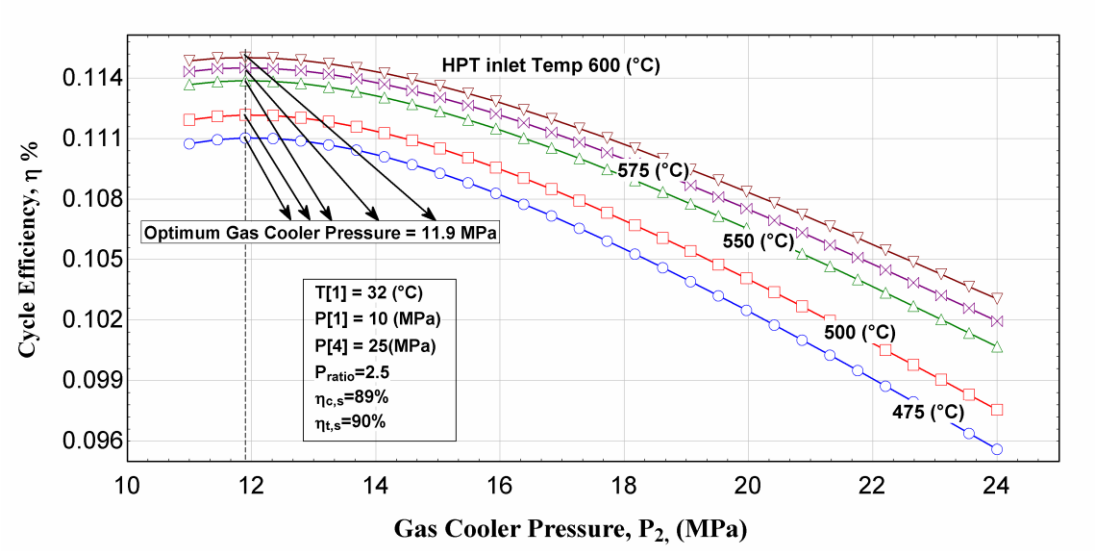


Figure 4.5 Cycle Efficiency vs. Gas Cooler Pressure at Different Turbine Inlet Temperatures for the Actual S-$CO_2$ Brayton Cycle with Intercooling

### 4.2.2 The Effect of High Pressure Turbine Inlet Temperature

A steady increase in $\eta_{th}$ of supercritical Brayton cycle with intercooler at different pressure ratios is shown by a solid line in Figure 4.6. It is seen from the figure that as turbine inlet temperature rises from 450 ºC to 650 ºC at $P_{ratio}$=2.2, $\eta_{th}$ is improved by 4.92% from 9.62% to 10.09%. As pressure ratio increases, thermal efficiency also increases.

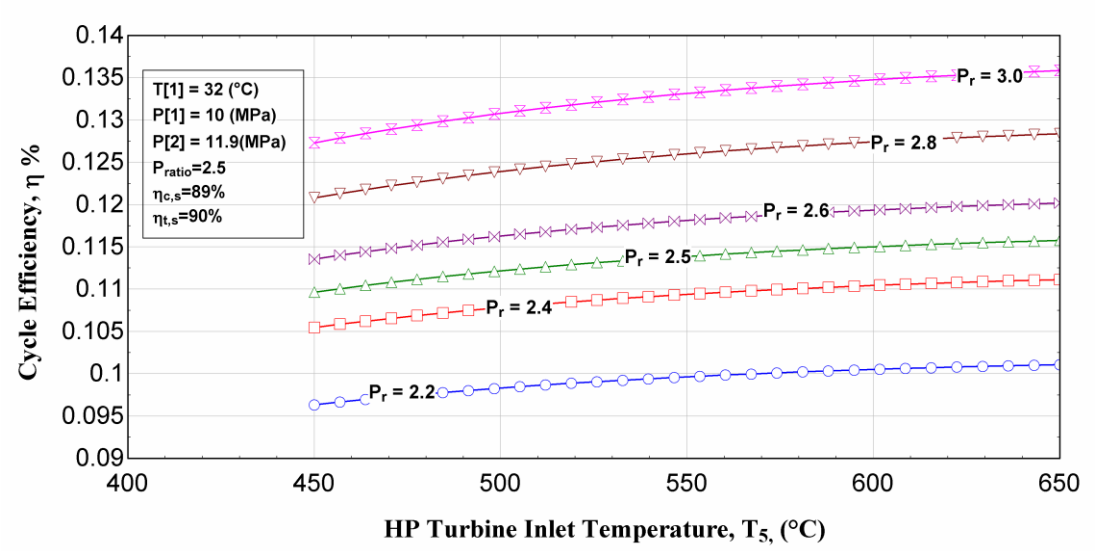


Figure 4.6 Cycle Efficiency vs. High Pressure Turbine Inlet Temperature at Different Pressure Ratios for the Actual S-$CO_2$ Brayton Cycle with Intercooling

### 4.2.3 The Effect of Gas Cooler Pressure on Cycle Work

The effect of gas cooler pressure $P_2$ of supercritical $CO_2$ Brayton cycle with intercooler on $W_{net}$ is shown in Figure 4.7 for an example of different high-pressure turbine inlet temperature. Total cycle work of the cycle takes a maximum value, 56.754 kJ/kg at $P_2 = 15.8$ MPa for present case (HPT inlet temp. 550 ºC).

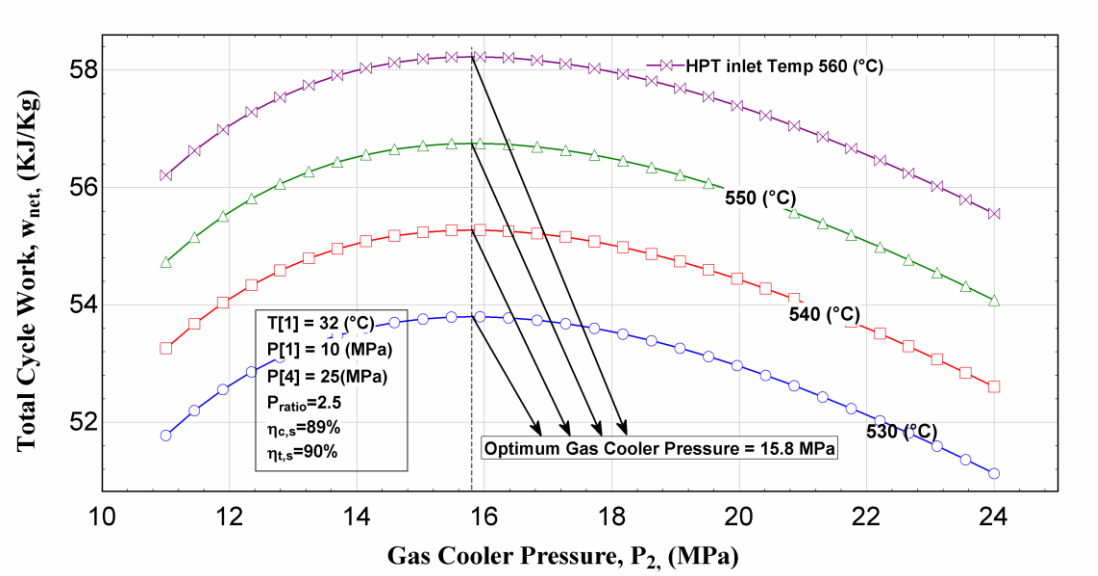


Figure 4. 7 Gas Cooler Pressure vs. Total Cycle Work at Different Turbine Inlet Temperatures for the Actual S-$CO_2$ Brayton Cycle with Intercooling

### 4.2.4 The Effect of Pressure Ratio

The cycle efficiency $\eta_{th}$ and the total cycle work $w_{net}$ are shown against the pressure ratio of cycle in figure 4.8. Their values increase with the raise in $P_{ratio}$. For instance, $\eta_{th}$ increases by about 27.86% while we have 0.5 unit increase in pressure ratio for HPT inlet temperature = 550 °C line. On the other hand, the right side of the figure describes the behavior of work net $W_{net}$. When the pressure ratio increased from 20 to 2.5 for 550 °C maximum fluid temperature, with net increases about 24.07%.

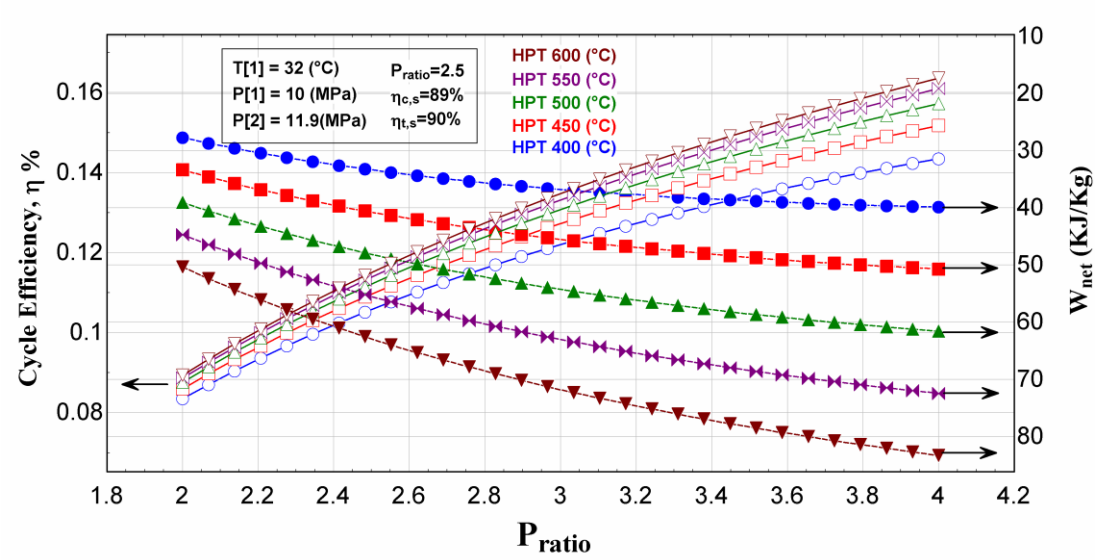


Figure 4.8 Cycle Efficiency and Total Cycle Work vs. Pressure Ratio at Different Turbine Inlet Temperatures for the Actual S-$CO_2$ Brayton Cycle with Intercooling

### 4.2.5 The Effect of Pressure Ratio on Compressor and Turbine Work

The variation of $W_{in}$ and $W_{out}$ with pressure ratio of cycle at turbine inlet temperature ($T_5 = 550$ °C), is shown in figure 4.9. As can be seen in the figure both works experienced a steady rise which are 35.15% and 29.9% for $w_{in}$ and $w_{out}$ respectively as the pressure ratio increased from 2 to 2.5.

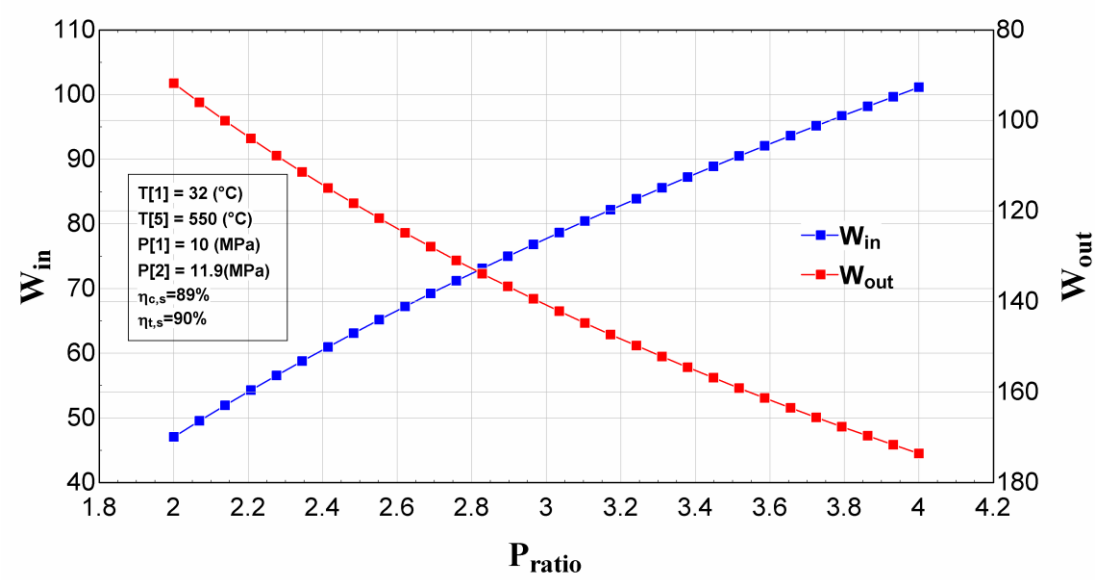


Figure 4.9 Total Compressor and Turbine Work vs. Pressure Ratio for the Actual S-$CO_2$ Brayton Cycle with Intercooling

### 4.2.6 The Effect of Minimum cycle Temperature

Figure 4.10 shows the variation of cycle efficiency and minimum cycle temperature (precompressor inlet temperature $T_1$) for a supercritical $CO_2$ Brayton cycle with intercooler with $T_{max}$ = 550 °C, $P_{min}$ = 10 MPa and $P_2 = 11.9$ MPa at several pressure ratios. As the minimum cycle temperature increase, the efficiency of cycle decrease steadily.

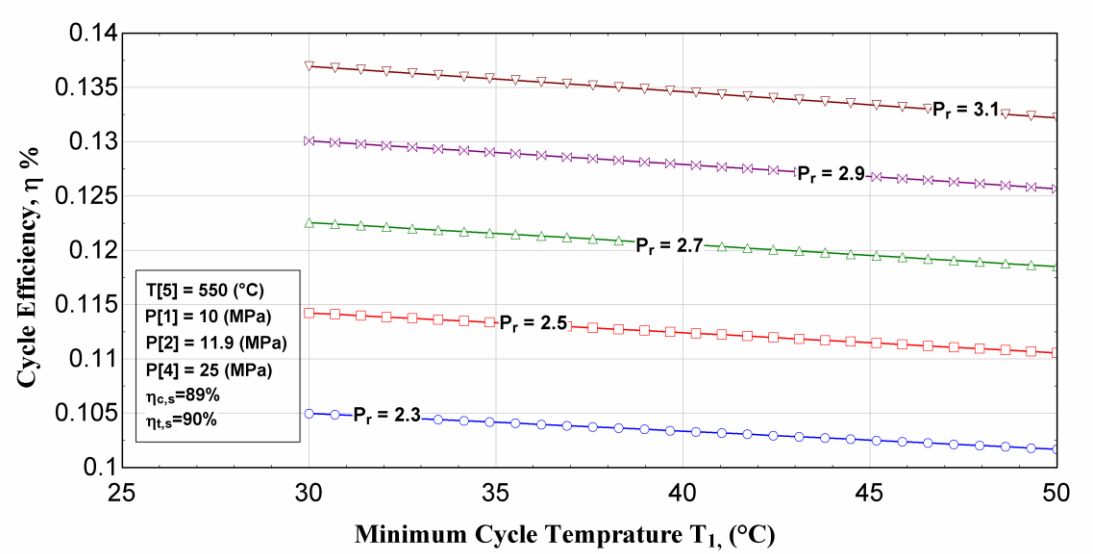


Figure 4.10 Cycle Efficiency vs. Minimum cycle Temperature at Different Pressure Ratios for the Actual S-$CO_2$ Brayton Cycle with Intercooling

## 4.3 Actual Supercritical Carbon Dioxide Brayton Cycle with Reheat

### 4.3.1 The Effect of Gas Reheater Pressure

Figure 4.11 illustrate cycle thermal efficiency versus high pressure turbine outlet pressure from 12 MPa to 24 MPa for several HP turbine inlet temperatures. As it obvious, the efficiency start to rise remarkably from the lowest cycle efficiency (12 MPa) to the highest (23.1 MPa) and then it follows a downward trend. At the optimum pressure of $P_4$= 23.1 MPa, the efficiency of the cycle is about 11.3% for the HPT inlet temperature=500 °C line.

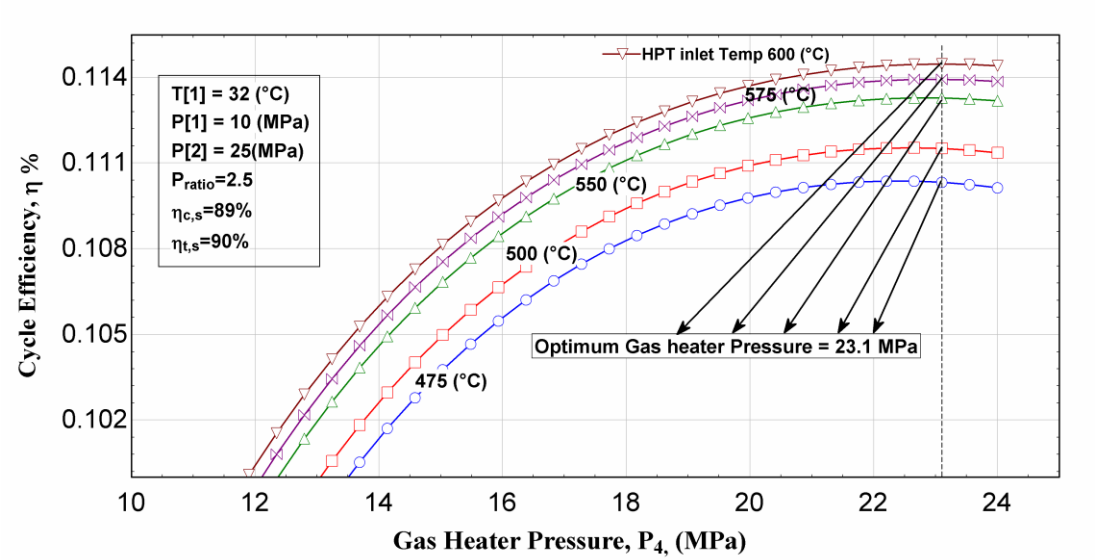


Figure 4.11 Cycle Efficiency vs. Gas Heater Pressure at Different Turbine Inlet Temperatures for the Actual S-$CO_2$ Brayton Cycle with Reheat

### 4.3.2 The Effect of High Pressure Turbine Inlet Temperature

The effect of inlet temperature of a high-pressure turbine $T_3$ on the cycle efficiency for different pressure ratios is shown in figure 4.12. It is clear from the figure that as turbine inlet temperature rises from 450 ºC to 650 ºC cycle efficiency increases for all pressure rates. For example, at $P_{ratio}$=2.5, $\eta_{th}$ is improved by 5.93% from 11.28% to 11.95%.

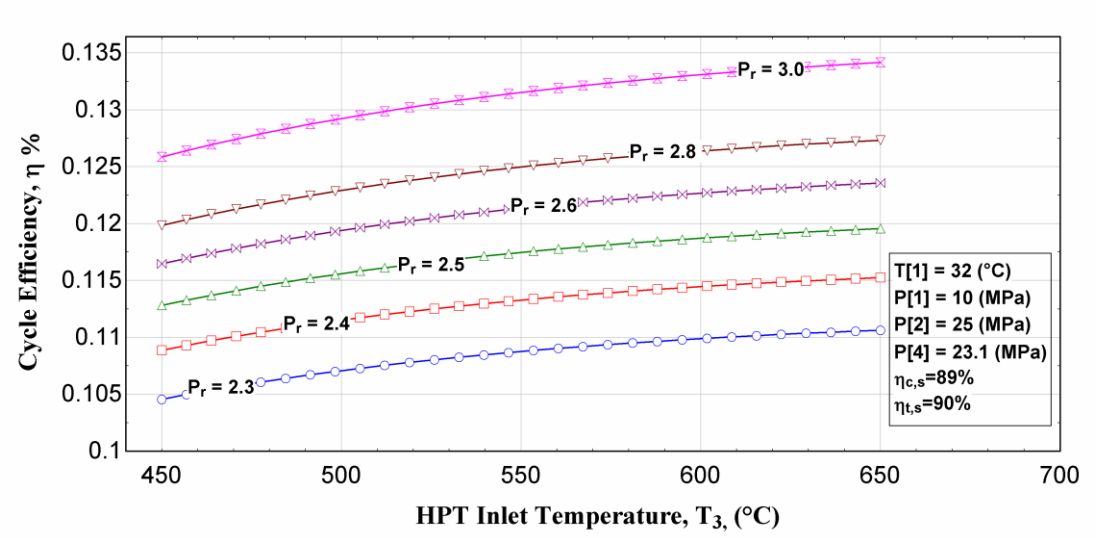


Figure 4. 12 Cycle Efficiency vs. High Pressure Turbine Inlet Temperature at Different Pressure Ratios for the Actual S-$CO_2$ Brayton Cycle with Reheat

### 4.3.3 The Effect of Reheater Pressure

The effect of reheater pressure $P_4$ on work net $w_{net}$, which is presented in Fig. 4.13 for different HP turbine inlet temperature. As the pressure of carbon dioxide increase in the reheater, the work net increases rapidly until to a peak point (i.e., optimum pressure that gives the optimum amount of work net. Then, as pressure increases beyond the optimum pressure $w_{net}$ decreases.

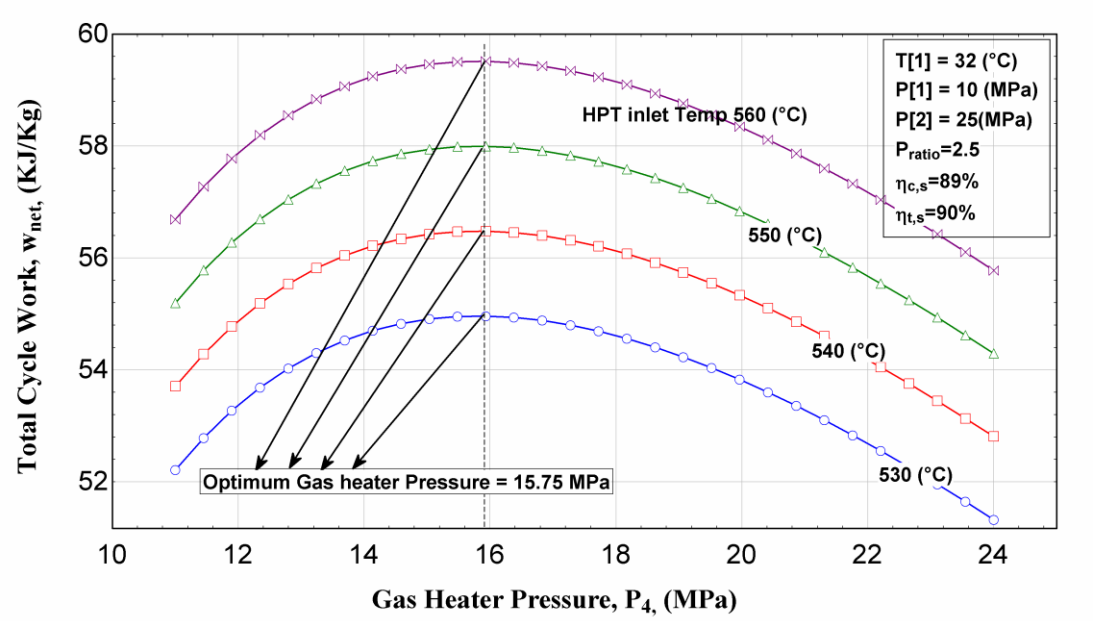


Figure 4. 13 Cycle Efficiency vs. Gas Heater Pressure at Different Turbine Inlet Temperatures for the Actual S-$CO_2$ Brayton Cycle with Reheat

It can be noticed from figure 4.13 that for 10 °C raise in HPT inlet temperature from 530 to 540, 540 to 550 and 550 to 560 there are 2.75%, 2.71% and 2.58% increase in the net work respectively. However, by increasing the HPT inlet temperature beyond optimum $P_4$, the percentage of increase in $W_{net}$ decreases smoothly.

### 4.3.4 The Effect of Cycle Pressure Ratio on Cycle Efficiency and Total Cycle Work

The influence of pressure ratio on thermal efficiency $\eta_{th}$ and the work net are shown in figure 4.14. It can be seen from the figure that efficiency and the work net

increase as pressure ratio increased. For instance, $\eta_{th}$ increases about 7.94% while we have 0.5 unit (2 to 2.5) increase in the pressure ratio for HPT inlet temperature = 550°C line. Furthermore, the right side of the figure describes the behavior of work net $W_{net}$. As the pressure ratio varied from 2 to 2.5 that gives 9.16% increase in work net for 550 ºC. There is a limitation in pressure ratio as higher pressure ratios mean higher pressure ratio in the system.

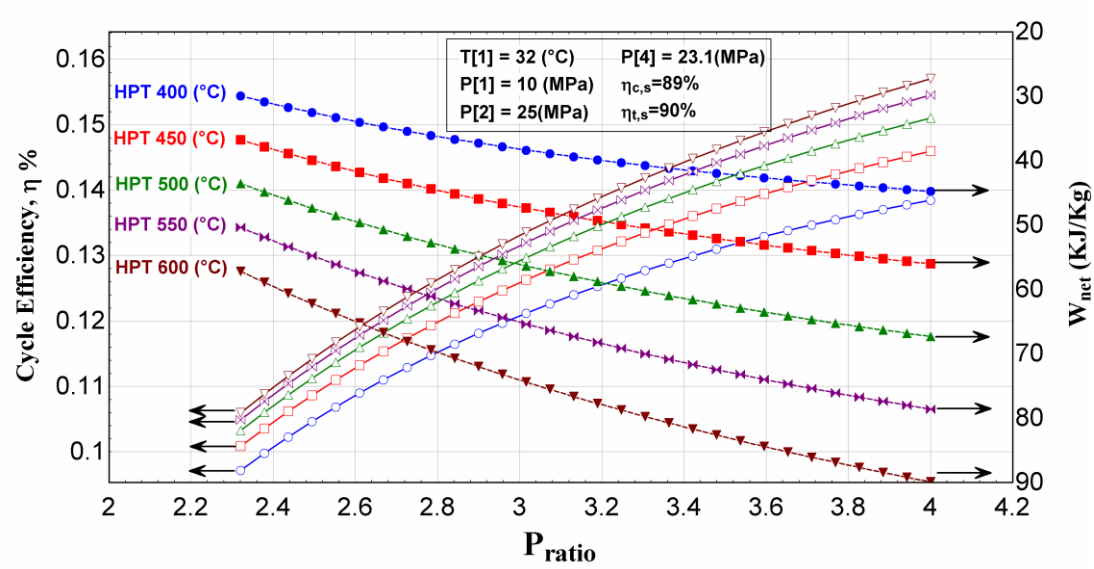


Figure 4. 14 Cycle Efficiency and Total Cycle Work vs. Pressure Ratio at Different Turbine Inlet Temperatures for the Actual S-$CO_2$ Brayton Cycle with Reheat

### 4.3.5 The Effect of Pressure Ratio on Compressor Work and Turbine Work

Figure 4.15 shows a trend of compressor and turbine work vs. the pressure ratio for actual S-$CO_2$ Brayton cycle with reheat. The compression inlet temperature $T_1$ is 32 °C, compression inlet pressure $P_1$is 10 MPa, HPT inlet temperature $T_3$ is 550 °C, HPT outlet pressure $P_4$ sets to optimum at of 23.1 MPa. The results indicate 49.4% and 44.11% increase in $w_{in}$ and $w_{out}$ respectively which can be obtainable by increasing the pressure ratio from 2.32 to 3.32.

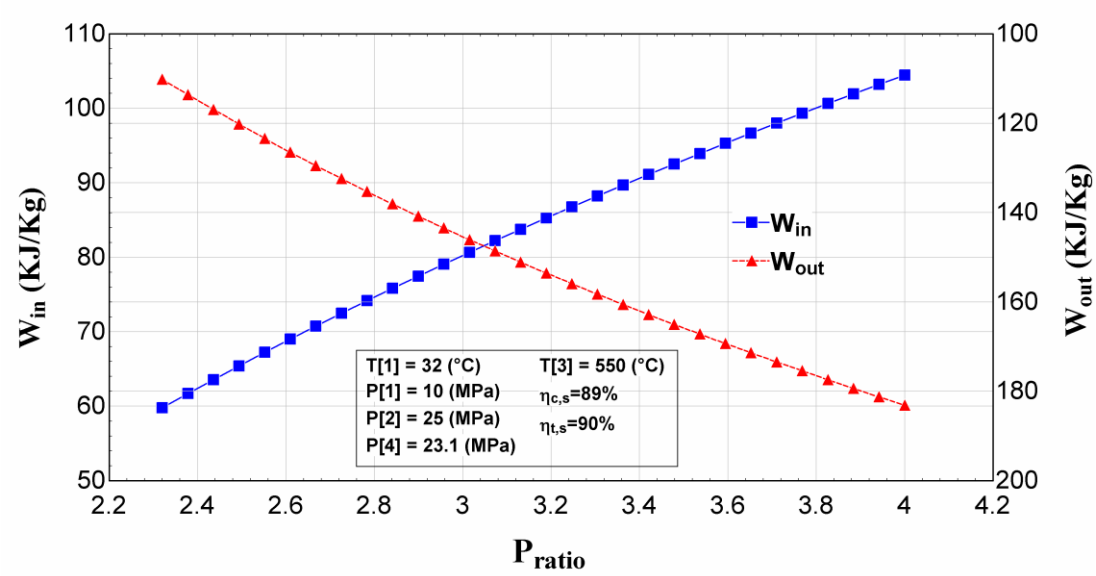


Figure 4. 15 Compressor Work and Turbine Work vs. Pressure Ratio for the Actual S-$CO_2$ Brayton Cycle with Reheat

### 4.3.6 The Effect of Minimum cycle Temperature

Figure 4.16 shows the variation of cycle efficiency and minimum cycle temperature (precompressor inlet temperature$T_1$) for a supercritical $CO_2$ Brayton cycle with reheat with $T_{max}$ = 550 °C, $P_{min}$ = 10 MPa and $P_2$ = 11.9 MPa at several pressure ratios. As the minimum cycle temperature increase, the efficiency of cycle decrease steadily. The reason that can be pointed out is about the area under the T-S diagram of cycle which goes to be more small and smaller by increasing the compressor inlet temperature. For example, for every 5°C increase in $T_1$, the efficiency decrease for about 0.8% at default pressure ratio of cycle ($P_{ratio}$=2.5).

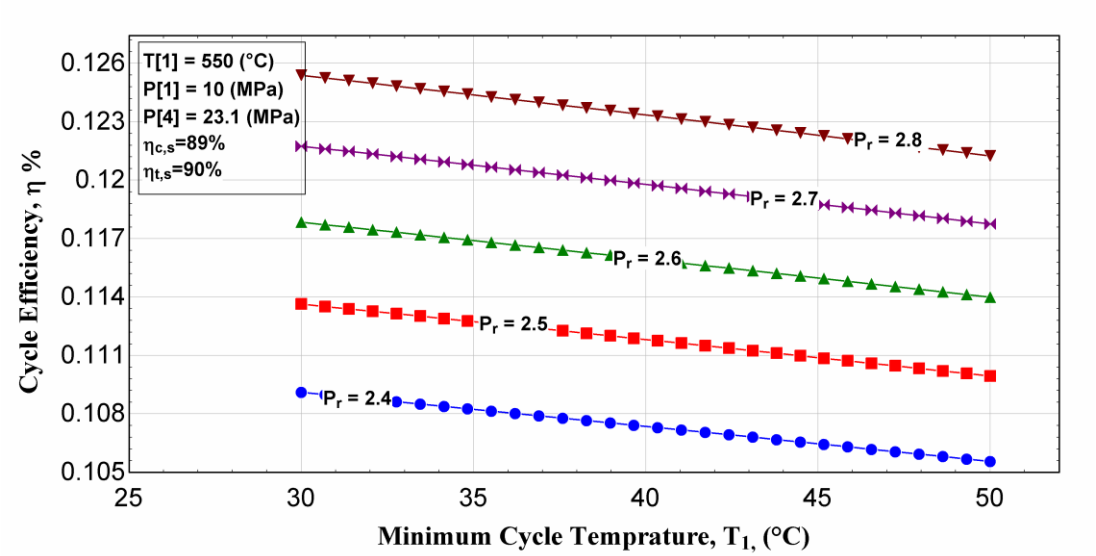


Figure 4. 16 Cycle Efficiency vs. Minimum Cycle Temperature at Different Pressure Ratios for the Actual S-$CO_2$ Brayton Cycle with Reheat

## 4.4 Actual Supercritical Carbon Dioxide Brayton Cycle with Intercooling and Reheat

### 4.4.1 The Effect of Gas Cooler Pressure

Figure 4.17 displays how the cycle efficiency is affected by precompressor outlet pressure $P_2$ alteration for an actual supercritical carbon dioxide Brayton cycle with intercooling and reheat. It can be seen from the figure that for a certain precompressor outlet pressure, there is an optimum compression pressure (11.9MPa), which enables the maximum thermal efficiency for about 11.4%. The results indicate that the precompressor has a significant critical influence on the system's efficiency.

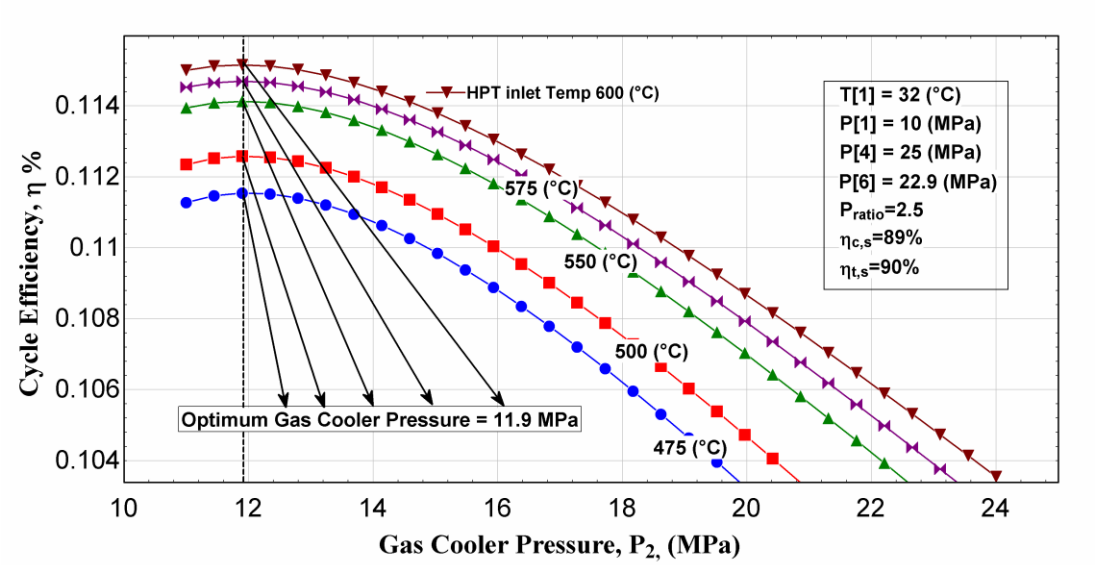


Figure 4. 17 Cycle Efficiency vs. Precompressor Outlet Pressure at Different Turbine Inlet Temperatures for the Actual S-$CO_2$ Brayton Cycle with Intercooling and Reheat

### 4.4.2 The Effect of High Pressure Turbine Inlet Temperature

The effect of inlet temperature $T_5$ of the high-pressure turbine on the efficiency of cycle for different pressure ratios is shown in figure 4.18. It is clear from the figure that as turbine inlet temperature rises from 450 ºC to 650 ºC for all pressure ratios there is an improvement in the cycle efficiency.

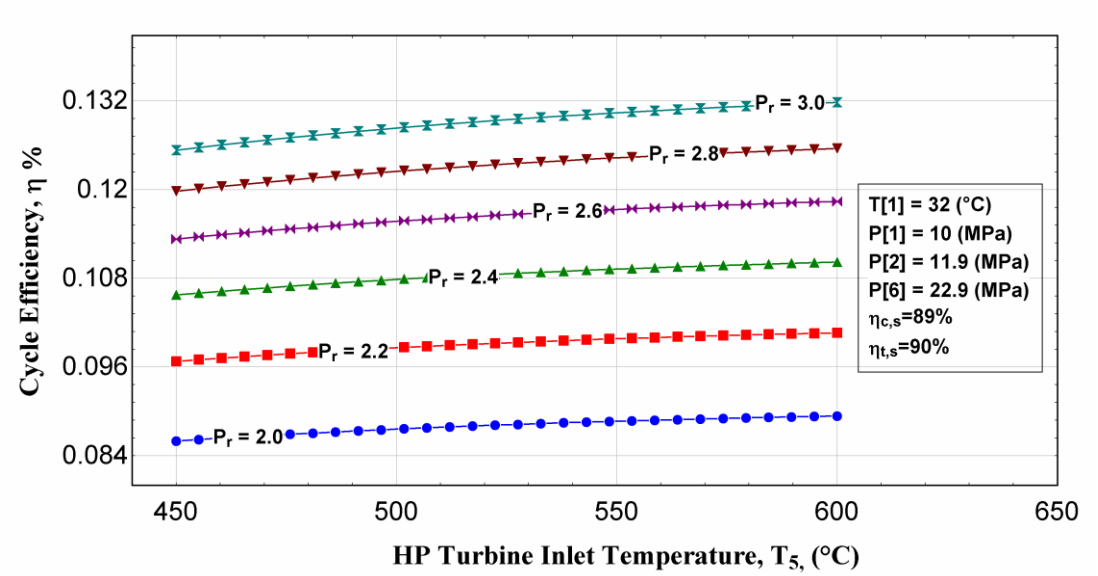


Figure 4. 18 Cycle Efficiency vs. High Pressure Turbine Inlet Temperature at Different Pressure Ratios for the Actual S-$CO_2$ Brayton Cycle with Intercooling and Reheat

### 4.4.3 The Effect of Gas Heater Pressure on Total Cycle Work

The effect of outlet pressure of recompressor $P_4$ on the work net for various amount of HPT inlet temperatures is shown in figure 4.19. As the pressure of carbon dioxide increased, the cycle's work net also increased. An optimum precompressor pressure ($P_4$=15.9 MPa) increasing, precompressor pressure above the optimum leads to a decrease in the work net. As expected higher turbine inlet temperature increases the work net.

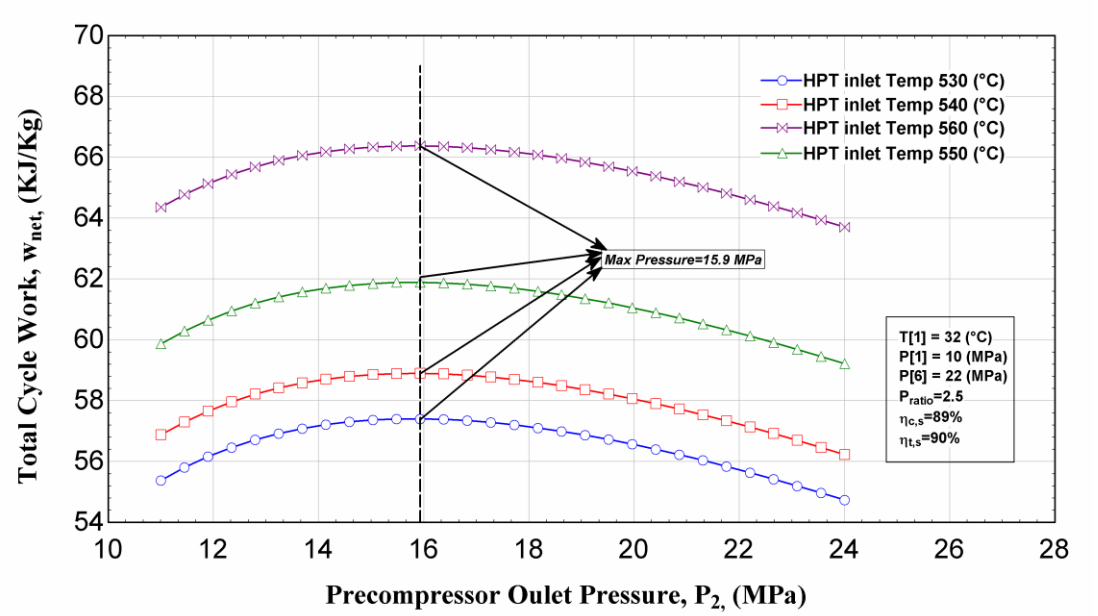


Figure 4. 19 Total Cycle Work vs. Precompressor Outlet Pressure at Different Turbine Inlet Temperatures for the Actual S-$CO_2$ Brayton Cycle with Intercooling and Reheat

### 4.4.4 The Effect of Pressure Ratio vs. Cycle Efficiency

The influence of pressure ratio of cycle on the thermal efficiency $\eta_{th}$ is shown in figure 4.20. It can be seen from the figure that efficiency values increase as pressure ratio is increased.

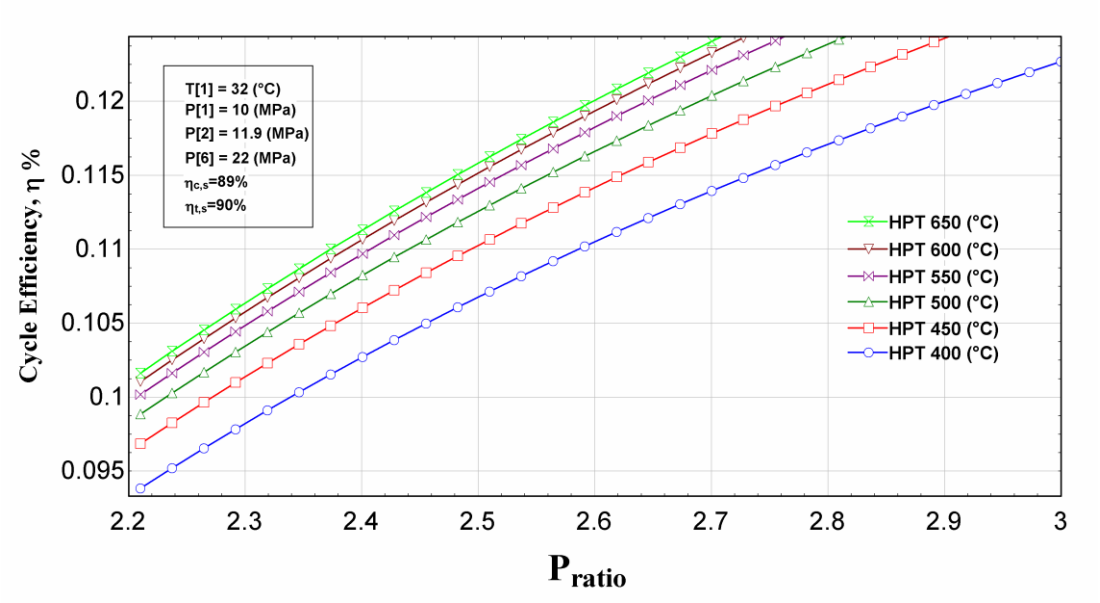


Figure 4. 20 Cycle Efficiency vs. Pressure Ratio at Different Turbine Inlet Temperatures for the Actual S-$CO_2$ Brayton Cycle with Intercooling and Reheat

### 4.4.5 The Effect of Pressure Ratio on Compressor and Turbine Work

Figure 4.21 shows the effect of pressure ratio on compressor work input and turbine work output, while precompressor inlet temperature $T_{min}$ is 32°C, HPT inlet temperature $T_{max}$ is 550°C, precompressor inlet pressure $P_{min}$ is 10 MPa, intercooler pressure $P_2$ is 11.9 MPa and reheater pressure is 22MPa.

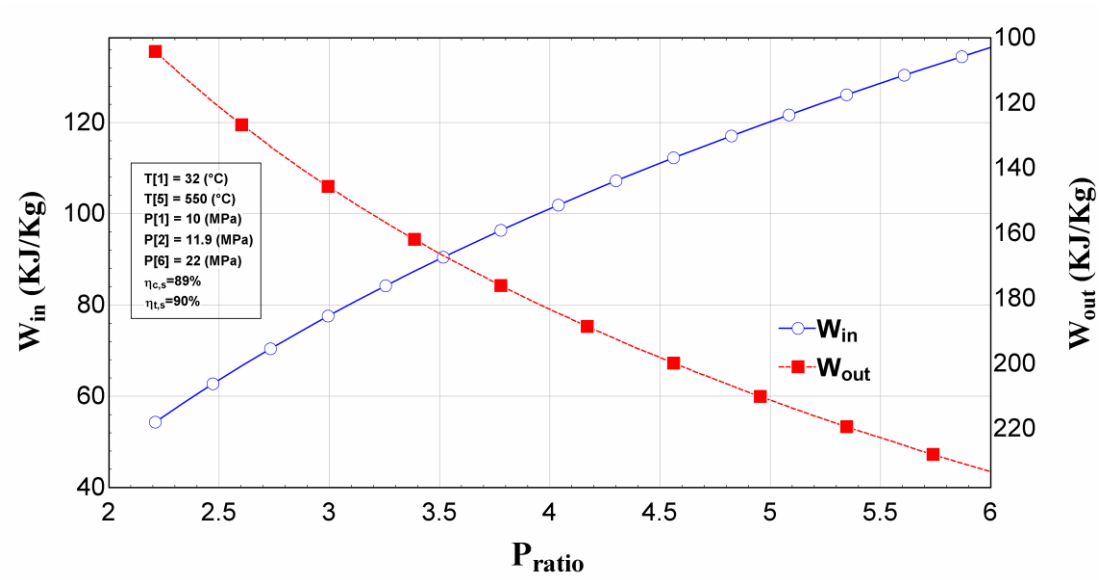


Figure 4. 21 Compressor Work and Turbine Work vs. Pressure Ratio for the Actual S-$CO_2$ Brayton Cycle with Intercooling and Reheat

Inspection of figure 4.21 reveals that compressor work and turbine work increases with pressure ratio whereas the thermal efficiency is relatively sensitive to pressure ratio.

### 4.4.6 Minimum cycle Temperature vs. Cycle Efficiency

Figure 4.22 shows the variation of cycle efficiency with the variation of minimum cycle temperature (precompressor inlet temperature $T_1$) for a supercritical $CO_2$ Brayton cycle with intercooler and reheater. As the minimum cycle temperature increased, the efficiency of cycle decrease steadily. The reason that can be pointed out is about the effect of increment in pressure ratio on cycle efficiency, which is going to be small and smaller.

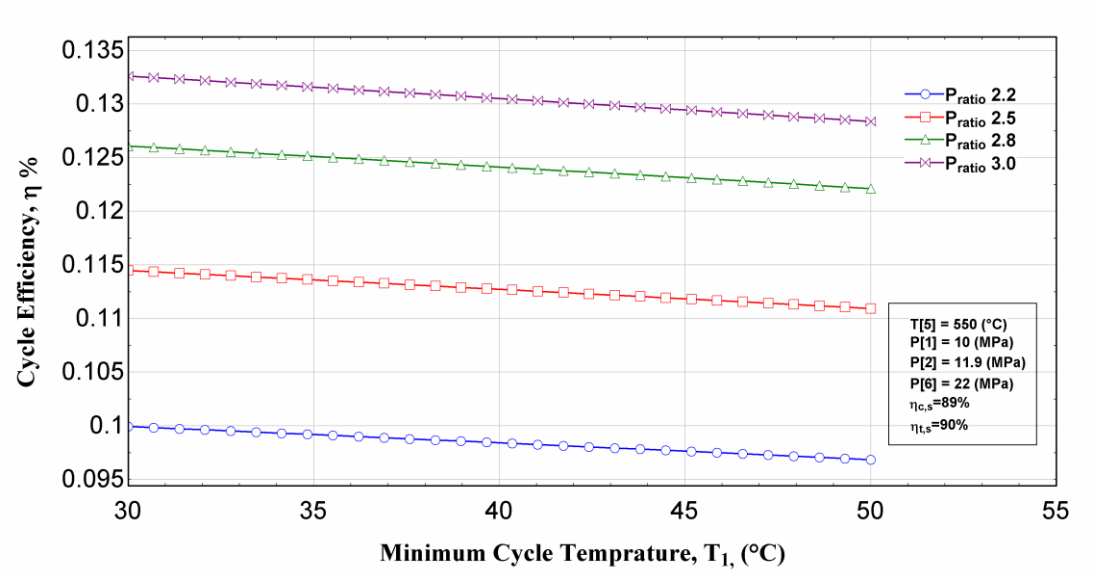


Figure 4. 22 Cycle Efficiency vs. Minimum Cycle Temperature at Different Pressure Ratios for the Actual S-$CO_2$ Brayton Cycle with Intercooling and Reheat

### 4.4.7 The Effect of Recompression Pressure Ratio

Figure 4.23 shows the variation of the work net output and cycle efficiency with the recompressor pressure ratio for the actual S-$CO_2$ Brayton cycle with intercooling and reheat. The work net increases with the recompression pressure ratio for different reheater pressure. The trend goes up to reach maximum at the point of 1.57 (pressure

ratio) with $W_{net}$= 60.85 kJ/kg Then the process experiences a slight fall until the break point which is the default pressure ratio of cycle ($P_{ratio}$=2.5). Exactly after a sharp downward trend makes a huge decrease in amount of work net. A cycle efficiency shows the same trend however there is a peak point is at where the pressure ratio is 2.5 and afterward sharp decrease in efficiency.

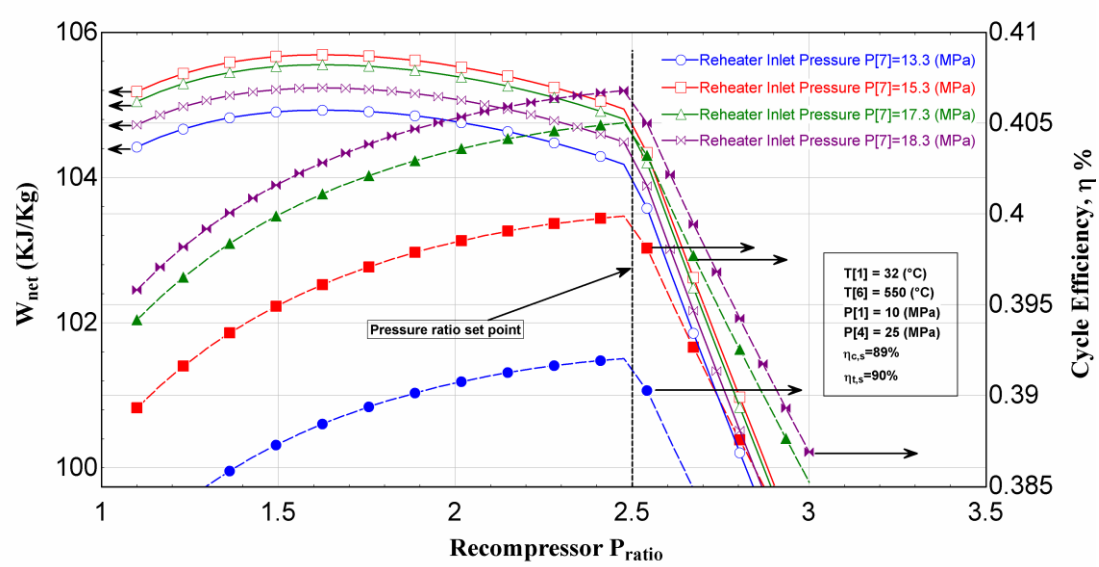


Figure 4. 23 Total Cycle Work and Cycle Efficiency vs. Recompression Pressure Ratio at Different Reheater Inlet Pressures for the Actual S-$CO_2$ Brayton Cycle with Intercooling and Reheat

## 4.5 Actual Supercritical Carbon Dioxide Brayton Cycle with Intercooling, Reheat and Regenerator

### 4.5.1 The Effect of Gas Cooler Pressure

The effect of first compressor outlet pressure ($P_2$) on thermal efficiency of the cycle is shown in figure 4.24. In the figure, the dash line shows the maximum thermal efficiency points for different turbine inlet temperature lines. The optimum pressure obtained for the first compressor is equal to 13.6 MPa for each case. As $P_2$ increased above its optimum value, efficiency decrease.

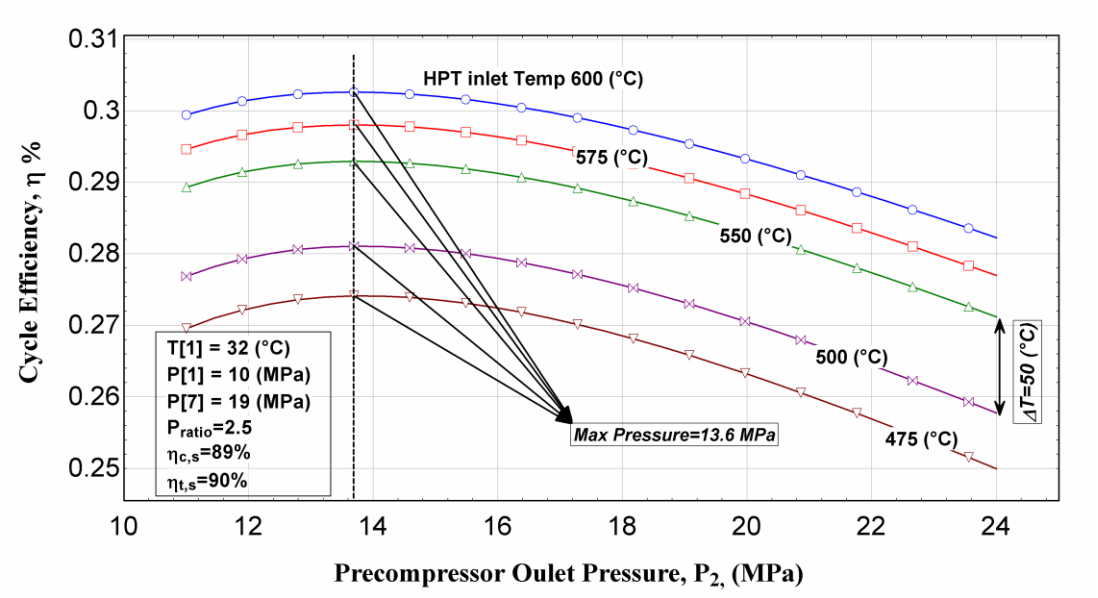


Figure 4. 24 Cycle Efficiency vs. Precompressor Outlet Pressure at Different Turbine Inlet Temperatures for the Actual S-$CO_2$ Brayton Cycle with Intercooling, Reheat and Regeneration

### 4.5.2 The Effect of High Pressure Turbine Inlet Temperature

A steady increase in cycle efficiency $\eta_{th}$ of actual supercritical Brayton cycle with intercooler, reheat and generator at different pressure ratios is shown by a solid line in figure 4.25. It is seen from the figure that as turbine inlet temperature rises from 450 ºC to 600 ºC cycle efficiency increases. For example at $P_{ratio}$=2.5, $\eta_{th}$ is improved by 10.05% from 26.63% to 29.31%.

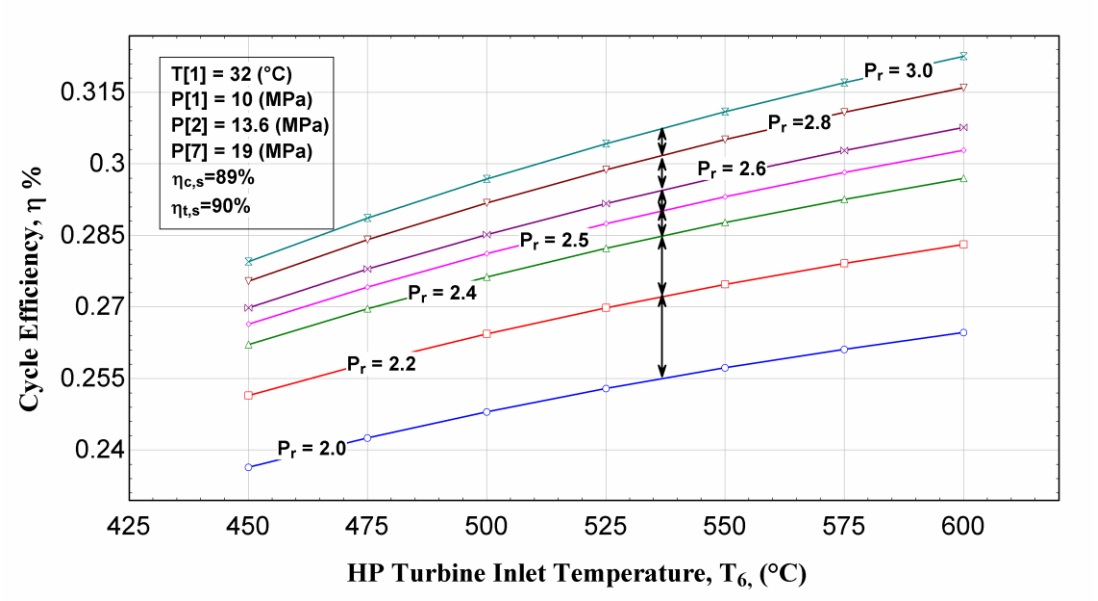


Figure 4. 25 Cycle Efficiency vs. High Pressure Turbine Inlet Temperature at Different Pressure Ratios for the Actual S-$CO_2$ Brayton Cycle with Intercooling, Reheat and Regeneration

### 4.5.3 The Effect of Gas Cooler Pressure on Total Cycle Work

The effect of precompressor outlet pressure $P_2$ of supercritical $CO_2$ Brayton cycle with intercooler, reheat and generator on $w_{net}$ is shown in Fig 4.26.

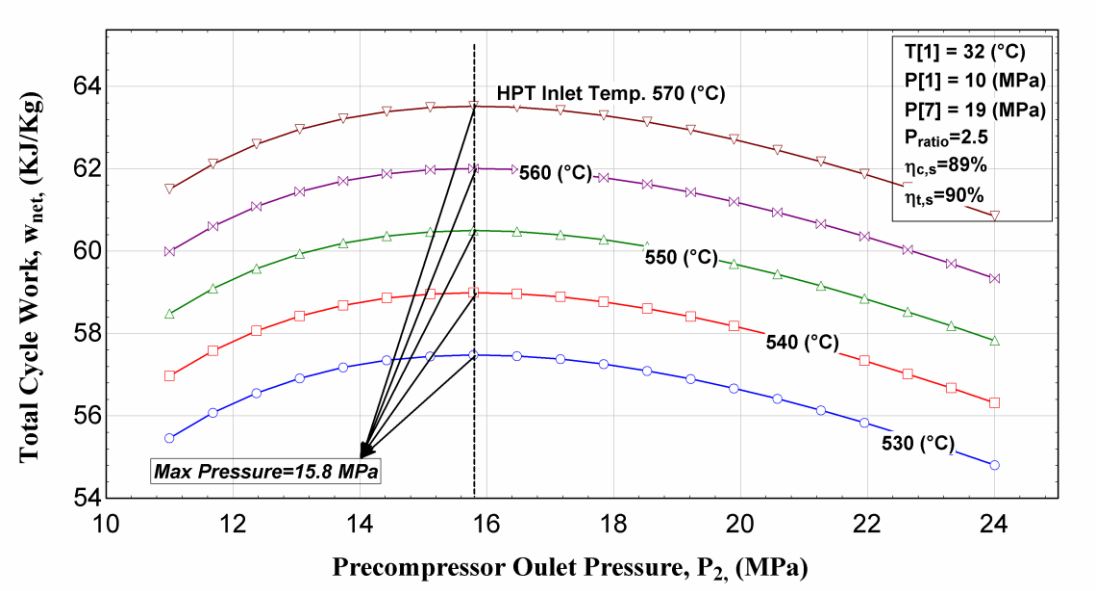


Figure 4. 26 Total Cycle Work vs. Precompressor Outlet Pressure at Different Turbine Inlet Temperatures for the Actual S-$CO_2$ Brayton Cycle with Intercooling, Reheat and Regeneration

The work net of the cycle reaches a maximum value, 60.5 kJ/kg at $P_2 = 15.8$ MPa for the present case (HPT inlet temp. 550 ºC).

### 4.5.4 The Effect of Cycle Pressure Ratio

The thermal efficiency of cycle depends on pressure ratio at various regenerator's effectiveness, as shown in Fig. 4.27. It is seen from the figure that the efficiency increases rapidly at lowest rate of pressure ratios until reaching the peak point, which means the highest amount of efficiency, can be obtained by the cycle. It can be pointed out that as the regenerator effectiveness up rise the maximum thermal efficiency happens at undermost rate of pressure ratios. For example, for a case of 85% regenerator effectiveness the topmost efficiency 35.42% is at pressure ratio of 4.5 however, for a 90% effectiveness the best efficiency is about 38.31% at pressure ratio of 3.7.

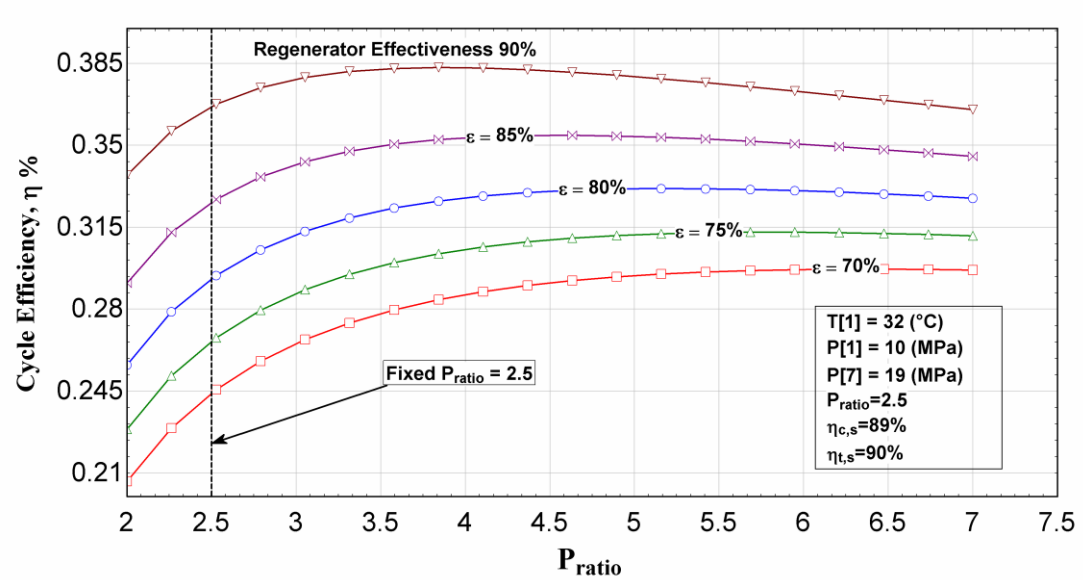


Figure 4. 27 Cycle Efficiency vs. Pressure Ratio at Different Regenerators Effectiveness for the Actual S-$CO_2$ Brayton Cycle with Intercooling, Reheat and Regeneration

### 4.5.5 The Effect of Pressure Ratio on Compressor and Turbine Work

The variation of $W_{in}$ and $W_{out}$ with pressure ratio of cycle at turbine inlet temperature ($T_5 = 550$ °C), is shown in figure 4.28. As can be seen in the figure both works experienced a steady rise in value, which is 34.01% and 33.1% for $W_{in}$ and $W_{out}$ respectively for pressure ratio range of 2 to 2.5.

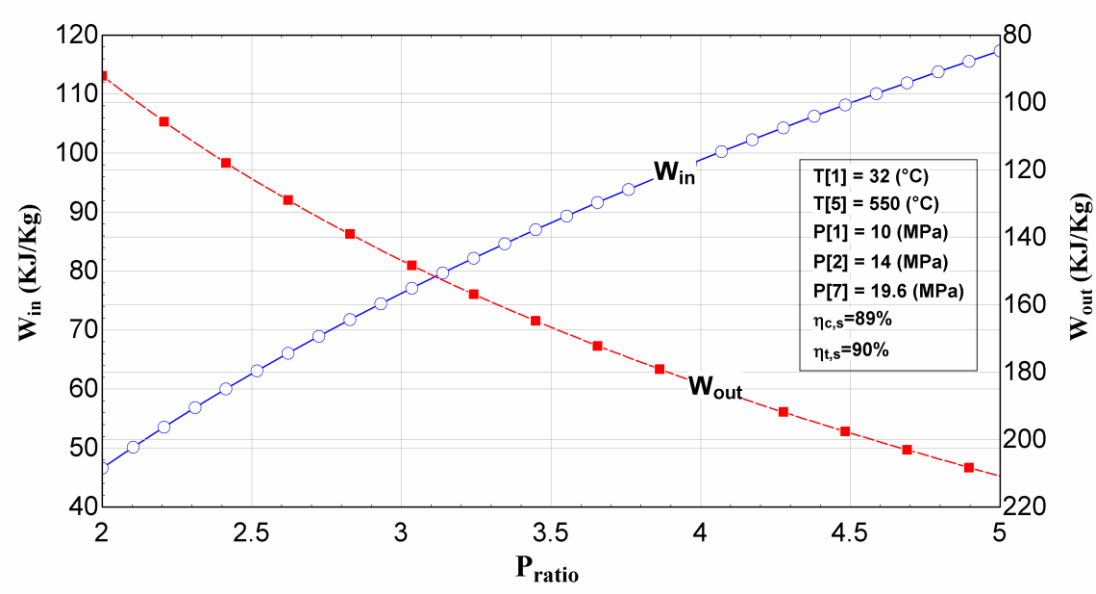


Figure 4. 28 Compressor Work and Turbine Work vs. Pressure Ratio for the Actual S-$CO_2$ Brayton Cycle with Intercooling, Reheat and Regeneration

### 4.5.6 The Effect of Minimum cycle Temperature

Figure 4.29 shows the variation of cycle efficiency and minimum cycle temperature (precompressor inlet temperature $T_1$) for a supercritical $CO_2$ Brayton cycle with intercooler, reheat and regenerator with $T_{max}$ = 550 °C, $P_{min}$ = 10 MPa and $P_2 = 14$ MPa at several pressure ratios. As the minimum cycle temperature increase, the efficiency of cycle decrease steadily. The reason that can be pointed out is that as the precompressor inlet temperature increases heat is rejected at higher temperature which lead to a decrease in the efficiency. For example, for every 5°C increase in $T_1$, the efficiency decreased about 2.91% at default pressure ratio of cycle ($P_{ratio}$=2.5).

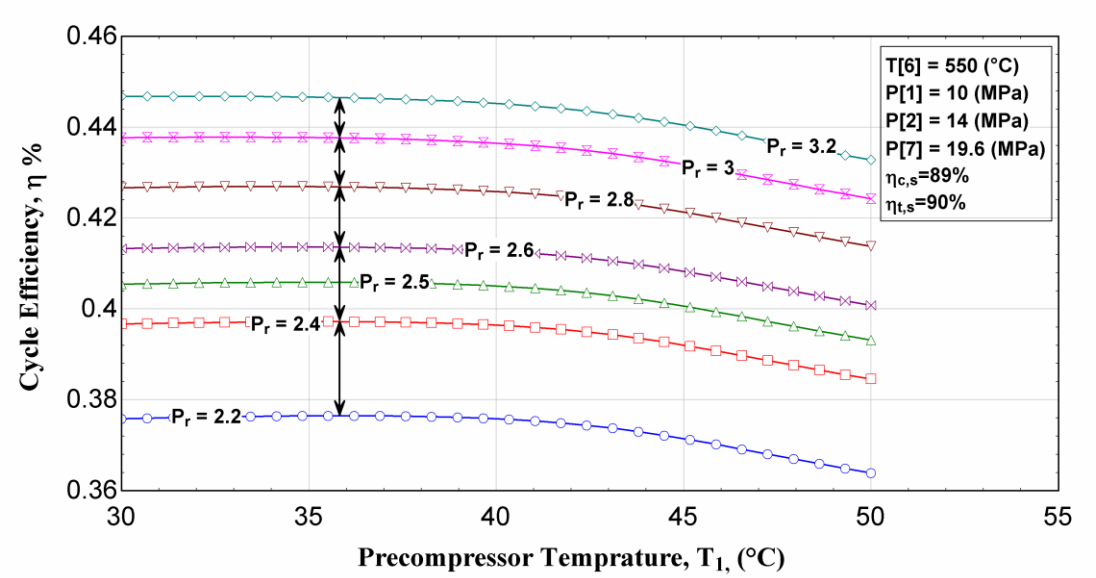


Figure 4. 29 Cycle Efficiency vs. Minimum Cycle Temperature at Different Pressure Ratios for the Actual S-$CO_2$ Brayton Cycle with Intercooling, Reheat and Regeneration

### 4.5.7 The Effect of Recompression Pressure Ratio

Figure 4.30 shows the variation of the work net output and cycle efficiency with the recompressor pressure ratio for the actual S-$CO_2$ Brayton cycle with intercooling, reheat and regenerator. The work net increases with the recompression pressure ratio for different reheater pressure. The trend goes up to reach a climax at the pressure ratio 1.57 with $W_{net}$= 60.85 kJ/kg. Then the process experiences a slight fall until the break point which is the default pressure ratio of cycle ($P_{ratio}$=2.5). Exactly after a sharp downward trend makes a huge decrease in amount of work net. A same trend applied to efficiency of cycle however the difference is the peak point is the pressure ratio set point ($P_{ratio}$=2.5) and afterward same sharp decrease in the cycle efficiency.

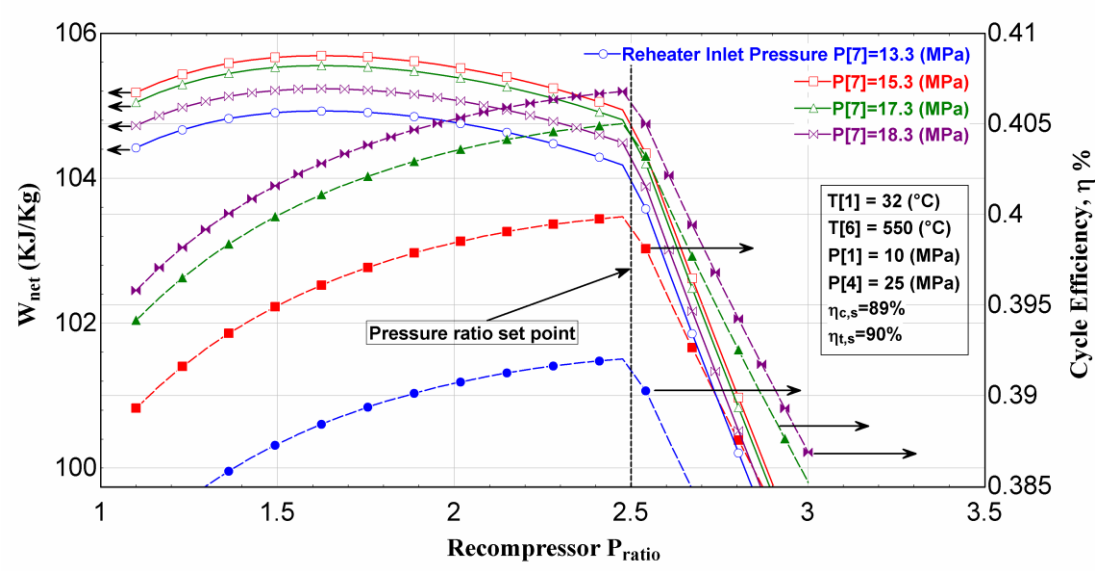


Figure 4. 30 Total Cycle Work and Cycle Efficiency vs. Recompression Pressure Ratio at Different Reheater Inlet Pressures for the Actual S-$CO_2$ Brayton Cycle with Intercooling, Reheat and Regeneration

For the current configuration couple of key parameters has been investigated by increasing the listed parameters to observe how they affect cycle efficiency, the results are presented in Table 4.1.

Table 4.1 Cycle efficiency sensitivity to key cycle parameters

| Cycle Parameters | Change in Cycle Parameter | Change in Cycle Efficiency (%) |
|---|---|---|
| Turbine Inlet Temperature | 50 ºC | +4.25 |
| Compressor Inlet Temperature | 5 ºC | -0.25 |
| Compressor Inlet Pressure | 2 MPa | -3.4 |
| Maximum pressure | 5 MPa | +6.38 |
| Gas Heater pressure | 2 MPa | +0.63 |
| Gas Cooler Pressure | 2 MPa | -1.23 |
| Pressure Ratio | 1 | +5.1 |
| Recuperator Effectiveness | 5% | +14.7 |

## 4.6 Carbon Dioxide Transcritical Power Cycle

When the function of the cycle shifts from Brayton cycle to a transcritical Brayton cycle, the heat rejection process will take place under the supercritical region and the condenser will be used instead of gas cooler (intercooler). The same efficiencies as chosen for the compressor and the expansion machine for carbon dioxide Brayton cycles are adopted for the pump and the expansion machine for carbon dioxide transcritical power cycles as initial analysis conditions (i.e. 89% for the pump and 90% for the expansion machine). The gas heater pressure and gas cooler pressure are assumed, 20 MPa and 10 MPa respectively for the initial cycle analysis.

### 4.6.1 The Effect of Turbine Inlet Temperature

By plotting the expansion inlet temperature vs. cycle efficiency for a given pump efficiency with various expansion efficiencies, and by plotting the expansion inlet temperature vs. cycle efficiency for a given expansion efficiency with various pump efficiencies (Fig. 4.31 & Fig. 4.32), it is found that the cycle efficiency will be improved by increasing the expansion inlet temperature. However, after a sharp increase at the beginning, the efficiency slope becomes flat if one further increases the expansion inlet temperature to the high temperature region. These figures also illustrate that the efficiencies of expansion units will have more crucial impact on the cycle efficiency than the efficiencies of compression units.

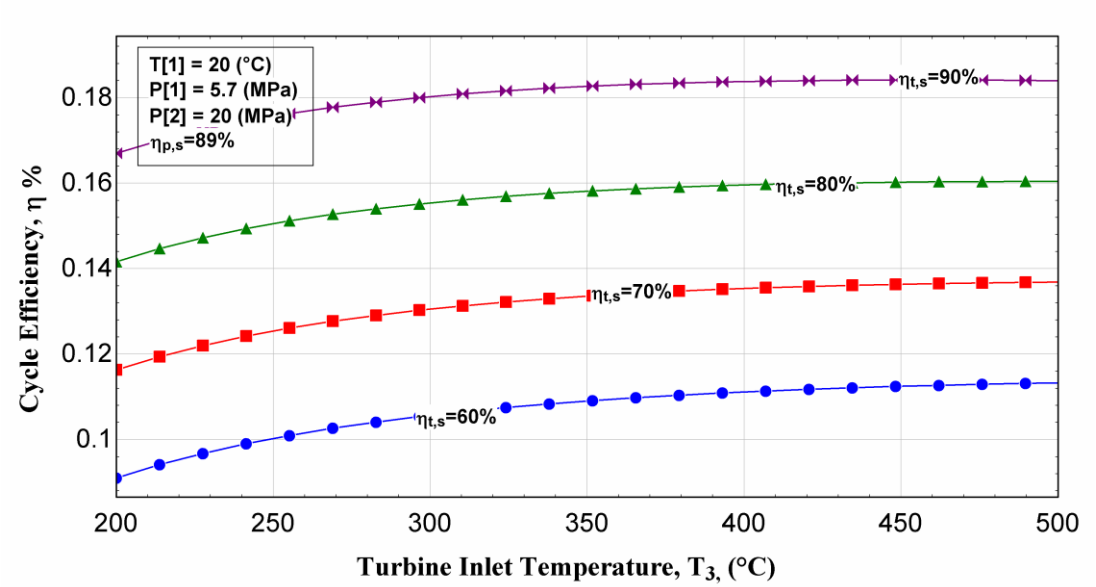


Figure 4. 31 Cycle Efficiency vs. Turbine Inlet Temperature at Different Turbine Efficiency for the Carbon Dioxide Transcritical Power Cycle

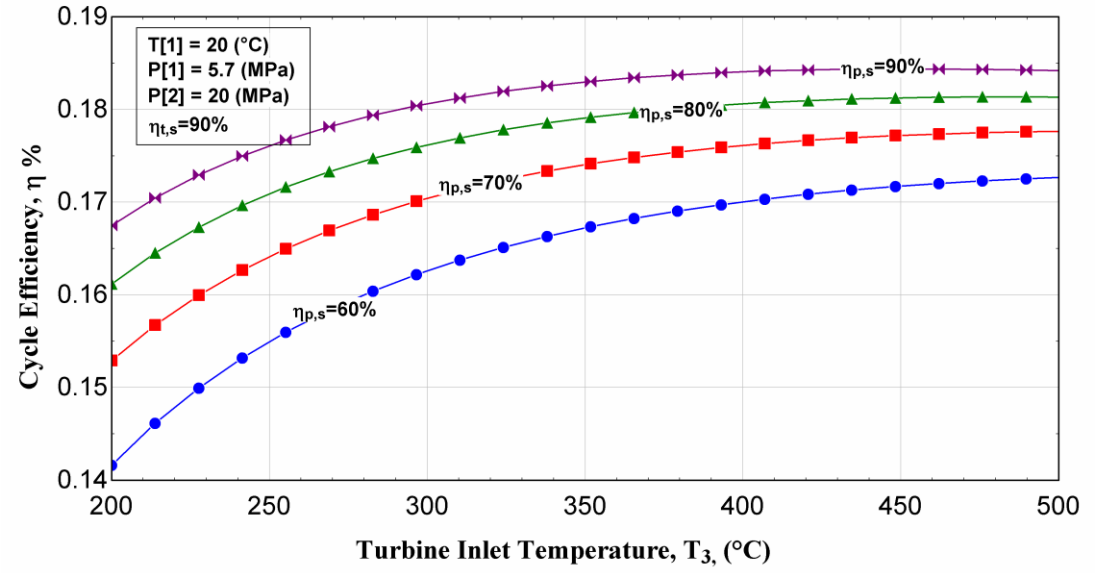


Figure 4. 32 Cycle Efficiency vs. Turbine Inlet Temperature at Different Pump Efficiency for the Carbon Dioxide Transcritical Power Cycle

### 4.6.2 The Effect of Gas Heater Pressure

Furthermore, the influence of the cycle gas heater pressure on the cycle efficiency of a carbon dioxide transcritical power cycle without IHX is plotted for different expansion inlet temperatures (see Fig. 4.33). It is shown that there is an optimum gas heater pressure for a certain expansion inlet temperature and condensing temperature.

At a certain condensing pressure, the lower the expansion inlet temperature, the lower the optimum gas heater pressure.

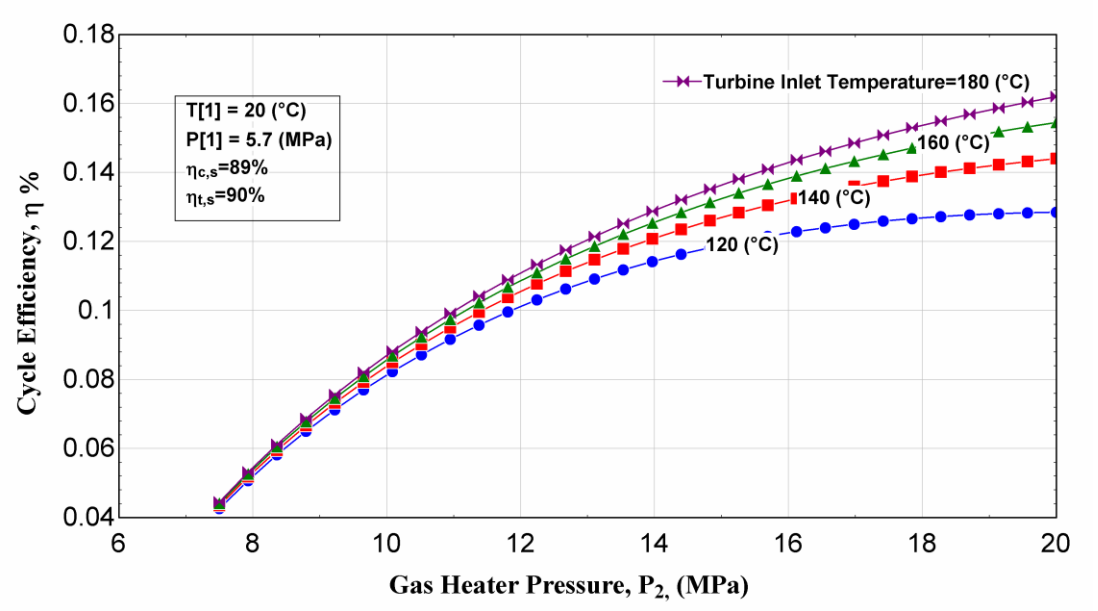


Figure 4. 33 Cycle Efficiency vs. Gas Heater Pressure at Different Turbine Inlet Temperature for the Carbon Dioxide Transcritical Power Cycle

# Chapter 5

# CONCLUSION

The reduction of the cost of power produced by all type of industrial plants is a crucial step toward the successful future utilization of low-grade waste heat sources. Therefore, efforts to redesign and reduce the cost of power cycles are vital. Compared to steam cycles, closed cycle gas turbines are simple, compact, less expensive and have shorter construction periods, thus reducing capital cost of the system.

The helium Brayton cycle has the highest thermal efficiency among other closed gas turbine cycles. However, helium Brayton cycles require core outlet temperatures around 900°C in order to achieve attractive efficiencies (45-48%)[42]. The necessity of high temperature sources for helium Brayton cycles and for any ideal gas cycle in general, is a serious challenge that makes some sort of difficulties in order to achieve that level of efficiency. Therefore, a power conversion cycle that would be capable of achieving high efficiencies at temperatures ranging from 70°C to at most 600°C is of considerable interest. Such a power cycle could close the gap between low temperature and high temperature sources. The supercritical $CO_2$ cycle and transcritical power cycle can achieve this goal.

In the this study, the capability of utilizing carbon dioxide power cycles in recovering energy in low-grade heat sources and waste heat has been investigated. Two major systems as carbon dioxide transcritical power cycle and supercritical

Brayton cycle are proposed. The performance of the corresponding cycles as simple supercritical carbon dioxide Brayton cycle, supercritical carbon dioxide Brayton cycle with intercooling, supercritical carbon dioxide Brayton cycle with reheat, supercritical carbon dioxide Brayton cycle with both intercooling and reheat, supercritical carbon dioxide Brayton cycle with intercooling, reheat and regenerator and carbon dioxide transcritical power cycle are studied. The influence of different cycle working parameters on the cycle performance is simulated by computer simulations. The simulation results show that there will be an optimum gas heater pressure for carbon dioxide power cycles at certain cycle working conditions. The optimum gas heater pressure will increase with increasing heat source temperature. Furthermore, the efficiency of the expansion machine will have more crucial influence on the cycle thermal efficiency than the pump efficiency does. For carbon dioxide Brayton cycles, there is also an optimum gas cooler pressure besides the optimum gas heater pressure for a certain cycle working condition.

# References


1. World Energy Outlook 2013. 2013; International Energy Agency ]. Available from: http://www.iea.org/.

2. Horuz, I. and B. Kurt, Absorption heat transformers and an industrial application. Renewable Energy, 2010. 35(10): p. 2175-2181.

3. Klein, S.A. and F. Alvarado, Engineering Equation Solver, version 9.237, F-Chart Software. Middleton 2012.

4. Kim, Y.M., C.G. Kim, and D. Favrat, Transcritical or supercritical CO2 cycles using both low- and high-temperature heat sources. Energy, 2012. 43(1): p. 402-415.

5. Institute, P. Energy Source: Solar Energy. Renewable Energy. . 2011; Available from: http://www.pembina.org/re/sources/solar.

6. Chen, H., The Conversion of Low-Grade Heat into Power Using Supercritical Rankine Cycles, in Chemical and Biomedical Engineering. 2010, University of South Florida.

7. Stijepovic, M.Z. and P. Linke, Optimal waste heat recovery and reuse in industrial zones. Energy, 2011. 36(7): p. 4019-4031.

8. International Energy Outlook. 2013; Available from: http://www.eia.gov/forecasts/ieo/index.cfm.

9. (EIA), U.S.E.I.A. World Energy Outlook 2013; Available from: http://www.worldenergyoutlook.org/publications/weo-2013/.

10. Sawyer, J.W., Sawyer's Gas Turbine Engineering Handbook: Theory & design. 1972: Gas Turbine Publications.

11. Cengel, Y. and M. Boles, Thermodynamics: An Engineering Approach with Student Resources DVD. 2010: McGraw-Hill Education.

12. Shepherd, D.G., Introduction to the gas turbine. 1960: Van Nostrand.

13. Zhang, X., M. He, and Y. Zhang, A review of research on the Kalina cycle. Renewable and Sustainable Energy Reviews, 2012. 16(7): p. 5309-5318.

14. Korobitsyn, M.A., New and Advanced Conversion Technologies: Analysis of Cogeneration, Combined and Integrated Cycles. 1998, University of Twente: Enschede.

15. Rogdakis, E.D. and K.A. Antonopoulos, A high efficiency NH3/H2O absorption power cycle. Heat Recovery Systems and CHP, 1991. 11(4): p. 263-275.

16. Ibrahim, M.B. and R.M. Kovach, A Kalina cycle application for power generation. Energy, 1993. 18(9): p. 961-969.

17. Lolos, P.A. and E.D. Rogdakis, A Kalina power cycle driven by renewable energy sources. Energy, 2009. 34(4): p. 457-464.

18. Nag, P.K. and A.V.S.S.K.S. Gupta, Exergy analysis of the Kalina cycle. Applied Thermal Engineering, 1998. 18(6): p. 427-439.

19. Yogi Goswami, D., Solar Thermal Power Technology: Present Status and Ideas for the Future. Energy Sources, 1998. 20(2): p. 137-145.

20. Vijayaraghavan, S. and D.Y. Goswami, A combined power and cooling cycle modified to improve resource utilization efficiency using a distillation stage. Energy, 2006. 31(8–9): p. 1177-1196.

21. Ng, K.C., T.Y. Bong, and T.B. Lim, A thermodynamic model for the analysis of screw expander performance. Heat Recovery Systems and CHP, 1990. 10(2): p. 119-133.

22. geo1.jpg (JPEG Image, 897 × 716 pixels) - Scaled (91%). 2014; Available from: http://www.tas.com/images/userfiles/geo1.jpg.

23. Converting Low- and Mid- Temperature Heat into Electrical Power. 2014; Available from: http://www.eng.usf.edu/~hchen4/Organic%20Rankine%20Cycle.htm.

24. Maizza, V. and A. Maizza, Working fluids in non-steady flows for waste energy recovery systems. Applied Thermal Engineering, 1996. 16(7): p. 579-590.

25. Gawlik, K. and V. Hassani. Advanced binary cycles: optimum working fluids. in Energy Conversion Engineering Conference, 1997. IECEC-97., Proceedings of the 32nd Intersociety. 1997.

26. Maizza, V. and A. Maizza, Unconventional working fluids in organic Rankine-cycles for waste energy recovery systems. Applied Thermal Engineering, 2001. 21(3): p. 381-390.

27. Angelino, G. and P. Colonna di Paliano, Multicomponent Working Fluids For Organic Rankine Cycles (ORCs). Energy, 1998. 23(6): p. 449-463.

28. Wang, X.D., et al., Performance evaluation of a low-temperature solar Rankine cycle system utilizing R245fa. Solar Energy, 2010. 84(3): p. 353-364.

29. Stine, W.B. and R.W. Harrigan, Solar energy fundamentals and design: with computer applications. 1985: John Wiley & Sons, Incorporated.

30. Andersen, W.C. and T.J. Bruno, Rapid Screening of Fluids for Chemical Stability in Organic Rankine Cycle Applications. Industrial & Engineering Chemistry Research, 2005. 44(15): p. 5560-5566.

31. Superc8.jpg (JPEG Image, 315 × 276 pixels). 2014; Available from: http://www.eng.usf.edu/~hchen4/Superc8.jpg.

32. Superc9.jpg (JPEG Image, 319 × 272 pixels). 2014; Available from: http://www.eng.usf.edu/~hchen4/Superc9.jpg.

33. Chen, Y., et al., A comparative study of the carbon dioxide transcritical power cycle compared with an organic rankine cycle with R123 as working fluid in waste heat recovery. Applied Thermal Engineering, 2006. 26(17-18): p. 2142-2147.

34. Chen, Y., Thermodynamic Cycles using Carbon Dioxide as Working Fluid CO2 transcritical power cycle study, in KTH, School of Industrial Engineering and Management (ITM), Energy Technology, Applied Thermodynamics and Refrigeration. 2011, KTH Royal Institute of Technology: Stockholm. p. xxii, 128.

35. Chen, Y., P. Lundqvist, and P. Platell, Theoretical research of carbon dioxide power cycle application in automobile industry to reduce vehicle's fuel consumption. Applied Thermal Engineering, 2005. 25(14–15): p. 2041-2053.

36. Zhang, X.-R., H. Yamaguchi, and D. Uneno, Experimental study on the performance of solar Rankine system using supercritical CO2. Renewable Energy, 2007. 32(15): p. 2617-2628.

37. Yamaguchi, H., et al., Preliminary Study on a Solar Water Heater Using Supercritical Carbon Dioxide as Working Fluid. Journal of Solar Energy Engineering, 2010. 132(1): p. 011010-011010.

38. Zhang, X.R., et al., Analysis of a novel solar energy-powered Rankine cycle for combined power and heat generation using supercritical carbon dioxide. Renewable Energy, 2006. 31(12): p. 1839-1854.

39. Yamaguchi, H., et al., Solar energy powered Rankine cycle using supercritical CO2. Applied Thermal Engineering, 2006. 26(17–18): p. 2345-2354.

40. Dostal, V., P. Hejzlar, and M.J. Driscoll, High-performance supercritical carbon dioxide cycle for next-generation nuclear reactors. Nuclear Technology, 2006. 154(3): p. 265-282.

41. File:Carbon dioxide pressure-temperature phase diagram.svg - Wikipedia, the free encyclopedia. 2010; Available from: http://en.wikipedia.org/wiki/File:Carbon_dioxide_pressure-temperature_phase_diagram.svg.

42. Dostal, V., A supercritical carbon dioxide cycle for next generation nuclear reactors, in Massachusetts Institute of Technology. Dept. of Nuclear Engineering. 2004, MASSACHUSETTS INSTITUTE OF TECHNOLOGY: Massachusetts Institute of Technology.

43. Feher, E.G., The supercritical thermodynamic power cycle. Energy Conversion, 1968. 8(2): p. 85-90.

44. Hiep T. Hoang, M.R.C., John W. Wuthrich. Thermodynamic Study of a Supercritical CO2 Brayton Cycle Concept. in SCCO2 Power Cycle Symposium. 2009. University of Colorado.

45. Gokhstein D. P, V.G.P., Future Design of Thermal Power Stations Operating on Carbon Dioxide. Thermal Engineering, 1971: p. 36-38.

46. Gokhshtein, D.P. and G.P. Verkhivker, Use of carbon dioxide as a heat carrier and working substance in atomic power stations. Soviet Atomic Energy, 1969. 26(4): p. 430-432.

47. Angelino, G., REAL GAS EFFECTS IN CARBON DIOXIDE CYCLES. ASME- Paper 69-Gt-102, 1969.

48. Petr V., K.M., A Study on Application of a Closed Cycle C02 Gas Turbine in Power Engineering (in Czech). 1997: Czech Technical University in Prague.

49. Kato, Y.N., T. ; Yoshizawa, Y., Carbon Dioxide Partial Condensation Direct Cycle for Advanced Gas Cooled Fast and Thermal Reactors. 2001: p. 2 Pages.

50. Dostal V, H.P., Todreas NE, Kazimi MS, Plant Design and Cost Assessment of Forced Circulation Lead-Bismuth Cooled Reactor with Conventional Power

Conversion Cycles. Advanced Nuclear Power Program. Vol. MIT-ANP-TR-082. 2001.

51. Craig S. Turchi, Z.M., Ty W. Neises and Michael J. Wagner Thermodynamic Study of Advanced Supercritical Carbon Dioxide Power Cycles for Concentrating Solar Power Systems. Journal of Solar Energy Engineering 2013. 135(4): p. 7.

52. Besarati, S.M. and D. Yogi Goswami, Analysis of Advanced Supercritical Carbon Dioxide Power Cycles With a Bottoming Cycle for Concentrating Solar Power Applications. Journal of Solar Energy Engineering, 2013. 136(1): p. 011020-011020.

53. Cayer, E., et al., Analysis of a carbon dioxide transcritical power cycle using a low temperature source. Applied Energy, 2009. 86(7–8): p. 1055-1063.

54. Yang Chen, W.P.a.P.L. Low-grade heat source utilization by carbon dioxide transcritical power cycle. in ASME/JSME 2007 Thermal Engineering Heat Transfer Summer Conference. 2007. Vancouver, British Columbia, Canada, July 8–12, 2007.

55. Dunham, M.T. and B.D. Iverson, High-efficiency thermodynamic power cycles for concentrated solar power systems. Renewable and Sustainable Energy Reviews, 2014. 30(0): p. 758-770.

56. Kalina, A.I., Combined-Cycle System With Novel Bottoming Cycle. Journal of Engineering for Gas Turbines and Power, 1984. 106(4): p. 737-742.

# APPENDIX

# APPENDIX A: The EES Code for Super Critical Carbon Dioxide Brayton Cycle

```
"============================================================"
                        "Actual Brayton"
"============================================================"

"Input variables"
T[1]=32
T[3]=550
P[1]=10
P_ratio=2.5
eta_compressor=0.89
eta_turbine=0.9

"========================================================="

"state 1"                       "Inlet to Compressor"
h[1]=ENTHALPY(CarbonDioxide,T=T[1],P=P[1])
s[1]=ENTROPY(CarbonDioxide,T=T[1],P=P[1])

"state 2"                       "Inlet to Combustor"
P_ratio=P[2]/P[1]
s_s[2]=s[1]
T_s[2]=TEMPERATURE(CarbonDioxide,s=s_s[2],P=P[2])
h_s[2]=ENTHALPY(CarbonDioxide,T=T_s[2],P=P[2])
eta_compressor=(h_s[2]-h[1])/(h[2]-h[1])
T[2]=temperature(CarbonDioxide,h=h[2],P=P[2])
s[2]=entropy(CarbonDioxide,T=T[2],P=P[2])

"state 3"                       "Inlet to Turbine"
P[3]=P[2]
h[3]=ENTHALPY(CarbonDioxide,T=T[3],P=P[3])
s[3]=ENTROPY(CarbonDioxide,T=T[3],P=P[3])

"state 4"                       "Turbine Outlet / Inlet to Heat Exchanger"
s_s[4]=s[3]
P[4]=P[1]
T_s[4]=TEMPERATURE(CarbonDioxide,s=s_s[4],P=P[4])
h_s[4]=ENTHALPY(CarbonDioxide,T=T_s[4],P=P[4])
eta_turbine=(h[4]-h[3])/(h_s[4]-h[3])
T[4]=TEMPERATURE(CarbonDioxide,h=h[4],P=P[4])
s[4]=ENTROPY(CarbonDioxide,T=T[4],P=P[4])

"========================================================="
"Energy Balance Equations"

w_in_compressor=abs(h[2]-h[1])
w_out_turbine=abs(h[3]-h[4])
```

```
w_net=w_out_turbine-w_in_compressor

q_in_combustor=abs(h[3]-h[2])
q_out_hex=abs(h[4]-h[1])

"========================================================="
"Thermal Efficiency"
eta=w_net/q_in_combustor
```

# APPENDIX B: The EES Code for Super Critical Carbon Dioxide Brayton Cycle with Intercooling

```
"============================================================"
                    "Actual Brayton with Intercooler"
"============================================================"

"Input variables"
T[1]=32
T[5]=550
P[1]=10
P[2]=11.9
eta_precompressor=0.89
eta_recompressor=0.89
eta_turbine=0.90
P_ratio=2.5

"============================================================"

"state 1"                                   "Inlet to Precompressor"
h[1]=ENTHALPY(CarbonDioxide,T=T[1],P=P[1])
s[1]=ENTROPY(CarbonDioxide,T=T[1],P=P[1])

"state 2"                                   "Inlet to Intercooler"
s_s[2]=s[1]
T_s[2]=TEMPERATURE(CarbonDioxide,s=s_s[2],P=P[2])
h_s[2]=ENTHALPY(CarbonDioxide,T=T_s[2],P=P[2])
eta_precompressor=(h_s[2]-h[1])/(h[2]-h[1])
T[2]=temperature(CarbonDioxide,h=h[2],P=P[2])
s[2]=entropy(CarbonDioxide,T=T[2],P=P[2])

"state 3"                                   "Inlet to Recompressor"
P[3]=P[2]
T[3]=T[1]
h[3]=ENTHALPY(CarbonDioxide,T=T[3],P=P[3])
s[3]=ENTROPY(CarbonDioxide,T=T[3],P=P[3])

"state 4"                                   "Inlet to Combustor"
s_s[4]=s[3]
P_ratio=P[4]/P[1]
T_s[4]=TEMPERATURE(CarbonDioxide,s=s_s[4],P=P[4])
h_s[4]=ENTHALPY(CarbonDioxide,T=T_s[4],P=P[4])
eta_recompressor=(h_s[4]-h[3])/(h[4]-h[3])
T[4]=TEMPERATURE(CarbonDioxide,h=h[4],P=P[4])
s[4]=ENTROPY(CarbonDioxide,T=T[4],P=P[4])

"state 5"                                   "Inlet to Turbine"
P[5]=P[4]
```

```
s[5]=ENTROPY(CarbonDioxide,T=T[5],P=P[5])
h[5]=ENTHALPY(CarbonDioxide,T=T[5],P=P[5])

"state 6"                                   "Turbine Outlet / Inlet to Heat
Exchanger"
s_s[6]=s[5]
P_ratio=P[5]/P[6]
T_s[6]=TEMPERATURE(CarbonDioxide,s=s_s[6],P=P[6])
h_s[6]=ENTHALPY(CarbonDioxide,T=T_s[6],P=P[6])
eta_turbine=(h[6]-h[5])/(h_s[6]-h[5])
T[6]=TEMPERATURE(CarbonDioxide,h=h[6],P=P[6])
s[6]=ENTROPY(CarbonDioxide,T=T[6],P=P[6])

"========================================================="
"Energy Balance Equations"

w_in_precompressor=abs(h[2]-h[1])
w_in_recompressor=abs(h[4]-h[3])
w_in=w_in_precompressor+w_in_recompressor

w_out=abs(h[5]-h[6])

w_net=w_out-w_in

q_in=abs(h[5]-h[4])

q_out_intercooler=abs(h[2]-h[3])
q_out_hex=abs(h[6]-h[1])
q_out=q_out_intercooler+q_out_hex



"========================================================="
"Thermal Efficiency"

eta=w_net/q_in

"net power"
m_dot=5.807
W_dot_cycle=m_dot*w_net
```

# APPENDIX C: The EES Code for Super Critical Carbon Dioxide Brayton Cycle with Reheat

```
"============================================================"
                    "Actual Brayton with Reheating"
"============================================================"

"Input variables"
T[1]=32
T[3]=550
P[1]=10
{P[2]=25}
P[4]=23.1
eta_compressor=0.89
eta_HPturbine=0.95
eta_LPturbine=0.95
P_ratio=2.5
"============================================================"

"state 1"                          "Inlet to compressor"
h[1]=ENTHALPY(CarbonDioxide,T=T[1],P=P[1])
s[1]=ENTROPY(CarbonDioxide,T=T[1],P=P[1])

"state 2"                          "Inlet to Combustor"
P_ratio=P[2]/P[1]
s_s[2]=s[1]
T_s[2]=TEMPERATURE(CarbonDioxide,s=s_s[2],P=P[2])
h_s[2]=ENTHALPY(CarbonDioxide,T=T_s[2],P=P[2])
eta_compressor=(h_s[2]-h[1])/(h[2]-h[1])
T[2]=temperature(CarbonDioxide,h=h[2],P=P[2])
s[2]=entropy(CarbonDioxide,T=T[2],P=P[2])

"state 3"                          "Inlet to High Pressure Turbine"
P[3]=P[2]
h[3]=ENTHALPY(CarbonDioxide,T=T[3],P=P[3])
s[3]=ENTROPY(CarbonDioxide,T=T[3],P=P[3])

"state 4"                          "Inlet to Reheater"
s_s[4]=s[3]
T_s[4]=TEMPERATURE(CarbonDioxide,s=s_s[4],P=P[4])
h_s[4]=ENTHALPY(CarbonDioxide,T=T_s[4],P=P[4])
eta_HPturbine=(h[4]-h[3])/(h_s[4]-h[3])
T[4]=TEMPERATURE(CarbonDioxide,h=h[4],P=P[4])
s[4]=ENTROPY(CarbonDioxide,T=T[4],P=P[4])

"state 5"                          "Inlet to Low Pressure Turbine"
T[5]=T[3]
P[5]=P[4]
```

```
s[5]=ENTROPY(CarbonDioxide,T=T[5],P=P[5])
h[5]=ENTHALPY(CarbonDioxide,T=T[5],P=P[5])

"state 6"                                   "Outlet of Low Pressure Turbine "
s_s[6]=s[5]
P[6]=P[1]
T_s[6]=TEMPERATURE(CarbonDioxide,s=s_s[6],P=P[6])
h_s[6]=ENTHALPY(CarbonDioxide,T=T_s[6],P=P[6])
eta_LPturbine=(h[6]-h[5])/(h_s[6]-h[5])
T[6]=TEMPERATURE(CarbonDioxide,h=h[6],P=P[6])
s[6]=ENTROPY(CarbonDioxide,T=T[6],P=P[6])


"======================================================="
"Energy Balance Equations"

w_in_compressor=abs(h[2]-h[1])

w_out_HPturbine=abs(h[3]-h[4])
w_out_LPturbine=abs(h[5]-h[6])
w_out=w_out_HPturbine+w_out_LPturbine

w_net=w_out-w_in_compressor

q_in_combustor=abs(h[3]-h[2])
q_in_reheater=abs(h[5]-h[4])
q_in=q_in_combustor+q_in_reheater


"======================================================="
"Thermal Efficiency"

eta=w_net/q_in
```

# APPENDIX D: The EES Code for Super Critical Carbon Dioxide Brayton Cycle with Intercooling and Reheat

```
"============================================================"
                "Actual Brayton with Intercooler and Reheating"
"============================================================"

"Input variables"
T[1]=32
{T[5]=550}
P[1]=10
P[2]=11.9
P[6]=22.9
eta_precompressor=0.89
eta_recompressor=0.89
eta_HPturbine=0.90
eta_LPturbine=0.90
P_ratio=2.5

"============================================================"

"state 1"                                   "Inlet to Precompressor"
h[1]=ENTHALPY(CarbonDioxide,T=T[1],P=P[1])
s[1]=ENTROPY(CarbonDioxide,T=T[1],P=P[1])

"state 2"                                   "Inlet to Intercooler"
s_s[2]=s[1]
T_s[2]=TEMPERATURE(CarbonDioxide,s=s_s[2],P=P[2])
h_s[2]=ENTHALPY(CarbonDioxide,T=T_s[2],P=P[2])
eta_precompressor=(h_s[2]-h[1])/(h[2]-h[1])
T[2]=temperature(CarbonDioxide,h=h[2],P=P[2])
s[2]=entropy(CarbonDioxide,T=T[2],P=P[2])

"state 3"                                   "Inlet to Recompressor"
P[3]=P[2]
T[3]=T[1]
h[3]=ENTHALPY(CarbonDioxide,T=T[3],P=P[3])
s[3]=ENTROPY(CarbonDioxide,T=T[3],P=P[3])

"state 4"                                   "Inlet to Combustor"
s_s[4]=s[3]
P_ratio=P[4]/P[1]
T_s[4]=TEMPERATURE(CarbonDioxide,s=s_s[4],P=P[4])
h_s[4]=ENTHALPY(CarbonDioxide,T=T_s[4],P=P[4])
eta_recompressor=(h_s[4]-h[3])/(h[4]-h[3])
T[4]=TEMPERATURE(CarbonDioxide,h=h[4],P=P[4])
s[4]=ENTROPY(CarbonDioxide,T=T[4],P=P[4])
```

```
"state 5"                                   "Inlet to High Pressure Turbine"
P[5]=P[4]
s[5]=ENTROPY(CarbonDioxide,T=T[5],P=P[5])
h[5]=ENTHALPY(CarbonDioxide,T=T[5],P=P[5])

"state 6"                                   "Inlet to Reheater"
s_s[6]=s[5]
T_s[6]=TEMPERATURE(CarbonDioxide,s=s_s[6],P=P[6])
h_s[6]=ENTHALPY(CarbonDioxide,T=T_s[6],P=P[6])
eta_HPturbine=(h[6]-h[5])/(h_s[6]-h[5])
T[6]=TEMPERATURE(CarbonDioxide,h=h[6],P=P[6])
s[6]=ENTROPY(CarbonDioxide,T=T[6],P=P[6])

"state 7"                                   "Inlet to Low Pressure Turbine "
T[7]=T[5]
P[7]=P[6]
s[7]=ENTROPY(CarbonDioxide,T=T[7],P=P[7])
h[7]=ENTHALPY(CarbonDioxide,T=T[7],P=P[7])

"state 9"                                   "Outlet of Low Pressure Turbine / Inlet
to Heat Exchanger"
s_s[8]=s[7]
P_ratio=P[5]/P[8]
T_s[8]=TEMPERATURE(CarbonDioxide,s=s_s[8],P=P[8])
h_s[8]=ENTHALPY(CarbonDioxide,T=T_s[8],P=P[8])
eta_LPturbine=(h[8]-h[7])/(h_s[8]-h[7])
T[8]=TEMPERATURE(CarbonDioxide,h=h[8],P=P[8])
s[8]=ENTROPY(CarbonDioxide,T=T[8],P=P[8])

"========================================================"
"Energy Balance Equations"

w_in_precompressor=abs(h[2]-h[1])
w_in_recompressor=abs(h[4]-h[3])
w_in=w_in_precompressor+w_in_recompressor

w_out_HPturbine=abs(h[6]-h[5])
w_out_LPturbine=abs(h[8]-h[7])
w_out=w_out_HPturbine+w_out_LPturbine

w_net=w_out-w_in

q_in_combustor=abs(h[5]-h[4])
q_in_reheater=abs(h[7]-h[6])
q_in=q_in_combustor+q_in_reheater

q_out_intercooler=abs(h[2]-h[3])
q_out_hex=abs(h[8]-h[1])
q_out=q_out_intercooler+q_out_hex
```

"=================================================="
"Thermal Efficiency"

eta=w_net/q_in

# APPENDIX E: The EES Code for Super Critical Carbon Dioxide Brayton Cycle with Intercooling and Reheat and Regeneration

```
"============================================================"
    "Actual Brayton with Intercooler and Reheating and Regeneration"
"============================================================"

"Input variables"
T[1]=32
T[6]=550
P[1]=10
P[2]=14
P[7]=19.6
eta_precompressor=0.89
eta_recompressor=0.89
eta_HPturbine=0.90
eta_LPturbine=0.90
P_ratio=2.5
{EPSILON=0.8}"Typical regenator effectivenesses range from 60 to 80%. Further increases in effectivenesses are typically not economical due to the large capital expenditures required to achieve these increases."

"============================================================"

"state 1"                                   "Inlet to Precompressor"
h[1]=ENTHALPY(CarbonDioxide,T=T[1],P=P[1])
s[1]=ENTROPY(CarbonDioxide,T=T[1],P=P[1])

"state 2"                                   "Inlet to Intercooler"
s_s[2]=s[1]
T_s[2]=TEMPERATURE(CarbonDioxide,s=s_s[2],P=P[2])
h_s[2]=ENTHALPY(CarbonDioxide,T=T_s[2],P=P[2])
eta_precompressor=(h_s[2]-h[1])/(h[2]-h[1])
T[2]=temperature(CarbonDioxide,h=h[2],P=P[2])
s[2]=entropy(CarbonDioxide,T=T[2],P=P[2])

"state 3"                                   "Inlet to Recompressor"
P[3]=P[2]
T[3]=T[1]
h[3]=ENTHALPY(CarbonDioxide,T=T[3],P=P[3])
s[3]=ENTROPY(CarbonDioxide,T=T[3],P=P[3])

"state 4"                                   "Inlet to Regenerator"
s_s[4]=s[3]
P_ratio=P[4]/P[1]
T_s[4]=TEMPERATURE(CarbonDioxide,s=s_s[4],P=P[4])
h_s[4]=ENTHALPY(CarbonDioxide,T=T_s[4],P=P[4])
```

```
eta_recompressor=(h_s[4]-h[3])/(h[4]-h[3])
T[4]=TEMPERATURE(CarbonDioxide,h=h[4],P=P[4])
s[4]=ENTROPY(CarbonDioxide,T=T[4],P=P[4])

"state 5"                                   "Inlet to Combustor"
P[5]=P[4]
EPSILON=(h[5]-h[4])/(h[9]-h[4])
h[5]=ENTHALPY(CarbonDioxide,T=T[5],P=P[5])
s[5]=ENTROPY(CarbonDioxide,T=T[5],P=P[5])

"state 6"                                   "Inlet to High Pressure Turbine"
P[6]=P[4]
s[6]=ENTROPY(CarbonDioxide,T=T[6],P=P[6])
h[6]=ENTHALPY(CarbonDioxide,T=T[6],P=P[6])

"state 7"                                   "Inlet to Reheater"
s_s[7]=s[6]
T_s[7]=TEMPERATURE(CarbonDioxide,s=s_s[7],P=P[7])
h_s[7]=ENTHALPY(CarbonDioxide,T=T_s[7],P=P[7])
eta_HPturbine=(h[7]-h[6])/(h_s[7]-h[6])
T[7]=TEMPERATURE(CarbonDioxide,h=h[7],P=P[7])
s[7]=ENTROPY(CarbonDioxide,T=T[7],P=P[7])

"state 8"                                    "Inlet to Low Pressure Turbine "
T[8]=T[6]
P[8]=P[7]
s[8]=ENTROPY(CarbonDioxide,T=T[8],P=P[8])
h[8]=ENTHALPY(CarbonDioxide,T=T[8],P=P[7])

"state 9"                                    "Outlet of Low Pressure Turbine"
s_s[9]=s[8]
P_ratio=P[6]/P[9]
T_s[9]=TEMPERATURE(CarbonDioxide,s=s_s[9],P=P[9])
h_s[9]=ENTHALPY(CarbonDioxide,T=T_s[9],P=P[9])
eta_LPturbine=(h[9]-h[8])/(h_s[9]-h[8])
T[9]=TEMPERATURE(CarbonDioxide,h=h[9],P=P[9])
s[9]=ENTROPY(CarbonDioxide,T=T[9],P=P[9])

"state 10"                                    "Regenerator Outlet"
P[10]=P[1]
h[4]+h[9]=h[5]+h[10]
T[10]=Temperature(CarbonDioxide,h=h[10],P=P[10])
s[10]=Entropy(CarbonDioxide,T=T[10],P=P[10])


"================================================="
"Energy Balance Equations"

w_out_HPturbine=abs(h[7]-h[6])
w_out_LPturbine=abs(h[9]-h[8])
```

```
w_out=w_out_HPturbine+w_out_LPturbine

w_in_precompressor=abs(h[2]-h[1])
w_in_recompressor=abs(h[4]-h[3])
w_in=w_in_precompressor+w_in_recompressor

w_net=w_out-w_in

q_in_combustor=abs(h[6]-h[5])
q_in_reheater=abs(h[8]-h[7])
q_in=q_in_combustor+q_in_reheater

q_out_intercooler=abs(h[2]-h[3])
q_out_reg=abs(h[7]-h[6])
q_out_precooler=abs(h[10]-h[1])
q_out=q_out_intercooler+q_out_reg+q_out_precooler

"========================================================="
"Thermal Efficiency"
eta=w_net/q_in
```

# APPENDIX F: The EES Code for Carbon Dioxide Transcritical Power Cycle

```
"============================================================"
                    "Carbon Dioxide Transcritical Power Cycle"
"============================================================"

"Input variables"
T[1]=20
T[3]=180
P[1]=5.73
P[2]=20
eta_pump=0.9
eta_turbine=0.9

"============================================================"

"state 1"                                   "Inlet to pump"
h[1]=ENTHALPY(CarbonDioxide,T=T[1],P=P[1])
s[1]=ENTROPY(CarbonDioxide,T=T[1],P=P[1])

"state 2"                                   "Inlet to Gas Heater"
s_s[2]=s[1]
T_s[2]=TEMPERATURE(CarbonDioxide,s=s_s[2],P=P[2])
h_s[2]=ENTHALPY(CarbonDioxide,T=T_s[2],P=P[2])
eta_pump=(h_s[2]-h[1])/(h[2]-h[1])
T[2]=temperature(CarbonDioxide,h=h[2],P=P[2])
s[2]=entropy(CarbonDioxide,T=T[2],P=P[2])


"state 3"                                    "Inlet to Turbine"
P[3]=P[2]
x[3]=Quality(CarbonDioxide,P=P[3],s=s[3])
h[3]=ENTHALPY(CarbonDioxide,T=T[3],P=P[3])
s[3]=ENTROPY(CarbonDioxide,T=T[3],P=P[3])

"state 4"                                   "Turbine Outlet / Inlet to Condenser"
s_s[4]=s[3]
P[4]=P[1]
x[4]=0
T_s[4]=TEMPERATURE(CarbonDioxide,s=s_s[4],P=P[4])
h_s[4]=ENTHALPY(CarbonDioxide,T=T_s[4],P=P[4])
eta_turbine=(h[4]-h[3])/(h_s[4]-h[3])
T[4]=TEMPERATURE(CarbonDioxide,x=x[4],P=P[4])
s[4]=ENTROPY(CarbonDioxide,x=x[4],P=P[4])

"============================================================"
"Energy Balance Equations"
```

```
w_in_pump=abs(h[2]-h[1])
w_out_turbine=abs(h[3]-h[4])
w_net=w_out_turbine-w_in_pump

q_in_combustor=abs(h[3]-h[2])
q_out_hex=abs(h[4]-h[1])

"========================================================="
"Thermal Efficiency"
eta=w_net/q_in_combustor
```